# GEOCHEMISTRY OF THE HACKETT RIVER VOLCANICS, NORTHWEST TERRITORIES

A Thesis

Presented to

the Faculty of the Department of Geosciences

New Mexico Institute of Mining and Technology

In Partial Fulfillment

of the Requirements for the Degree

Master of Science

in Geochemistry

by

Thomas Ewing

August, 1977

## ABSTRACT

Twenty-two [illegible] rare-earth analyses, are reported for the Archean Hackett River volcanic sequence, Slave structural province of the [illegible]. The presence and effects of alteration and multi-element mobility are documented by the use of correlation coefficients and cluster techniques.

The Hackett River samples display a calc-alkaline overall differentiation trend with substantial Mg and Fe enrichment. Two basalts are highly enriched in Mg and Fe, resembling basaltic komatiites. Five distinct groups of samples are re recognized on the basis of rare-earth abundances and trace- and major-element data: enriched Archean tholeiite (EATH), depleted Archean tholeiite (DATH), undepleted andesites and dacites (AADH), undepleted siliceous volcanics (USVH) and depleted siliceous volcanics (DSVH). Similar but distinct differentiation trends appear for the sequence AADH-USVH and for DSVH.

Trace-element modelling indicates that AADH and USVH were derived by partial melting of a peridotite, possibly containing plagioclase and amphibole, while DSVH and EATH were derived by partial melting of a garnet peridotite. DATH could have been produced by a highly depleted plagioclase peridotite. As AADH-USVH and DSVH samples are intercalated in the volcanic sequence, two distinct sources of magma were simultaneously active during the eruption of the Hackett River volcanics.

TABLE OF CONTENTS



TABLES



FIGURES

FIGURES (continued)



PHOTOGRAPHS



INTRODUCTION

Archean volcanic and [illegible] "greenstone belts" for the abundant metabasalts they contain, are scattered fragments of variably metamorphosed mafic to felsic volcanics. Their base is generally obscured by intrusion of both younger and remobilized older granites and migmatites; they are overlain by Archean sedimentary and volcanic rocks dominated by mudstone and greywacke turbidites. They range in age from about 3500 to 2700 Ma, occurring within cratonic "nuclei" such as the Yilgarn and Pilbara blocks in Australia, the Transvaal and Rhodesian cratons of southern Africa, and the Superior and Slave provinces of the Canadian Shield. Although these sequences have been recognized and studied since the late 1800s, wide recognition and formation of comprehensive tectonic and genetic models has only occurred in recent years. A comprehensive review of the subject is found in Anhaeusser and others (1969); recent tectonic interpretations include Anhaeusser (1973) and Langford and Morin (1976).

Geochemical studies are likewise of recent vintage. Abundant major-element studies of the volcanics first became available in the 1960s, with work on the Superior province by Wilson and others (1965), on the Yellowknife volcanics by Baragar (1966), and on Canadian Shield rhyolites by Baragar and Goodwin (1969). Many recent studies on the Canadian Shield, as well as the work of Viljoen and others (1969) in South Africa, have increased our knowledge of their geochemistry.

Trace-element geochemistry and geochemical modeling of the

Archean volcanic successions is of still more recent date. Hart and others (1970a,b) use K, Rb, Cs, Sr and Ba to compare Archean and modern basalts; Glikson (1971) uses trace elements to follow differentiation patterns through time; Jahn and others (1975) use geochemical modeling techniques with both these elements and the rare earth elements in samples from Minnesota, as do Arth and Hanson (1976). The techniques of trace-element geochemistry and geochemical modeling have been widely applied by Condie and co-workers; results of these studies have been summarized in a review article (Condie, 1976).

There is still a need for further studies in new areas of major and trace element geochemistry. Field relationships in Archean terrains are generally obscured by intrusion and deformation, and petrographic study is frustrated by later metamorphism; geochemistry, especially of trace elements not affected by alteration and metamorphism, may be the only means to effect a tectonic reconstruction of the Archean. Extant rare-earth analyses come from less than twenty distinct belts in North America, Africa and Australia. With the variety of patterns and processes displayed by these results (Condie, 1976), additional data are needed to better define distinct populations.

The Hackett River volcanic sequence is admirably suited for one such study. Located in an isolated and geochemically little-known area of the Slave Province of the Canadian Shield, the volcanic sequence was discovered only within the decade; it is currently being mapped by the Geological Survey of Canada and explored for mineral deposits by several mining companies.



The belt consists largely of intermediate to silicic volcanics, contrasting sharply with the largely mafic sequences of other areas. As a new area with abundant siliceous volcanics and substantial economic interest, it was chosen for geochemical analysis and modelling.

ACKNOWLEDGEMENTS

I wish to acknowledge and thank:

Dr. R. A. Frith of the Geological Survey of Canada, for permitting use of the field camp, for providing transport to and within the area, for valuable orientation and conversations in the field, and for providing preliminary maps and thirty-odd thin sections;

Dr. Kent C. Condie of New Mexico Institute of Mining and Technology, for creating the opportunity to undertake this study, for providing the equipment, the expertise and the funds for the analysis and interpretation of the samples;

John Hill, John Ostler and John Percival, summer assistants with the Geological Survey of Canada, for orientation, companionship and advice;

Dr. W. E. Padgham of the Department of Indian Affairs and Northern Development, Yellowknife, for assistance in time of need;

Jim Mather of Missouri Research Laboratories, Albuquerque, for making available equipment and expertise at favorable rates, which led to the resurrection of a gamma-ray spectrometer and the completion of this study;

The Geoscience Department, New Mexico Institute of Mining and Technology, for providing 25 thin sections and various equipment and supplies;

The Office of Education, Department of Health, Education and Welfare, for support on a Domestic Mining, Mineral and Mineral Fuel Conservation Fellowship for the year 1976-1977.

## GEOGRAPHICAL AND GEOLOGICAL SETTING

### Location

The Hackett River volcanic sequence lies within the quadrilateral bounded by meridians 107° and 109° West and parallels 65° and 66° North, District of Mackenzie, Northwest Territories, Canada (Figures 1, 2). The supply base and Territorial capitol is Yellowknife, 340 km southwest of the camp at Uist Lake, in the south-central part of the area. The nearest settlement, Bathurst Inlet, is 90 km to the north of D'Arcy Lake camp, in the northern part of the area. The area is mapped at scales of 1:500,000 and 1:250,000; aerial photographs are available at scales of 1:50,000 and 1:25,000. All names used in this report, except for Nose, Regan and Beechey Lakes and Mara, Hackett, Contwoyto, Back and Western Rivers, are unofficial.

The entire area lies within the Contwoyto upland physiographic subprovince. Elevation averages about 1300 feet above sea level; relief may reach 300 feet on the volcanic and granitic terrains. Glacial scouring has been intense (Photo 2), with continental glaciers moving across the area until about 10,000 years B.P. Outcrops are abundant and very fresh; weathering rinds are poorly developed and less than $\frac{1}{2}$" thick. Drainage is poor, with numerous lakes. Quaternary overburden is sparse, consisting primarily of scattered till and alluvium, a few large eskers, and one moraine east of D'Arcy Lake (Figure 2). The extreme freshness of outcrops aids mapping and sampling in the area.

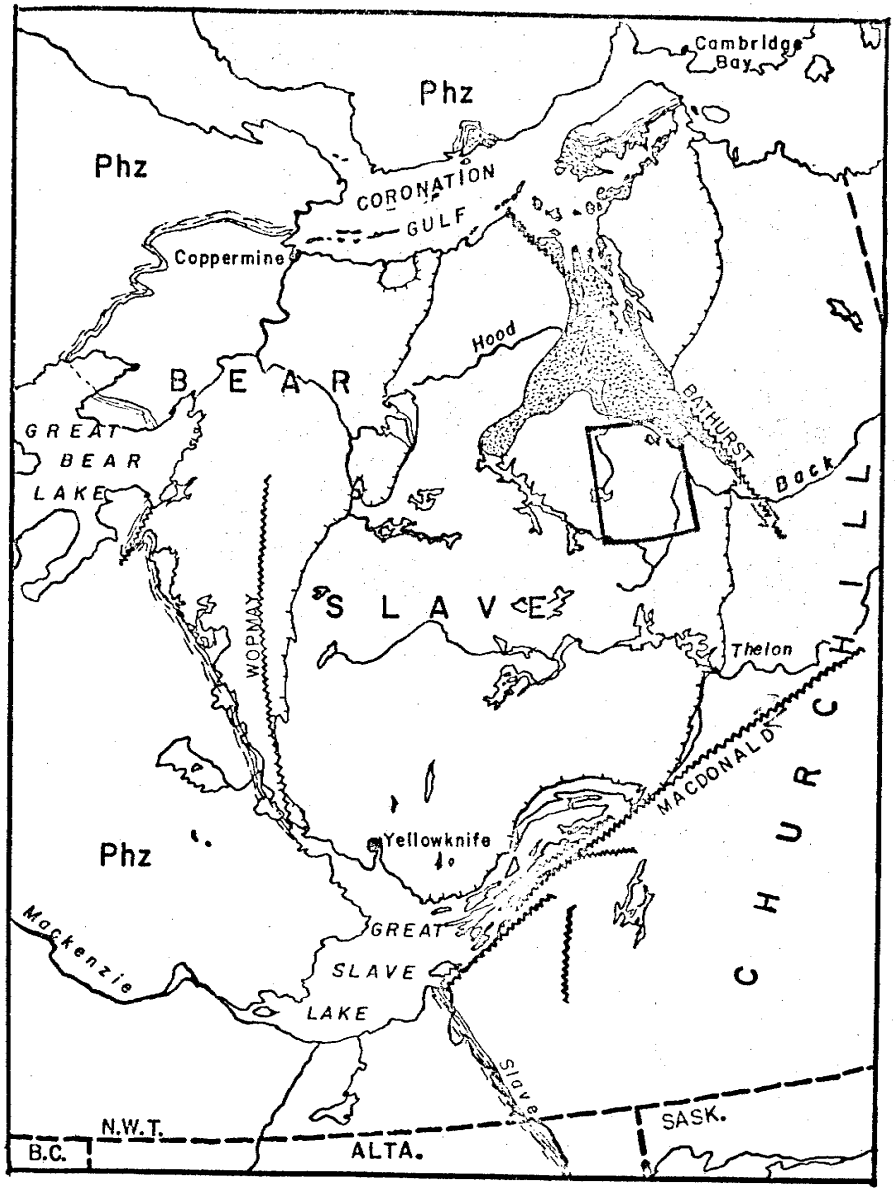


Figure 1. Location map of the Hackett River area, District of Mackenzie (after Douglas, 1968). Scale: 1:4,900,000. Rectangle is area of Figure 2. Large faults are represented by wavy lines, while hachured lines represent boundaries between structural provinces within the Canadian Shield. The stippled area is underlain by Aphebian and Helikian epicontinental sediments of the Goulburn and Bathurst Groups. Phz = Phanerozoic cover.

## Previous Work

The first reconnaissance mapping of the Hackett River area was that of Wright (1957) and Fraser (1964). These air-support operations discovered the extensive Back River volcanic complex south of the area, but failed to locate the Hackett River volcanics.

The Hackett River sequence was discovered during the follow-up of geochemical anomalies found during the Bear-Slave lake sediment sampling operation. This work (Cameron and Durham, 1974; Cameron, 1975) delineated extensive gossan zones and massive sulfide mineralization within felsic volcanic rocks in the Agricola Lake area, and gossans with intermediate to felsic rocks in the Uist Lake area.

To aid mineral exploration in the area, the Department of Indian Affairs and Northern Development sponsored the geologic mapping of the entire belt at 1:31,680 by Padgham and others (1974a-e; 1975a,b; 1976),Jefferson and others (1976a-c), and Bryan and others (1975). This confirmed the extent and felsic nature of the volcanics. R.A. Frith of the Geological Survey of Canada began a study of the sequence as an Archean succession of genetic interest and economic importance. Progress reports on this project have been published (Frith and Hill, 1975; Frith, Fyson and Hill, 1977), and aspects of rock and ore genesis considered (Frith and Roscoe, 1977). In the southern part of the area, Lambert is studying the volcanic geology of the Back River complex (Lambert, 1976).



## Geologic Setting

The Hackett River volcanic sequence is located in the northeastern part of the Slave structural province of the Caradian Shield, the geology of which has been reviewed by McGlynn and Henderson (1972). The sequence is part of a north-south trending band of volcanic and sedimentary basins in the eastern part of the province. The metamorphic and structural Thelon Front which marks the northwestern boundary of the Churchill province lies 80 km east-southeast of Uist Lake. The Bathurst fault zone, the site of sinistral Proterozoic transcurrent faulting (Thomas and others, 1976), lies 60 km northeast of D'Arcy Lake at nearest approach.

Detailed studies of the Yellowknife Supergroup volcanic and sedimentary rocks of the Slave province have been made in only a few areas, most notably at Yellowknife (Boyle, 1961; Henderson and Brown, 1966). Geochemical studies have been largely confined to the Yellowknife area (Baragar, 1966; Condie and Baragar, 1974), except for the Bear-Slave Operation and follow-ups mentioned above.

Aside from scattered inconclusive K/Ar dates, the best information on geochronology in the Slave province comes from Frith and others (1977), studying the Indin Lake region on the western border of the province. Three groups os Rb/Sr ages have been defined: a 3000-Ma group of granodiorites which form a basement to the Yellowknife volcanics in the area; a 2700-Ma group of synvolcanic granites; and a 2560-Ma group of

migmatitic diapirs which penetrate the supracrustal sequence. Later events at 2300 and 1970 Ma may record rifting of the Archean crust correlative with the formation of the Coronation Geosyncline; an 1800-Ma episode in the Bear province marks the Hudsonian orogeny of Stockwell (1972). Green and Baadsgaard (1971) recognize 2650-Ma volcanism and 2600-Ma granitic intrusion in the Yellowknife area. These dates are correlative with those from Indin Lake, suggesting that these events were province-wide, and may apply to the undated rocks of the Hackett River area.

## Description of Rock Units

The following descriptions are taken from progress reports by Frith and Hill (1975) and Frith, Fyson and Hill (1977). All unit numbers refer to Figure 2.

### "Basement" gneisses (unit 1)

Deformed and metasomatized granitic gneiss forms the core of the diapiric Hackett River dome. Pebbles in the surrounding metasediments suggest that these gneisses once were a granitic basement; but later intrusion and metasomatism have obscured the contact relationships.

### Metasediments (unit 2)

Overlying the "basement" gneisses is a unit containing quartzofeldspathic paragneiss and conglomerate. Deformed granitic clasts are present, often in a magnesium- and aluminum-rich matrix interpreted by Frith, Fyson and Hill (1977) as



volcanogenic.

### Hackett River Volcanic Sequence (unit 3)

Around the Hackett River dome, a largely felsic volcanic sequence conformably overlies the metasediments of unit 2. To the south, a similar volcanic sequence has no observed base, but grades into an extensively fumarolized and metasomatized area northeast of Uist Lake. The top of the sequence is often marked by iron-formation, carbonates and gossans, the "exhalite facies" rocks of Ridler (1973). Frith, Fyson and Hill (1977) suspect that the lower part of the sequence has been tectonically removed, leaving the (more felsic) upper portions behind; but mafic-to-felsic cycles are not well defined in this area. The sequence is estimated to contain about one third felsic ash flows, breccia and tuff (unit 3r), and two thirds andesitic to basaltic flows and tuffs (unit 3a)(Frith, Fyson and Hill, 1977). Massive sulfides occur at Camp Lake and at Agricola Lake, associated at both locations with silicic tuffs (Frith and Roscoe, 1977). Sections have not yet been measured; the thickness of the volcanics is estimated to vary from several hundred meters at Camp Lake to several kilometers at Uist Lake.

In the Uist Lake area, a thin upper volcanic sequence of mafic and felsic flows and tuffs is separated from the thicker lower sequence by a thin layer of shallow-water carbonaceous sediments and gossan. The upper sequence is interpreted

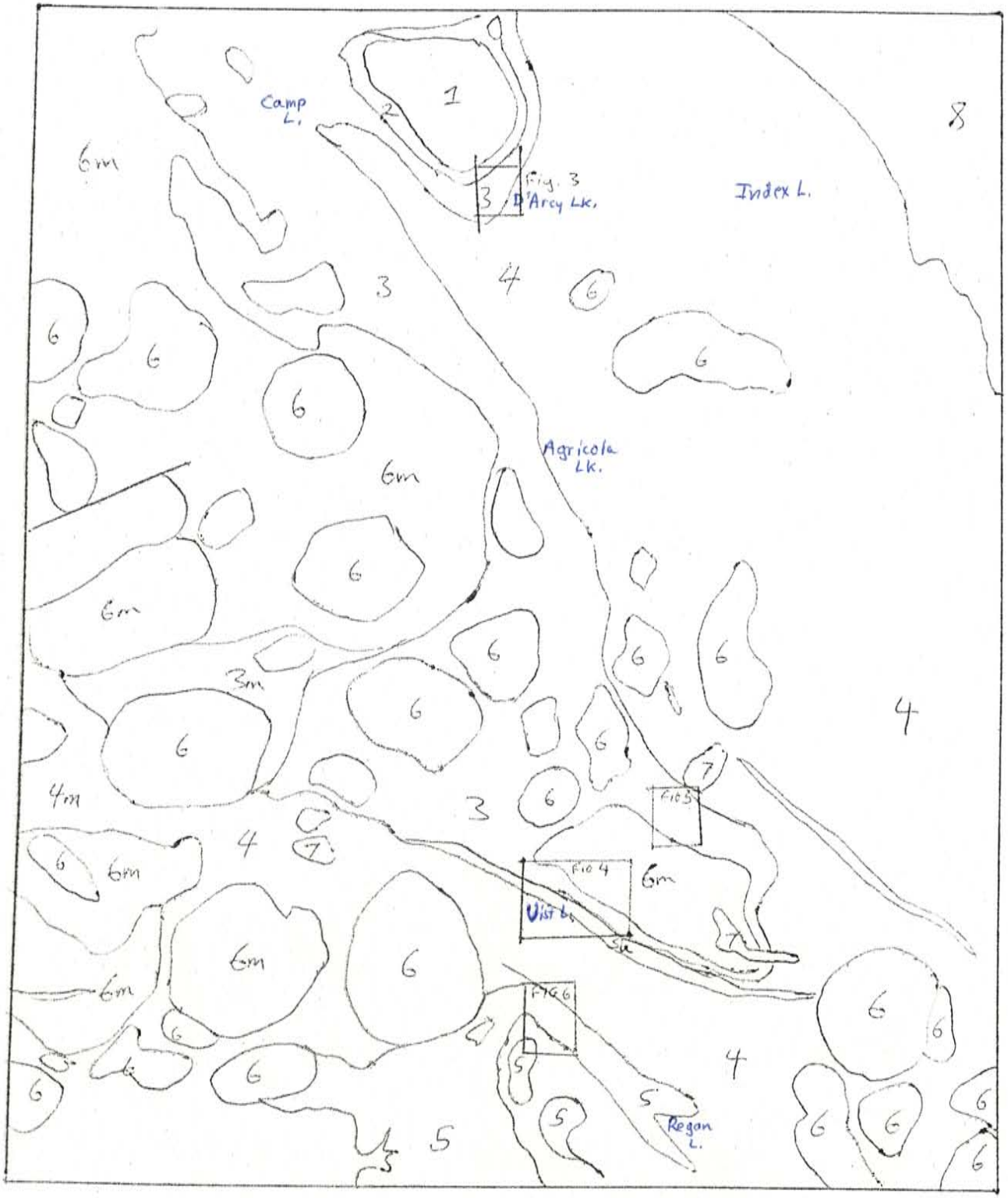


FIGURE 2. GEOLOGIC MAP HACKETT R. VOLCANIC SEQUENCE

FOR DESCRIPTION OF UNITS SEE TEXT.

as a later phase of Hackett River volcanism (Frith, Fyson and Hill, 1977) in the area.

Yellowknife sediments (unit 4)

Above the Hackett River volcanic sequence are mudstone and greywacke turbidites characteristic of the Yellowknife Supergroup (Henderson, 1975). Small amounts of exhalite facies rocks (gossan, iron-formation, carbonate and carbonaceous shale) are common immediately adjacent to the volcanics. Frith, Fyson and Hill (1977) propose a northwest-trending sedimentary basin, whose western boundary corresponds roughly to the present outcrop of volcanic rocks. Greater than 3 km of sediments may be present in the area.

Back River Volcanic Sequence (unit 5)

The Back River sequence conformably overlies and interfingers with Yellowknife sediments. In the map area, the complex is floored with andesitic to dacitic tuff-breccias and flows, above which rhyolite domes and tuffs, and andesite flows are found. To the south, these rhyolitic units show relict shards, welded pumice fragments and perlitic cracks (Lambert, 1976), identifying them as subaerial ash-flow tuffs. Lambert has also found possible cauldron subsidence structures in the complex.

Granitic complexes and plutons (unit 6)

Granites, granodiorites and diorites with associated granite gneisses and migmatites intrude and replace units 3, 4



and 5. These intrusions are commonly oval diapiric intrusions similar to those found in other Archean areas. Adjacent volcanic rocks have been extensively metasomatized and migmatized, creating large gradational granite-gneiss areas (unit 6m). Some intrusions are zoned (shown by dashes on Figure 2), with granodiorite margins and monzonitic cores (Frith, Fyson and Hill, 1977).

Late muscovite-bearing granites (unit 7)

Small potassium-rich granites intrude all earlier rock types, forming small stocks. They show no metamorphic fabric, indicating post-deformational emplacement.

Goulburn Group sediments (unit 8)

The northeastern corner of the map area is covered with gently-dipping sediments of the Aphebian Goulburn Group. Quartzites, quartz conglomerates and dolomites make up an epicontinental succession, which was once over 1200 m thick in the area.

Late gabbro and diabase (unit 9)

Diabase dikes and irregular gabbro bodies cut all previous units, and are possibly of Proterozoic age (McGlynn and Henderson, 1972).

## Structure and Metamorphism

Major structures in the map area are: the Hackett River dome; a southward-plunging syncline running southeast from

Camp Lake; and a large southward-plunging anticlinorium, here named the Island Lake anticlinorium, trending southeastward from the area north of Nose Lake to the area east of Uist Lake. Isograds drawn on biotite and on staurolite/andalusite outline in a general way the regions of uplift and intense diapiric intrusion (Frith, Fyson and Hill, 1977). Metamorphic facies are generally those of the low-pressure Abukuma-type facies series of Miyashiro (1961), characterized in this area by cordierite, andalusite and staurolite in the metasediments.

Three episodes of deformation have been identified in the Hackett River area (Frith, Fyson and Hill, 1977). The first formed large isoclinal folds in the sediments, and occasionally in the volcanics (Photos 3, 5), and was associated with diapiric intrusion. The second episode formed open northwest-striking folds, and was associated with the emplacement of plutons of unit 6. The third episode formed northeast-trending crenulation folds of small magnitude (Photo 4).

The volcanics have benerally been sampled in regions of fairly high metamorphic grade (see Modes reported in Table III, Appendix). The one suite of low-grade rocks, sampled from the Back River complex, has undergone extensive alteration, rendering it unsuitable for detailed analysis. This is in keeping with the observation of Viljoen and Viljoen (1969) that alteration is most intense in areas of low-grade metamorphism within Archean volcanic sequences. The question of the effects of metamorphism on rock chemistry will be taken up in a later section.

## SAMPLING

### General Considerations

Sampling of the Hackett River volcanic sequence was limited by several factors:

1) Field time was limited; sampling had to be completed in under 14 days;

2) During this time, the field party camped in only two locations, D'Arcy Lake and Uist Lake;

3) Air support was limited to two days with charter floatplane.

Within these limitations, an attempt was made to sample in some detail one traverse of the volcanic section, and one volcanic unit along strike for one or two miles. This was possible in the D'Arcy Lake and Uist Lake areas, as the base camp was close at hand. In the Island Lake and "Regan Lake" areas, only one traverse was made.

The resultant sampling of the volcanic sequence is therefore incomplete. Especially important are the absence of samples from the central portion of the belt, and the poor distribution of analyzed samples from the lower volcanic series at Uist Lake. During a two-week stay in the field, 62 samples were collected from the four areas; of these, major-element analyses were made of 22 and neutron-activation analyses of 11. As the map area is 10,500 $km^2$ and the belt extends over 190 km, the results must necessarily indicate more than they prove theories of petrogenesis. However, Cameron and Durham (1974) give 70 analyses of volcanics from the Agricola Lake area,

many of which were unaltered. These may be used to compare with the results of the present study, and to provide major-element control on the central part of the belt.

## Descriptions of Sample Areas

The stratigraphic, structural and petrologic descriptions that follow are intended to place the samples in a geologic framework. The geologic information is mostly derived from personal observation, and personal communications with R.A. Frith, J. Ostler, J. Hill, and J. Percival. Petrographic data is synthesized from personal study of thin-sections from all samples.

### D'Arcy Lake Area (Figure 3)

The traverse started in a sequence of sericitic felsites (unit 3) which overly both older metasediments (unit 1 = unit 2 of Figure 2) and lower volcanics (unit 2 of Figure 3; from Jefferson and others, 1976). These felsites are andesitic to rhyolitic in composition; minerals identified in thin section include chlorite, biotite and sericite. Poor optical determinations of plagioclase composition by the Michel-Levy method give anorthite contents from $An_6$ to $An_{22}$, showing sodic rims. One sample of this unit has been analyzed by X-ray fluorescence (XRF).

Above the felsites is a thick unit of bleached rhyolites (unit 4; Photos 1 and 3). These rhyolites are distinguished by their bone-white color, silica contents greater than 80%, and



Figure 3. Geologic map of the D'Arcy Lake sample area, Hackett River volcanic sequence, compiled from unpublished field data of Frith and others, supplemented by personal observations. Scale is 1:25,000. Units are (see text for description):

1--older metasediments
2--lower volcanics
3--sericitic felsites
4--bleached rhyolites
5--andesite
6--mostly rhyolites
7--basalts and andesites
8--Yellowknife sediments

A--recessional moraine
B--alluvium
C--felsenmeer on Yellowknife sediments

~~~~ --faults

 --gossans

Dots are sample localities; analyzed samples are shown with their sample numbers.
~~~~

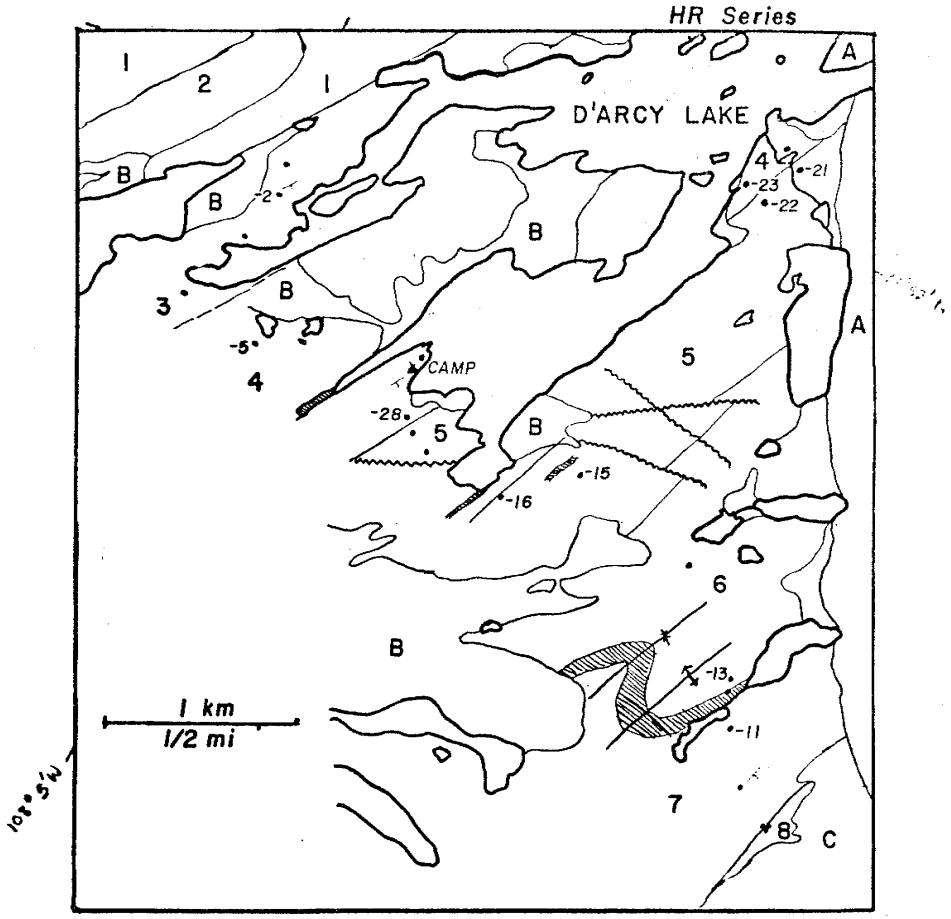




extensive gossan development. Large (2-3 cm) quartz eyes and minute quartz veins are often present. Identified minerals include quartz, muscovite and sericite, chlorite and biotite; sillimanite is occasionally present. Two samples were analyzed from the traverse (one for rare earths); two samples were also collected at the top of this unit 2 km northeast of the traverse.

Above the rhyolites is a unit of andesite (unit 5). Agglomeratic textures have been observed (Frith, pers. comm.); andesite breccias with a rhyolitic matrix are also frequent. Silica contents range from 55% to 62%; minerals present include biotite, hornblende and muscovite, as well as calcic-rimmed plagioclase ($An_{40}$-$An_{60}$). Two samples were analyzed from the traverse; one is of a rhyolitic agglomerate at the contact with unit 4. In addition, two samples were analyzed from the base of the unit about 2 km northeast of the traverse.

Above the andesite is a unit of mostly rhyolites(unit 6). These rhyolites are similar to those of unit 4, although less conspicuously bleached. Fragmental textures are present, although recrystallization has obscured most samples. Minerals present include quartz phenocrysts, muscovite and chlorite. One sample was analyzed from the top of the unit; it may represent a cherty interlayer, and occurs immediately below a wide gossan zone.

Topping the volcanic succession is a unit of basalts and andesites (unit 7). Near the base of the unit is a pillow basalt, with pillows showing extreme structural attenuation; sample HR-11 is from this rock. Andesitic volcanics and

volcanogenic sediments continue, with minor rhyolite interlayers, to the contact with the Yellowknife sediments (unit 8). Minor carbonate and ferruginous sediment mark the contact. Minerals identified in the basalts and andesites include calcic-rimmed plagioclase, chloritized hornblende, biotite and garnet.

Structure in this area is complex and mostly hidden. $F_1$ isoclinal folds strike northeastward, along the strike of the beds (Frith, pers. comm.); closure is seen only rarely (Photo 3). Two folds have been mapped (Jefferson and others, 1976) high in the section. However, at the scale at which sampling was conducted, this deformation does not affect any conclusions drawn from geochemistry; the folding does not appear to disrupt or repeat the stratigraphy outlined above. Cutting the sequence are several faults, marked by trenches across the upland surface. These faults displace the contacts of the major units a maximum of 1 km. The area has undergone fairly high-grade metamorphism, as shown by the occasional presence of garnet and sillimanite. Carbonate alteration is unimportant; sericitization is frequent, especially associated with the bleached and silicified rhyolites of unit 4. Epidotization and chloritication were not observed.

Uist Lake Area (Figure 4)

The base of the Hackett River volcanic succession in the Uist Lake area consists of tonalitic augen gneisses (unit 1, Figure 4) which form the core of the Island Lake anticlinorium.



Figure 4. Geologic map of the Uist Lake sample area, Hackett River volcanic sequence, compiled from unpublished field data of Frith and others, supplemented by personal observation. Scale is 1:50,000. Units are (see text for description):

1--tonalitic augen gneisses (a = amphibolite unit)
2--lower volcanics
3--shallow-water sediments
4--upper volcanics
5--Yellowknife sediments
6--diabase dike

--faults

--gossans

Dots are sample localities; analyzed samples are shown with their sample numbers.

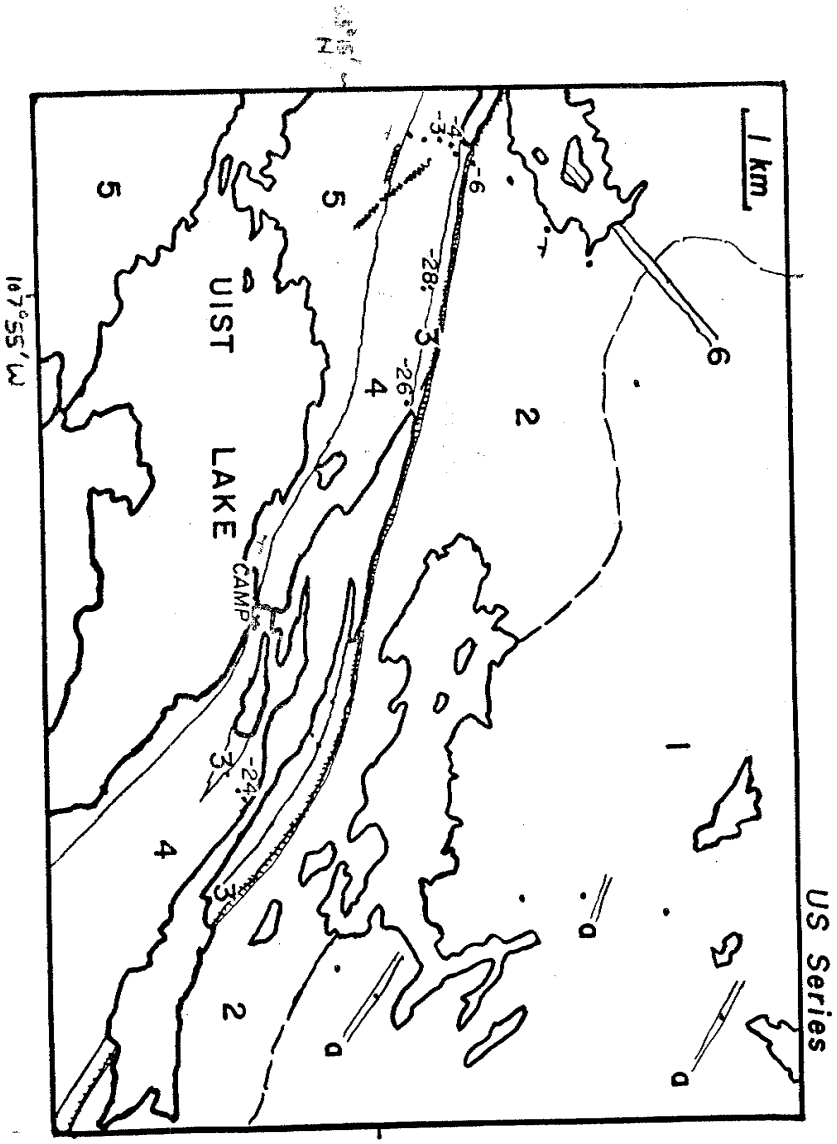




The gneisses contain large augen of plagioclase and orthoclase set in a matrix of hornblende ± biotite. Narrow (1-20 m) subunits of amphibolite cut the gneisses. These gneisses are the rock type that Frith, Fyson and Hill (1977) call "hybrid agmatitic rocks of uncertain petrologic affinity" produced by granodioritic intrusion. As their geochemistry has probably been profoundly altered, no samples are analyzed.

The augen gneisses grade into the less-altered intermediate to felsic volcanic rocks and associated sediments of the lower volcanics (unit 2). This unit grades upward from andesitic gneissic rocks to dacitic and rhyolitic fragmental rocks and tuffaceous sediments. Minerals identified include biotite, chlorite, epidote and garnet, as well as occasional calcite and sulfides. A traverse was made along Sanctuary Lake (west side of Figure 4); one sample, of a rhyolite at the top of the unit, was analyzed for rare earths.

The lower volcanics are succeeded by a thin unit of shallow-water sediments (unit 3; see Photo 2). The base of this unit is a remarkably continuous iron-rich gossan, which can be traced for over 20 km. This is succeeded by carbonaceous shales, tuffaceous sediments, and occasional felsic volcanic rocks. One of these volcanic units was sampled and analyzed.

Overlying the sediments is a unit of basaltic and intermediate rocks, the upper volcanics (unit 4). The unit frequently contains intermediate to felsic volcanics at its base, including rhyolite tuffs and lapilli-tuffs; but most of the unit consists of basaltic flows and tuffs, variably deformed and carbonated

(see Photo 4). Minerals identified include hornblende, biotite, garnet, epidote and calcite. Two samples were analyzed from the Sanctuary Lake traverse; two other samples were analyzed from the lower portion of the unit, along strike to the east.

Above the upper volcanics are greywacke and mudstone turbidites typical of the Yellowknife sediments. Graded beds on an interval of a few cm are well displayed (see Photo 6). Cutting the volcanics and the augen gneiss is a diabase dike (unit 6), about 100 m wide.

Complex structure is not apparent in this area outside of the augen gneiss. Good top determinations in the sediments indicate a homoclinal south-dipping sequence; few faults are indicated from mapping (Frith, pers. comm.). Small $F_3$ crenulation folds become prominent in units 4 and 5 (Photo 4), but do not disturb the stratigraphy. Metamorphism is high-grade and similar to that in the D'Arcy Lake area, with garnet, biotite and chlorite present. Epidote occurs in the area, but is not extensively developed. Carbonation is prevalent in much of the section, particularly the upper basalts; but sericitization is not as intense as in the D'Arcy Lake area.

Island Lake Area (Figure 5)

The basal unit in this area is the same mass of tonalitic augen gneiss (unit 1 on Figure 5) mentioned above, which forms the core of the Island Lake anticlinorium.

Overlying the augen gneiss is the volcanic series, undivided. Exposures in this area are not good, as relief is low; consequently, the volcanics are not divided. The sequence



Figure 5. Geologic map of the Island Lake sample area, Hackett River volcanic sequence, compiled from unpublished field data of Frith and others, supplemented by personal observation. Scale is 1:50,000. Units are (see text for description):

1--tonalitic augen gneiss
2--volcanic series, undivided
3--Yellowknife sediments

A--esker
B--alluvium and glacial debris

Dots are sample localities; analyzed samples are shown with their sample numbers.

Figure 6. Geologic map of the "Regan Lake" sample area, Back River volcanic belt; compiled from unpublished field data of Frith and others, supplemented by personal observation. Scale is 1:50,000. Units are (see text for description):

1--Yellowknife sediments
2--andesitic flows and tuff-breccias
3--dacite tuff-breccias
4--"Miller" andesite porphyry
5--dacite and dacite tuff
A--felsenmeer and alluvium

~~~~ --faults

Dots are sample localities; analyzed samples are shown with their sample numbers.
~~~~

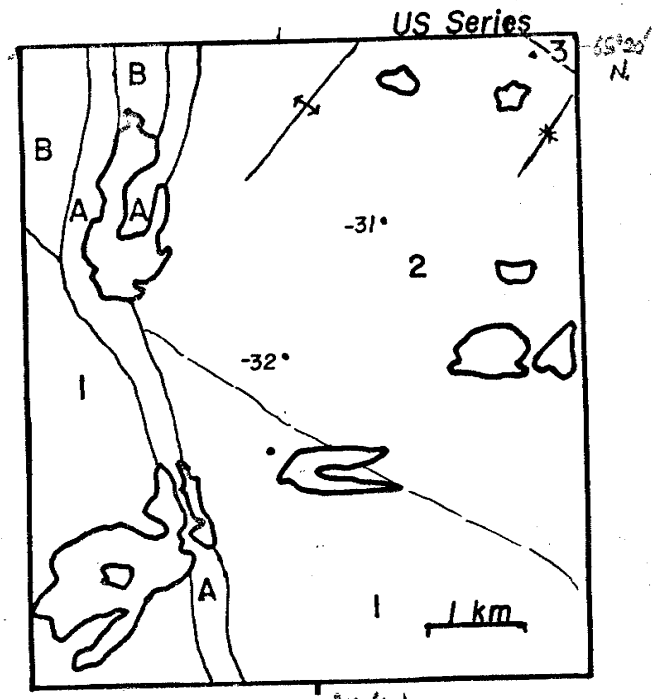


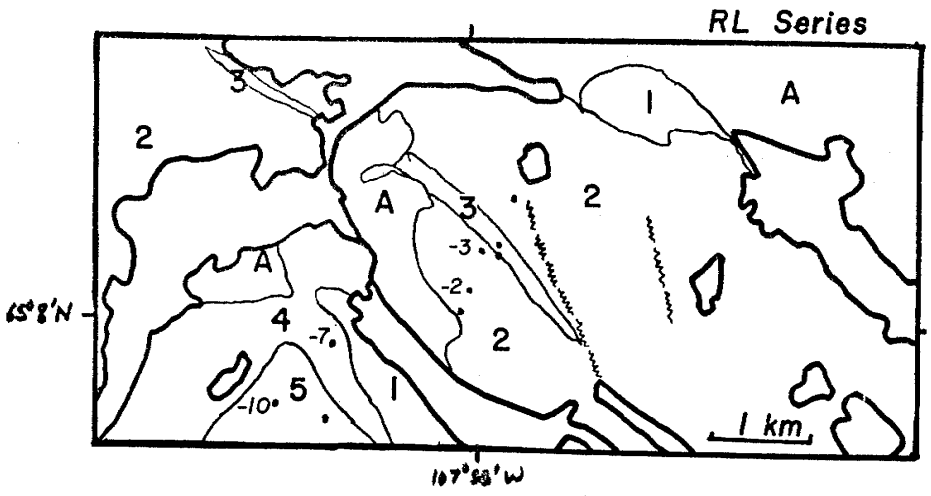




contains an amphibolite with large [illegible] of hornblende near its base (sampled by US-32), but [illegible] are felsic upwards; felsic and intermediate rocks interculate throughout the upper section. Two samples were analyzed from this unit. Overlying the volcanic series are typical Yellowknife sediments (unit 3), with a narrow band of shallow-water and exhalite facies sediments.

Metamorphism in this section is similar to that at Uist Lake. Minerals identified include hornblende, biotite, chlorite and cordierite. Calcite is present in some samples; sericite exists but is not a serious problem. The sequence forms a homocline, dipping northward from the augen gneiss core; small-scale northeast-trending folds cross the area (Frith, pers. comm.).

"Regan Lake" Area (Figure 6)

Overlying typical Yellowknife sediments (unit 1 of Figure 6) is a unit of andesitic to dacitic fragmental rocks (unit 2). Primary textures are well preserved; they are dominated by breccias and tuffs, with occasional beds of pillowed mafic andesites (sampled by RL-2) forming 20-30% of the section. One set of beds of dacitic tuff-breccia (unit 3) is included in this sequence. Both units are dominated in thin-section by calcite and sericite, but relict plagioclase phenocrysts and well-preserved quartz and calcite-filled amygdules are found. Chloritized hornblende and iron oxides are also abundant. Two samples were analyxed by X-ray fluorescence.

Also overlying Yellowknife sediments, and possibly above the previous units is a unit informally designated the "Miller" andesite porphyry (J. Ostler, pers. comm.; unit 4). This andesite is distinguished in the field by 5-10 mm plagioclase phenocrysts composing some 17% of the rock. In thin-section, the extent of calcite and sericite alteration becomes apparent; about 13% of the rock is calcite. The unit is distinctive and forms a marker bed in the volcanic complex. One sample was analyzed.

Above the "Miller" andesite is a unit of dacite and dacite tuff (unit 5). It is typical of several felsic "domes" found in the Back River complex. The unit is mineralogically simple, consisting of quartz and feldspar groundmass and phenocrysts, with occasional chloritized hornblende and sulfides; it is extensively replaced by calcite and sericite. One sample of massive dacite was analyzed.

Metamorphism in the area is at most lower greenschist facies, and obscure. Alteration, on the other hand, is intense throughout the area, with many samples having up to 35% modal calcite and 6-10% sericite. Structure is simple; the northern belt (units 2 and 3) forms a homoclinal steeply-dipping sequence, while the southern area is essentially flat-lying. A few faults cut the sequence with slight displacement.

## Methods of Sampling and Sample Preparation

At each locality, a sample was taken which was judged to represent the outcrop. Altered areas were avoided; but it was necessary to sample some of the weathering rind in order to



collect the sample. Generally only one piece weighing perhaps 2-5 lb was collected, although occasionally a composite sample was taken. Samples were marked with marking pens on a weathered surface. Due to the problem of transportation, as much of the rind was chipped off in the field, and samples were kept small.

Upon returning from the field, a slab was cut from each specimen, dividing it into three pieces: the slab, a small butt-end (which serves as a hand specimen), and a larger remainder (reserved for chemical analysis). Thin-section slabs were cut from each large slab; sections were made by the Geoscience Department, New Mexico Institute of Mining and Technology and the Thin Section Laboratory, Geological Survey of Canada.

The portion reserved for chemical analysis was run through large-size and medium-size steel jaw crushers, afterwards picking out weathered and altered pieces. The machines were cleaned with compressed air before and after each run. This sample was then run through a small jaw crusher and a ceramic-fitted "chipmunk" jaw crusher, again cleaning with compressed air between runs. Steel contamination was minimal, and could e easily be picked out of the crushed sample; contamination from the high-alumina ceramic plates is negligible.

About 10-20 grams of the crushed sample was then run through a ceramic-fitted rotary grinder, reducing the sample to a coarse powder. This was then ground in a Fisher automatic mortar grinder with an agate mortar for 30 minutes.

All but four grams was removed and stored for use in neutron activation analysis. The four-gram sample was then ground under acetone for at least 30 minutes, reducing the sample to a very fine powder.

Pellets for X-ray fluorescence analysis were made by the standard powder-press procedure in use at New Mexico Tech. About three grams was used for each pellet, which was then pressure-fused to a bakelite backing. USGS standard rocks had previously been prepared in this manner. Neutron activation samples were prepared by weighing out accurately ($\pm$ 0.1 mg) about 500 mg of the sample not ground under acetone, and placing it in a special polyethylene vial. This vial was then sealed with a soldering gun and placed in aluminum sample holders for irradiation.

Selection of Samples for Chemical Analysis

Sixty-two samples were received. Of these, five were not intended for analysis and were not crushed. Of the rest, twenty-two samples were selected for analysis by X-ray fluorescence; out of these, eleven were chosen for trace-element analysis by neutron activation. Selection for X-ray fluorescence was based on a preliminary neutron activation run of all samples for Na and Mn, as well as examination of thin sections and general considerations listed below. Selection for neutron activation was made with the additional information supplied by preliminary results for Si, Fe, Ti and K. The following considerations guided the choice of samples for analysis:



1) The sample should represent one rock type, not a mixture of types; therefore, the sample should be homogeneous. Breccias and layered samples were avoided.

2) The sample should be unaltered as far as possible. Rocks with extensive calcite, quartz veining, fractures or sericitization are avoided.

3) The sample should represent a rock type of interest. Thus, samples of carbonates and quartz gneiss were discarded in favor of volcanic rocks.

4) The suite of samples selected should include a substantial number of the rock types of special interest; here, felsic volcanics. However, sufficient variety should be included to assess differentiation trends and compare with other areas.

5) Samples should be geographically well-distributed.

## ANALYTICAL PROCEDURES

### Methods of Analysis

Twenty-two samples were analyzed by X-ray fluorescence. A Philips X-ray fluorescence unit with a Kicksort 706 Multichannel analyzer was used to analyze the pressed powder pellets mentioned above. Instrumental conditions for each run, as well as the elements sought, are listed on Table 1. The X-ray system was marginally operational throughout the analysis; in particular, the vacuum was not high enough to yield precise analyses of the lighter elements, expecially Mg.

All peak and background counts were averaged over four replications; these values were converted to net peaks, then corrected by the drift pellet to the analytical conditions of the first batch of standards. The standard analyses, replicated two and three times during a run, were averaged, discarding anomalous readings. Sample and standard values were then tabulated for use in the curve-fitting routine.

Three irradiations were made for neutron activation analysis. All irradiations were made at the Annular Core Pulse Reactor operated by Sandia Laboratories in Albuquerque, New Mexico. The first run was made on all samples to determine Na and Mn; the other two determined trace-element concentrations in eleven samples. Data was gathered using the Canberra 7000 series Gamma Ray Spectroscopy system, with a Ge(Li) detector and 4096-channel Digital Processor; instrumental conditions and dates of counting and irradiation are given on Table 1. Peak energies and basic methods come from Gordon and others (1968)



Table 1. Instrument Parameters

X-Ray Fluorescence

Run 1: Cr tube; Standards JB, [illegible], AGV, BCR, T-1, W-1, JG, SY, GSP GSP served as drift pellet. Gain = 20. time = 10 sec.

| | Vacuum | KV/ma | Col;Xtl | | Det. | HV | PHA window |
|---|---|---|---|---|---|---|---|
| Fe | air | 20/10 | F Qtz | 33.69 | Scint | 850 | .12+.4 |
| Ti | air | 40/20 | F Qtz | 48.58 | Scint | 850 | .08+.37 |
| K | air | 40/20 | F Qtz | 68.20 | P-10 | 1350 | .58+.45 |
| Ca | 500 um | 20/10 | F Qtz | 60.40 | P-10 | 1350 | .66+.5 |
| Si | 500 um | 40/20 | C Gyp | 26.25 | P-10 | 1350 | .17+.32 |

Run 2: Mo tube; Standards GSP, BCR, JB, AGV, JB, T-1, GH, G2; G-2 served as drift pellet. Gain = 20. Time=10 sec.
All elements run with LiF crystal, KV/ma=45/30, PHA window = .10-.50. Scintillation counter used.

| element | peak | background |
|---|---|---|
| Mo compton | 29.00 | none |
| Zr | 32.20 | 33.20 |
| Y | 33.95 | 33.20 |
| Sr | 35.95 | 36.95 |
| Rb | 38.05 | 39.05 |
| Zn | 60.70 | 61.00 |
| Cu | 65.70 | 66.20 |
| Ni | 71.45 | 72.45 |

Run 3: Cr tube; Standards JB, T1, G2, GH, BCR, JG, GSP, AGV, SY, PCC, DTS AGV served as drift pellet. Gain = 20. Time=1 sec.
Flow-proportional counter with P-10 used for all; HV=1350.

| | Vacuum | KV/ma | Col;Xtl | peak | bkgd. | window |
|---|---|---|---|---|---|---|
| P | 200 | 40/20 | C Gyp | 17.84 | 18.84 | .35-.57 |
| Si | 170 | 40/20 | C Gyp | 25.90 | none | .17-.57 |
| Al | 150 | 40/20 | C Gyp | 36.64 | 37.64 | .17-.40 |
| Mg | 140 | 50/35 | C Gyp | 51.30 | 51.30 | .10-.65 |

Neutron Activation Analysis
Sample size about 500 mg.

Run 1: Irradiated for 5 minutes, flux = $10^{11}$ n/cm$^2$-sec, Nov. 1976
Samples counted 600 sec each, within 48 h.
Elements sought: Na-24, Mn-56.

Run 2: Irradiated for 1 hour, flux = $2.5 \times 10^{12}$ n/cm$^2$-sec, 17 Feb.1
Samples counted as follows:

| elements | count time | Kev | date |
|---|---|---|---|
| La 140 | 5000 sec. | 1595 | 21 February 1977 |
| Np-239 (U) | " | 278 | " |
| Sm-153 | " | 103 | " |

Table 1--continued

Neutron Activation Analysis (continued)
Run 2 (continued)

| elements | count time | KeV | date |
|---|---|---|---|
| Sb-124 | 20,000 sec | 1691 | 3 May 1977 |
| Eu-152 | " | 1408 | " |
| Co-60 | " | 1333 | " |
| Ta-182 | " | 1222 | " |
| Tb-160 | " | 1178, 879 | " |
| Zn-65 | " | 1115 | " |
| Fe-59 | " | 1099 | " |
| Rb-86 | " | 1077 | " |
| Sc-46 | " | 889 | " |
| Co-58 (Ni) | " | 810 | " |
| Cs-134 | " | 796 | " |
| Zr-95 | " | 757 | " |
| Hf-181 | " | 482 | " |
| Cr-51 | " | 320 | " |
| Pa-233 (Th) | " | 312 | " |
| Yb-169 | " | 177 | " |
| Ce-141 | " | 145 | " |

Run 3: Irradiated as Run 2, on 10 May 1977.
Samples counted as follows:

| elements | count time | KeV | date |
|---|---|---|---|
| Ba-131 | 4000 sec | 496 | 17 May 1977 |
| Yb-175 | " | 396 | " |
| Lu-177 | " | 208 | " |

Seven samples from Run 3 were run with 10,000-second count times for those elements analyzed with 20,000-second count times in Run 2, beginning 7 June 1977.



and Condie and Lo (1971), with modifications derived from the analysis scheme used at the University of the Witwatersrand, Johannesburg.

Results were posted from the spectrometer printout by summation over all peak channels using fixed-width windows determined for each element and each run. Background was determined on each side of the peak, averaging when necessary, but maintaining uniformity in procedure from sample to sample.

## Statistical Analysis of Data

Values of USGS rock standards used for all data reduction are given in Table 2.

### X-Ray Fluorescence results

The basic procedure used for reducing the X-ray fluorescence major-element results is as follows: The standards are plotted on a percent element vs. counts graph. A visual best fit is obtained, and anomalous standards discarded. The remaining standard values are entered with the unknowns into program MAJOR, which calculates both a linear and a quadratic least-squares fit to the standard counts and concentrations, then evaluates the unknowns according to this fit. The program, however, neither calculates errors associated with the fit, nor does it optimize the number of standards used.

To overcome these limitations, I decided to use a least-squares confidence interval model derived in part from Krumbein and Graybill (1965). Briefly, one can estimate an

Table 2. Values for Standard Rocks.

| | W-1 | G-2 | GSP | AGV | PCC | DTS | BCR | GH | SY-1 |
|---|---|---|---|---|---|---|---|---|---|
| $SiO_2$ | 52.64 | 69.11 | 67.38 | 58.99 | 41.90 | 40.50 | 54.50 | 75.80 | 59.50 |
| $TiO_2$ | 1.07 | 0.50 | 0.66 | 1.04 | 0.015 | 0.013 | 2.20 | 0.08 | 0.49 |
| $Al_2O_3$ | 15.00 | 15.40 | 15.25 | 17.25 | 0.74 | 0.24 | 13.61 | 12.50 | 9.6 |
| $Fe_2O_3$ | 11.09 | 2.65 | 4.33 | 6.76 | 8.35 | 8.64 | 13.40 | 1.34 | 8.20 |
| MgO | 6.62 | 0.76 | 0.96 | 1.53 | 43.18 | 49.80 | 3.46 | 0.03 | 4.20 |
| CaO | 10.96 | 1.94 | 2.02 | 4.90 | 0.51 | 0.15 | 6.92 | 0.69 | 10.20 |
| $Na_2O$ | 2.15 | 4.07 | 2.80 | 4.26 | 0.006 | 0.007 | 3.27 | 3.85 | 3.30 |
| $K_2O$ | 0.64 | 4.51 | 5.53 | 2.89 | 0.004 | 0.001 | 1.70 | 4.76 | 2.67 |
| $P_2O_5$ | 0.14 | 0.14 | 0.28 | 0.49 | 0.002 | 0.002 | 0.36 | 0.01 | 0.22 |
| Zr | 105. | 300. | 500. | 225. | 7. | 3. | 190. | 160. | 3030. |
| Y | 25. | 12. | 30. | 21. | <5. | 0.05 | 37. | 70. | 441. |
| Rb | 21. | 168. | 254. | 67. | 0.06 | 0.05 | 47. | 390. | 195. |
| Sr | 190. | 479. | 233. | 657. | 0.41 | 0.35 | 330. | 10. | 286. |
| Zn | 86. | 85. | 98. | 84. | 36. | 45. | 120. | 80. | 219. |
| Cu | 110. | 13. | 33. | 60. | 11. | 7.0 | 18. | 12. | 23. |
| Ni | 76. | 5. | 12.5 | 18.5 | 2339. | 2369. | 16. | 3. | 43. |

| | T-1 | JG | JB |
|---|---|---|---|
| $SiO_2$ | 62.65 | 72.24 | 52.09 |
| $TiO_2$ | 0.59 | 0.26 | 1.34 |
| $Al_2O_3$ | 16.52 | 14.21 | 14.53 |
| $Fe_2O_3$ | 6.03 | 2.21 | 9.04 |
| MgO | 1.89 | 0.73 | 7.70 |
| CaO | 5.19 | 2.18 | 9.21 |
| $Na_2O$ | 4.39 | 3.39 | 2.79 |
| $K_2O$ | 1.23 | 3.96 | 1.42 |
| $P_2O_5$ | | 0.10 | 0.26 |
| Zr | 200. | (160.) | 155. |
| Y | 25. | | |
| Rb | 30. | 186. | 41. |
| Sr | 680. | 184. | 438. |
| Zn | 190. | 36. | 83. |
| Cu | 47. | 3.3 | 52. |
| Ni | 10. | 10. | 139. |

| | G-2 | AGV | BCR |
|---|---|---|---|
| Ba | 1870. | 1208. | 675. |
| Ce | 170. | 70. | 54. |
| Co | 5.5 | 14. | 38. |
| Cr | 7. | 12. | 18. |
| Cs | 1.4 | 1.4 | 0.95 |
| Eu | 1.4 | 1.7 | 2.0 |
| Hf | 7.4 | 5.2 | 4.7 |
| La | 90. | 35. | 26. |
| Lu | 0.12 | 0.28 | 0.55 |
| Mn | 260. | 763. | 1406. |
| Sb | 0.1 | 4.5 | 0.69 |
| Sc | 3.7 | 13. | 33. |
| Sm | 7.3 | 6.0 | 6.6 |
| Tb | 0.52 | 0.75 | 1.0 |
| Th | 24. | 6.4 | 6.0 |
| U | 2.0 | 1.9 | 1.7 |
| Yb | 0.66 | 1.7 | 3.4 |
| Ta | 0.9 | 0.9 | 0.88 |

Compiled by Condie (pers. comm.) from many sources.



100(1-a)% confidence interval for Y=f(X), where Y and X are random variables, by determining the standard deviation of the least squares fit, then applying the formula

$$\left|\hat{Y} - t_{a/2}(n-2)\hat{\sigma}\sqrt{\frac{1}{n} + \frac{(x-\bar{x})^2}{SS\ X^2}}\right| \leq Y \leq \left|\hat{Y} + t_{a/2}(n-2)\hat{\sigma}\sqrt{\frac{1}{n} + \frac{(x-\bar{x})^2}{SS\ X^2}}\right|$$

where n = number of standards used
$\bar{x}$ = mean of x-values (here, the counts)
x = the particular x-value under consideration
$t_{a/2}$ = the Student's t-value for a/2
$\hat{\sigma}$ = the standard deviation of the curve
$\hat{Y}$ = the calculated Y value for x
SS $X^2$ = sum of squares of the residuals of x; $(X-\bar{X})^2$

The term including t and the standard deviation is a measure of the precision of the least-squares fit at the 100(1-a)% degree of confidence. This error term is at a minimum when $x = \bar{x}$, that is, at the midrange of the standards; it increases away from this minimum, the rate of increase depending on the magnitudes of the x quantities. Values for this term are given for $x = \bar{x}$ (e-min) and for the maximum error encountered in the set of samples (e-max) for a given number of standards used in Table 3.

This error term includes, at least in part, the counting and sample replication error terms emphasized in the analytical literature. These errors affect both standards and samples; and although the standard counting errors are reduced by multiple analyses, yet the 95% confidence interval used (representing two standard devaitions of a normal variable) should encompass sample errors at one standard deviation.

To use the equation given above, it is necessary to calculate the standard deviation of the least-squares fit. For a simple

Table 3. Errors in X-Ray major-element curve fitting.

| | linear e-min | linear e-max | second-order e-min | second-order e-max | accept: |
|---|---|---|---|---|---|
| Si: | | | | | |
| 9 stds. | 0.68 | 2.64 | 0.66 | 2.52 | |
| 8 | 0.589 | 2.31 | 0.613 | 2.39 | linear,8 standards |
| Si(2): | | | | | |
| 11 | 0.537 | 2.04 | 0.439 | 1.668 | |
| 10 | 0.573 | 2.117 | 0.363 | 1.342 | second,10 " |
| Ti: | | | | | |
| 11 | 0.022 | 0.046 | 0.024 | 0.049 | linear,11 " |
| Al: | | | | | |
| 10 | 0.440 | 0.598 | 0.478 | 0.650 | |
| 9 | 0.303 | 0.409 | 0.334 | 0.450 | linear,9 " |
| Fe: | | | | | |
| 9 | 0.174 | 0.411 | 0.166 | 0.392 | |
| 8 | 0.166 | 0.403 | 0.145 | 0.351 | second,8 " |
| Mg: | | | | | |
| 7 | 2.888 | 3.95 | 1.707 | 2.01 | |
| 6 | 2.516 | 2.969 | 1.650 | 1.947 | second,6 " |
| Ca: | | | | | |
| 10 | 0.114 | 0.219 | 0.084 | 0.162 | second,10 " |
| K: | | | | | |
| 12 | 0.034 | 0.038 | 0.021 | 0.023 | second,12 " |

Errors are at two standard deviations; for derivation see text.
All errors are absolute, and expressed in oxide percent.



model, this is given by

$$\hat{\sigma} = \sqrt{\frac{1}{(n-2)} (y - y_i)^2}$$

Here, (n-2) is the number of degrees of freedom remaining in the data set. The problem is: how to calculate the standard deviation for a quadratic fit? To a first approximation, as the linear model reduces the degrees of freedom by 2 from n to (n-2), so the quadratic model reduces the degrees of freedom to (n-3). Standard deviations were therefore calculated for the quadratic fit by replacing (n-2) in the above equation by (n-3). The y residuals necessary to compute the standard deviation are obtained by entering the standards as unknowns in MAJOR's data deck. Values for the 95% confidence interval derived from these calculations are also presented on Table 3.

One may now optimize both the order of the curve fit and the number of standards used, by this procedure: Calculate the error terms at $x = \bar{x}$ and $x = x\text{-max}$ for both linear and quadratic regressions. However, when computing the standard deviations, write down the squares of the y residuals for each standard. After the errors are calculated, examine the lists of y residuals. If any one standard displays anomalously high values, eliminate it and rerun the program with one less standard. Repeat this process until no outstanding residuals remain; then choose the order of fit and the number of standards which yield the lowest error term.

It must be noted that preliminary graphical inspection must still be carried out; if large numbers of spurious values

are included, a wrong solution could be obtained. Also geological common sense must be used; standards should approximate the bulk chemistry of the samples. Given these caveats, however, such an optimization method based on analysis-of-variance concepts provides a more satisfactory way of handling the least-squares procedure and yielding values for error of fit.

Trace elements analyzed by X-ray fluorescence can also be analyzed satisfactorily. Trace element results are fed into the program MOLYCOMP, which calculates mass absorption coefficients for each sample and each element on the basis of the Mo Compton peak recorded for each sample. The program then adjusts the data for absorption effects, and compares all unknowns to one standard. The program is run several times against different standards, and the average of consistent results is the reported value. To assign error to the trace elements, we may consider two sources of error: counting error, and scatter of standards. Counting errors follow a simple Poisson distribution; $\sigma_c = \sqrt{N}$. Scatter of standards may be taking the relative standard deviation, or coefficient of variation, of the readings; this is constant from sample to sample. The relative counting errors for the best and worst case may also be calculated, and the square root of the sum of the squares of the errors taken as a measure of the relative error associated with the entire analysis. Results of this analysis are given in Table 4.



Table 4. Relative Errors of Trace Element Analyses by XRF.

| | Relative Error, XRF | | Relative Error, NA (Table 5) |
|---|---|---|---|
| | Min | Max | Min |
| Zr | 8.3% | 9.4% | 31% |
| Y | 43.2% | 45.7% | |
| Rb | 3.4% | 12.3% | 33% |
| Sr | 4.0% | 6.5% | |
| Zn | 6.8% | 17.4% | 25% |
| Cu | 36.5% | 38.7% | |
| Ni | 42.5% | 43.7% | 37% |
| P | 2.1% | 6.3% | |

Neutron Activation results

Neutron activation data are handled in essentially the same manner as X-ray fluorescence trace-element analyses. The raw numbers are fed into program NATRCE, which corrects for nuclide decay during the course of the run, subtracts background, compares all unknowns against one standard, normalizes rare earths to chondrite values and reports element concentration and associated error. The standard analysis is placed first in the data deck, as in MOLYCOMP; subsequent standards are treated as samples. Due to instrument drift, the standards analyzed as samples usually yield results consistently higher or lower than the accepted value. The results must therefore be corrected with an empirically derived factor, which represents an average of standard ratios (true value/calculated), casting out anomalous or poorly-known values.

Error analysis proceeds much as in X-ray trace analyses. Counting error is given by the program; a relative standard deviation of fit may be calculated from the empirical ratios. Total error is the square root of the sum of the squares of the

relative counting error and the relative fit error. These values at one standard deviation are quoted in Table 5 for those elements run for both Runs 2 and 3; values for other elements are given in Table II, Appendix. The values quoted are minima; maximum values are not generally meaningful, as many samples give negative or meaningless results.

Adjustment of Duplicate Analyses

These analytical schemes provide several sets of duplicate analyses; 1) two runs of certain samples for the long count by neutron activation; 2) two runs of silicon by X-ray fluorescence; and 3) iron run by both X-ray fluorescence and neutron activation. A single value must be adopted; therefore, the analyses must be compared and adjustments made.

Comparison of the two runs of the long neutron activation count is given in Table 5 for the seven samples affected. Results are generally in good agreement, except for Tb, where Run 2 (Batch 1) results were often too low; in these cases, the higher value was used, as determined by the best fit on the rare-earth spectrum plot (Figure 16 ). Results for Zn, Rb, Zr and Fe during Run 3 (Batch 2) were inferior and were discarded; values for all other elements were averaged. Results for trace elements analyzed by both neutron activation and X-ray fluorescence were also compared; Zn, Zr and Ni were averaged, while Rb results from neutron activation were inferior and were discarded. During averaging, the higher of the two relative errors was accepted for the final value,



Table 5. Comparison of Batch 1 and Batch 2 neutron activation results for seven samples.

| | HR-23 | | | HR-5 | | | us-28 | | | HR-22 | | | Remarks |
|---|---|---|---|---|---|---|---|---|---|---|---|---|---|
| | 1 | 2 | accept | 1 | 2 | accept | 1 | 2 | accept | 1 | 2 | accept | |
| Sb | 0.4 | 0.5 | 0.45 | 0.5 | 0.1 | 0.3 | 0.4 | 0.3 | 0.34 | 0.4 | 0.4 | 0.4 | average |
| Zn | 2.1 | (2.4) | 2.1 | 105. | 190. | 105. | 760. | 531. | 531. | 142. | 430. | 142. | Batch 1+XRF |
| Ni | 10. | -- | 10. | 15. | -- | 15. | 11. | 24. | 15.1 | 22.5 | 70. | 46. | ave.-XRF |
| Co | 2.4 | 4.4 | 3.2 | 2.2 | 3.0 | 2.5 | 12.2 | 20. | 8.7 | 26.7 | 33. | 26.3 | average |
| Cr | -- | -- | -- | -- | 2.9 | 2.9 | 6. | 6.5 | 7.3 | 95. | 69. | 82. | average |
| Sb | 26.7 | 26.7 | 26.7 | 85.0 | 95.0 | 85.0 | 58.2 | 58.2 | 58.2 | 37.7 | 45. | 37.7 | Batch 1+XRF |
| Cs | 0.5 | 0.6 | 0.55 | 1.4 | 1.7 | 1.55 | 1.7 | 1.6 | 1.65 | 1.4 | 1.7 | 1.55 | average |
| Th | 4.4 | 5.3 | 4.85 | 8.5 | 7.7 | 8.1 | 2.0 | 3.5 | 2.75 | 2.5 | 1.9 | 2.2 | average |
| Sc | 4.9 | 6.2 | 5.5 | 5.8 | 6.5 | 6.15 | 87. | 10.8 | 49. | 20.8 | 21.8 | 21.3 | average |
| Sr | 170. | 160. | 179. | 230. | 160. | 230. | 200. | 210. | 200. | 203. | 190. | 203. | Batch 1 |
| Hf | 6.3 | 5.5 | 5.9 | 7.7 | 6.6 | 7.15 | 6.2 | 6.5 | 6.35 | 5.3 | 4.3 | 5.8 | average |
| Ta | 0.89 | 1.4 | 1.04 | 1.38 | 1.7 | 1.54 | 0.82 | 1.0 | 0.91 | 0.76 | 1.1 | 0.93 | average |
| Ce | 65. | 70. | 67.5 | 56. | 40. | 48. | 50. | 42. | 50. | 49. | 43. | 46. | average |
| Eu | 1.3 | 1.6 | 1.3 | 0.8 | 0.8 | 0.8 | 1.6 | -- | 1.6 | 1.4 | 1.8 | 1.6 | average |
| Tb | 0.5 | 0.8 | 0.8 | 0.9 | 0.51 | 0.9 | -- | 0.58 | 0.58 | 0.7 | 0.88 | 0.79 | use best fit |
| " | 0.36 | 0.8 | 0.8 | 0.34 | 0.7 | 0.7 | 0.3 | 0.4 | 0.4 | 0.6 | 0.6 | 0.6 | on spectrum |
| Yb | 3.2 | 3.8 | 3.5 | 3.4 | 4.0 | 3.65 | 1.3 | 2.4 | 2.4 | 3.7 | 3.3 | 3.3 | not used |
| Fe | | 0.36 | 0.18 | | 2.4 | 2.23 | | 5.2 | 4.88 | | 9.2 | 9.49 | Batch 1+XRF |

| | HR-21 | | | HR-15 | | | US-32 | | | Errors | | |
|---|---|---|---|---|---|---|---|---|---|---|---|---|
| | 1 | 2 | accept | 1 | 2 | accept | 1 | 2 | accept | 1 | 2 | accept |
| Sb | 0.5 | 0.2 | 0.33 | 0.4 | 0.3 | 0.45 | 0.3 | 0.5 | 0.4 | 28% | 33% | 33% |
| Zn | 219. | 210. | 219. | 116. | (110.) | 116. | 95. | (50.) | 95. | 25% | 25% | 25% |
| Ni | 20. | 80. | 45. | 30. | 110. | 70. | 46. | 140. | 94. | 37% | 94% | 37% |
| Co | 22.6 | 24. | 23.3 | 26.3 | 29. | 27.6 | 54.1 | 31. | 43. | 1.8% | 48% | 4.5% |
| Cr | 61. | 59. | 75. | 83. | 68. | 75. | 220. | 144. | 182. | 12% | 4.5% | 14.6% |
| Rb | 70.6 | 80. | 70.6 | 9.10 | 15. | 9.10 | 16.1 | 20. | 16.1 | 33% | 14.6% | 14.6% |
| Cs | 3.9 | 4.2 | 4.0 | 0.7 | 0.5 | 0.6 | 0.9 | 0.7 | 0.8 | 8.1% | 33% | 33% |
| Th | 3.5 | 2.2 | 2.8 | 2.4 | 2.1 | 2.25 | 1.2 | 0.3 | 0.8 | 3.5% | 25% | 5.6% |
| Sc | 18.3 | 18.8 | 18.8 | 19.2 | 23.2 | 21.2 | 40.0 | 26.6 | 33.3 | 1.7% | 5.6% | 3.1% |
| Zr | 184. | 110. | 184. | 189. | -- | 189. | 79. | (70.) | 79. | 31% | 39% | 31% |
| Hf | 5.8 | 5.2 | 5.5 | 4.4 | 4.3 | 4.35 | (0.5) | 0.6 | 0.55 | 11.4% | 11.2% | 11.4% |
| Ta | 0.99 | 1.1 | 1.04 | 0.70 | 0.7 | 0.7 | 0.20 | (0.07) | 0.20 | 7.7% | 16.6% | 16.6% |
| Fe | 8.36 | 8.5 | 8.86 | 9.1 | 10.24 | 9.67 | 3.5 | ND | 3.5 | 2.6% | 11% | 2.6% |
| Ce | 25. | 24. | 24. | 43. | 51. | 47. | 7. | (0.7) | 7. | 3.7% | 2.9% | 3.7% |
| Eu | 1.2 | 1.6 | 1.4 | 1.3 | 1.6 | 1.45 | 0.82 | (0.4) | 0.82 | 7.7% | 14.5% | 14.5% |
| Tb | 0.4 | 0.2 | 0.4 | 0.3 | 0.73 | 0.5 | 0.5 | -- | 0.5 | 23% | 37% | 24% |
| " | -- | 0.4 | 0.4 | 0.3 | 0.5 | 0.5 | -- | -- | -- | 25% | 13% | 13% |
| Yb | -- | 2.3 | 2.3 | 3.6 | 3.0 | 3.3 | 3.5 | 2.9 | 3.5 | 22% | 31% | 31% |
| Fe | 8.36 | 8.5 | 8.43 | 9.1 | 10.24 | 9.67 | | ND | 15.16 | 2.6% | 11% | 2.6% |

and is reported in Table 5, and Table II, Appendix.

Two X-ray fluorescence runs for Si were made; one with ten-second counts in a poor vacuum, the other with one-second counts in a good vacuum. The results were treated as follows: After evaluation of the least-squares errors as detailed above, the two sets of analyses were tabulated with their 95% errors. The results were examined; those analyses of the first run that reported over 90% $SiO_2$ were discarded in favor of the more reasonable results of run 2 (HR-23, HR-13 and HR-28 were so affected). The remaining values were then averaged between the two runs. For these, the distance between the 95% intervals was calculated; that is, $D = |X_1 - X_2| - e_1 - e_2$, where $X_i$ = the value reported from run i, and $e_i$ = the 95% half-interval about $X_i$. If the D so calculated is less than zero, it is taken as zero. The final error is then: $e = \sqrt{(e_1)^2 + (e_2)^2 + D^2}$. The minimum absolute error thus found is reported in Table I, Appendix.

A similar procedure was used to reconcile the X-ray fluorescence and neutron activation values for iron. Here, samples HR-15, HR-11 and US-32 showed large discrepancies; the X-ray fluorescence value was favored for these samples. The values for the other samples affected were averaged, and the error reported as for Si. The minimum absolute error thus found is reported in Table I, Appendix.

The complete analyses of 22 samples, with error estimates and selected ratios are given in Tables I and II, Appendix.



## Modal and Normative Analysis

In order to evaluate the effects of metamorphism and alteration of the volcanic rocks of the study area, thin sections of all 62 samples were examined, noting mineralogy and texture. A modal analysis was made of each chemically analyzed sample. The analysis used a Swift electronic point counter attached to a Zeiss petrographic microscope; 500 points were used for most slides, with a few slides receiving 1000 points. By an analysis conducted by Hayslip (1973) on California volcanics, 2000 points are needed for an accurate mode; however, time did not permit this extensive a count. In addition, the discrimination of quartz and feldspars in the fine-grained groundmass, as well as pervasive sericite and carbonate encountered in a few, make accurate modes impossible to obtain. The results of the modal analysis are given in Table III, Appendix.

The modes were then used to obtain semiquantitative estimates for $CO_2$ and S. All $CO_2$ is assumed to be in calcite, while all S is in pyrite. The modal volume percents of these minerals were converted to weight percents by calculating a bulk density for the rock, using density figures for minerals from Hodgman and others, 1962), then multiplying the volume percent by the ratio of mineral density to whole-rock density. Chemical weight percent was then obtained by multiplying by the ratio of the molecular weights of $CO_2$ or S and the assumed mineral phase. These chemical percentages are listed in Table I of the Appendix. Accuracy is probably in the range of 15% for

$CO_2$ , and 60% for S. Because of the low abundance of sulfides in the samples, sulfur estimates are very poor; S is not considered in the geochemical portion of this report.

CIPW norms for the analyzed samples were calculated by using GNAP (Graphic Normative Analysis Program), written by Bowen (1971). In order to use this program, values for both $Fe_2O_3$ and FeO must be entered for each sample, whereas only total iron was determined. Fortunately, however, the analys s from Agricola Lake (Cameron and Durham, 1974) report both oxides. Therefore, each sample was compared to the Agricola Lake samples, using criteria of silica content, alteration patterns and general geochemistry, The $Fe^{III}/Fe^{II}$ ratios which were reported for those samples most like the presently-analyzed samples were then taken for the present study, and appropriate values of $Fe_2O_3$ and FeO calculated. The program was run both with and without the inclusion of $CO_2$ and S in the analysis; two norms are not computable with $CO_2$ present due to inadequate amounts of Ca. The norm for HR-28 could not be computed, as no CaO, MgO or FeO was detected. The norms as calculated are presented in Table IV, Appendix.

## DESCRIPTIVE GEOCHEMISTRY

### Evaluation of the Effects of Alteration and Metamorphism

Before viewing the results of the analytical procedures detailed above, it is important to consider the effects of alteration processes and metamorphism on rock chemistry. In particular, is it possible to identify altered samples with combined petrographic and chemical data?

Four alteration processes occur frequently in Archean volcanic sequences: silicification, carbonation, chloritization and sericitization. A fifth, serpentinization, applies only to ultramafic rocks and is not encountered in the study area. Spilitization is apparently rare in the Archean, and is not suggested by the data for Hackett River. Weathering is avoided by the choice of unweathered sample during crushing.

Silicification is especially important in felsic volcanics, identified by abundant quartz veins, removal of ferromagnesian components and frequent chert horizons (see Viljoen and Viljoen, 1969). Petrographically, altered rocks are distinguished by high quartz contents, absence of ferromagnesian minerals and quartz veining. In chemical analysis, such rocks have $SiO_2$ contents greater than 80%, with nearly complete removal of MgO, severe depletion of Fe, and low $Al_2O_3/SiO_2$ ratios (Figures 9c,9d, 11). Some silicified rocks are accompanied by sericitization, leading to a wide range of $K_2O$ contents and K/Na ratios (Figure 9g). In practice, analyses reporting greater than 80% silica were set aside. Although some natural rhyolites may exceed 80% $SiO_2$, they are few; all of the affected samples show

petrographic signs of alteration as well. All of the high-silica samples described here come from the two rhyolite units in the D'Arcy Lake area. Evidently silicification was widespread within certain stratigraphic units. Similar rocks are also found at Agricola Lake (Cameron and Durham, 1974).

Carbonation is frequent in Archean mafic and intermediate rocks, but is also present in felsites (Viljoen and Viljoen, 1969). The process is marked by pervasive replacement of silicates with calcite, often with accompanying quartz and sericite. Carbonation favors finer-grained rocks and those of low metamorphic grade, being rare in rocks of epidote-amphibolite and higher facies (Viljoen and Viljoen, 1969). Viljoen and Viljoen (1969) report the effects of carbonation to be: increase in FeO, $CO_2$, $Na_2O$ (slight), $TiO_2$, $H_2O$ and total Fe, with small decreases in other elements. In this study, rocks with a modal estimate of $CO_2$ greater than 2% were set aside. So affected are all samples of the Back River complex (RL-series); the fine grain size and low metamorphic grace of these rocks confirms theory. Of the carbonated rocks in this study, three behave coherently, with loss of $TiO_2$, total Fe and possible gain in CaO indicated (Figure 9); the fourth, RL-2, has unique features discussed later. Unfortunately, there are no unaltered samples of the Back River volcanics available to confirm the alteration origin of the variations noted above.

Chloritization is a brief name for a complex phenomenon, involving possible addition of Fe and Mg, and loss of Ca and



Na, often associated with the footwall of massive sulfide deposits. Petrographically, the process involves formation of hydrous iron-magnesium minerals such as chlorite at the expense of feldspar. Cameron (1974) and Cameron and Durham (1974) use the ratio (Fe+Mg)/(Ca+Na) to detect this alteration; anomalously high values (over 5 to 10) indicate alteration. Although such alteration is found in the Agricola Lake area (Cameron and Durham, 1974), none of the 22 analyzed samples show any chlorite anomaly.

Sericitization is often observed in Archean volcanics of all compositions. The process is not well-defined chemically, but must involve an addition of water and a redistribution or addition of K. As K is one of the most mobile elements in the geochemical system, it would be difficult to separate by chemical means those samples which have been especially affected. Petrographically it is found that with the exception of fractures, which are culled during crushing, extensive sericitization is generally found only with silicification or carbonation. Therefore no samples were set aside solely on the basis of sericite development.

It is possible, however, to estimate the mobility of K in the geochemical system. A K variation diagram (Figure 9g) shows a rough increase of $K_2O$ with silica with large scatter, and several anomalous samples. A line may be drawn through visually-estimated"normal" values, and residuals calculated at any $SiO_2$ value; these residuals yield a rough estimate of K enrichment or depletion, assuming that the samples form a

homogeneous, smoothly-varying population. High residuals should indicate cases of exceptional K mobility. Ignoring the high-silica samples, HR-21 and HR-2 show K enrichment, and US-26 and US-4 show K depletion.

The K residuals show a correlation of +0.54 with K/Na (Figure 7), once high-silica samples are eliminated. The significance of this correlation may be questioned, as K appears on both axes. However, Pearson's coefficient of v variation for potassium is calculated to be 0.62 for 18 points; according to Chayes (1975), spurious correlation for variable pairs of the sort X vs. X/Y rapidly approaches zero with small variance as the Pearson's coefficient increases past 0.50. Therefore, the graphs should approximate the true situation. The positive correlation indicates that K is more mobile than Na in the geochemical system at Hackett River; it is enriched faster than Na, and depleted faster. A similar plot of K residuals vs. K/Rb shows a much less well-defined trend (Figure 8). This analysis assumes that K, Rb and Na behave sympathetically during alteration, that is, they respond similarly to the same processes.

A further check on the effects of sericitization is the comparison of samples HR-21 and HR-22. Although these samples were taken from the same stratigraphic level only a few hundred meters apart, sample HR-21 has been enriched in K relative to HR-22. Effects of alteration, assuming the original chemistry to have been similar, are summarized on Table 6. In brief, all alkali elements including Sr and Ba increase, whereas



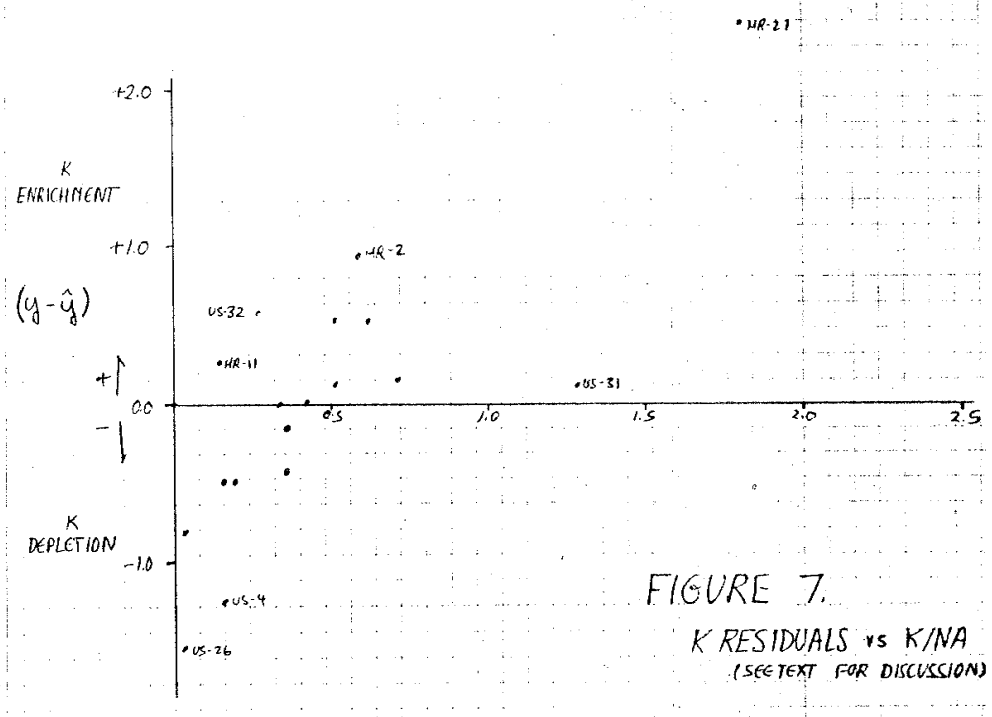


FIGURE 7.

K RESIDUALS vs K/NA

(SEE TEXT FOR DISCUSSION)

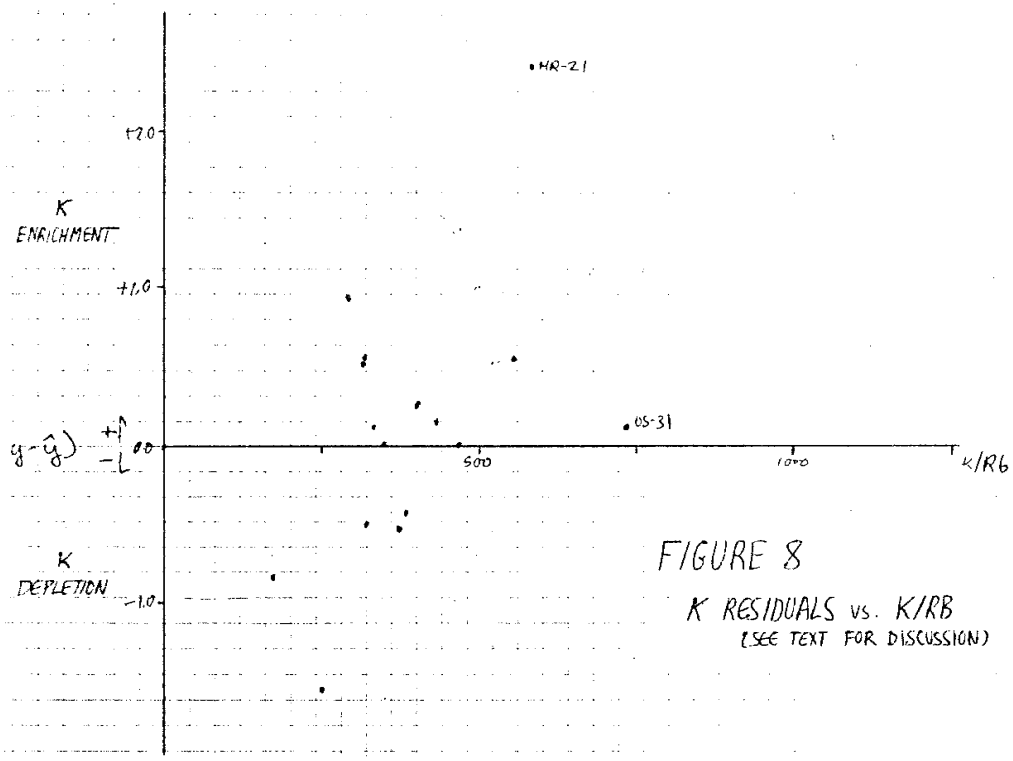


FIGURE 8

K RESIDUALS vs. K/RB
(SEE TEXT FOR DISCUSSION)



Table 6. Changes in Major and Trace Elements with Sericitization.

| Increase | Decrease | Unchanged |
|---|---|---|
| K | Na | Si |
| K/Na | Ca | Total Fe |
| Rb | Sc? | Mg |
| Cs | REE | P |
| Sr | (exc. Eu) | Mn |
| Ba | La/Yb | Co |
| Th? | | Cr |
| K/Rb | | Cu? |
| Rb/Sr | | Ni? |
| Ti | | Sb? |
| Al | | Y |
| Al/Si | | Zr? |
| Zn | | Hf |
| Eu/Eu* | | Ta |
| | | Zr/Y |
| | | Eu |

Data estimated from changes between samples HR-21 and HR-22.

transition metals (except Zn) and immobile elements (Y,Zr,Hf) remain unchanged, and rare-earth elements decrease, except for Eu. The best explanation for this behavior appears to be the replacement of plagioclase by orthoclase in the sample, as well as additional feldspar replacing other minerals. By this means, overall REE would be depleted, and a positive Eu anomaly created. Increases in Sr and Ba would then be related to their capturing by the feldspar. Sericite would then result from the alteration of the introduced orthoclase.

To sum up the results of this alteration study: Of 22 samples analyzed, four were found to be silicified beyond acceptable limits; four have been subjected to intense carbonation; and four have experienced much K mobilization.

The question of metamorphic effects on rock chemistry does not yet have a complete answer. No opportunity presented

itself during this study to sample one unit across a metamorphic gradient, or otherwise test for metamorphic effects. Two studies from other areas seem relevant to the question. Field and Elliott (1974) looked at progressive metamorphism of gabbro to amphibolite by studying inclusions within the amphibolite. Relative to the elements considered here, they found increase in $K_2O$, $P_2O_5$, Rb, Sr(occasionally), and decrease in Ca, Zn and sometimes Sr. La, Y, Co, Cu, Sc, Mg, Ni and Na remained unchanged. Engel and Engel (1962) examined progressive metamorphism of quartzofeldspathic gneiss and amphibolite from amphibolite to granulite facies. Significant increases were found in CaO, MgO, $Al_2O_3$, Fe and Cr; decreases in $K_2O$ and Cu; and no change in Yb, Ba, Zr, Y, Sr, Sc, Ni and Co.

These studies do not prove a case; nonetheless, they are signs that, although major elements and alkali elements may be mobile during metamorphism, other trace elements, including the rare earth elements, Zr, Y and Co remain unchanged to reflect original magmatic processes of melting and differentiation.

## Variation Diagrams

Diagrams showing the variation of the major elements with respect to $SiO_2$ are presented in Figure 9(a-g). The salient features are:

1) $TiO_2$ shows a poor trend, with basaltic samples plotting below the main curve; $TiO_2$ ranges near 1% in most samples. This pattern is generally similar to that observed from Talasea (see Carmichael, Turner and Verhoogen,1974, p. 540).



Figure 9-- Variation diagrams of major element oxides versus $SiO_2$. Black ellipses are errors at two standard deviation (see text). Dots = samples; crosses = altered samples (carbonated or silicified), "'K" = potassium-enriched samples. Sample numbers given for distinctive or anomalous samples on each diagram.

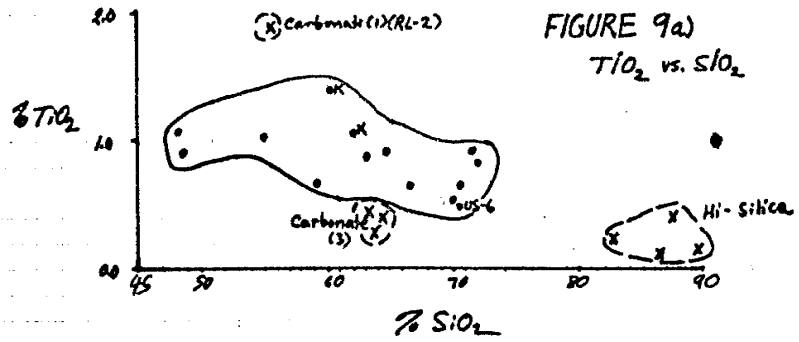


FIGURE 9a)

$TiO_2$ vs. $SiO_2$

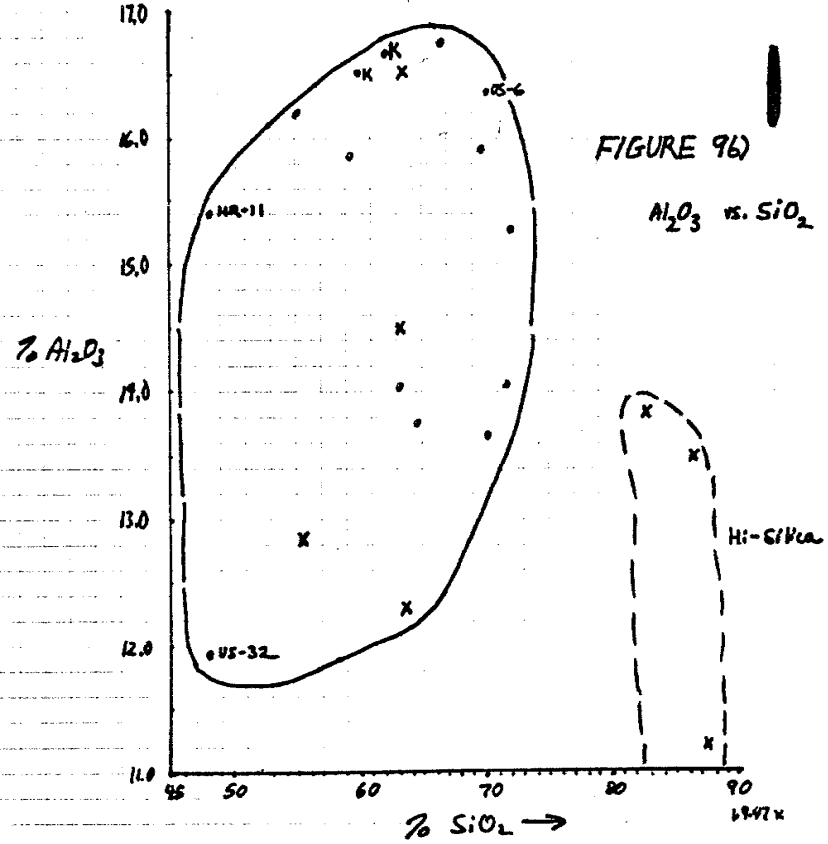


FIGURE 9b)

$Al_2O_3$ vs. $SiO_2$



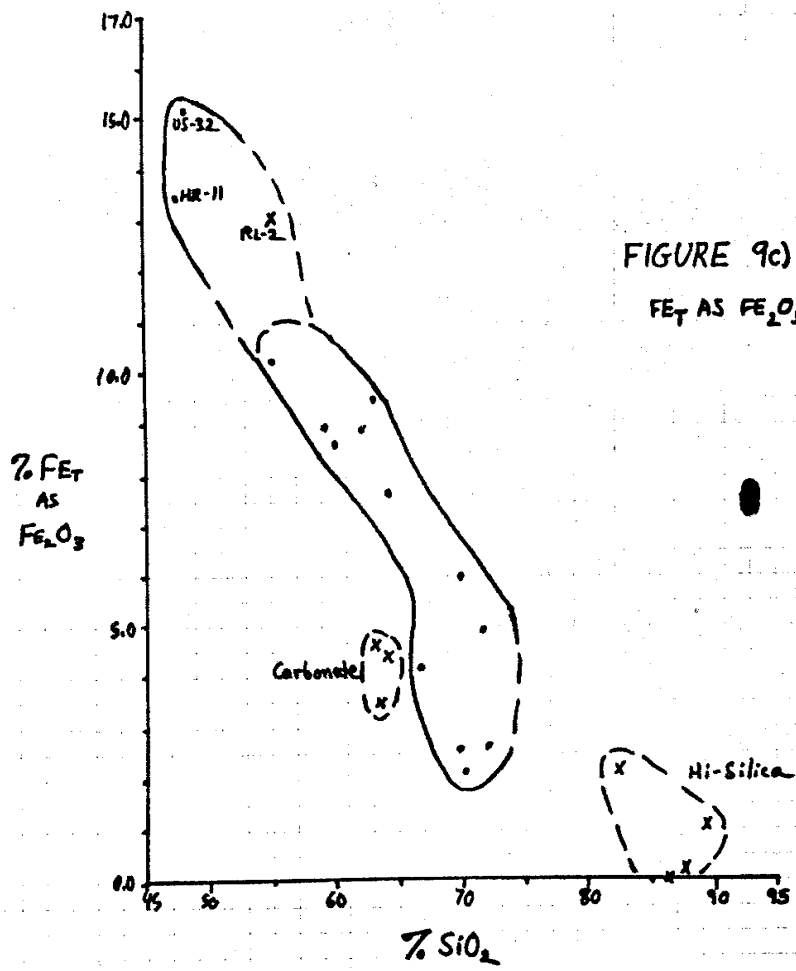


FIGURE 9c)

$FE_T$ AS $FE_2O_3$ VS $SiO_2$

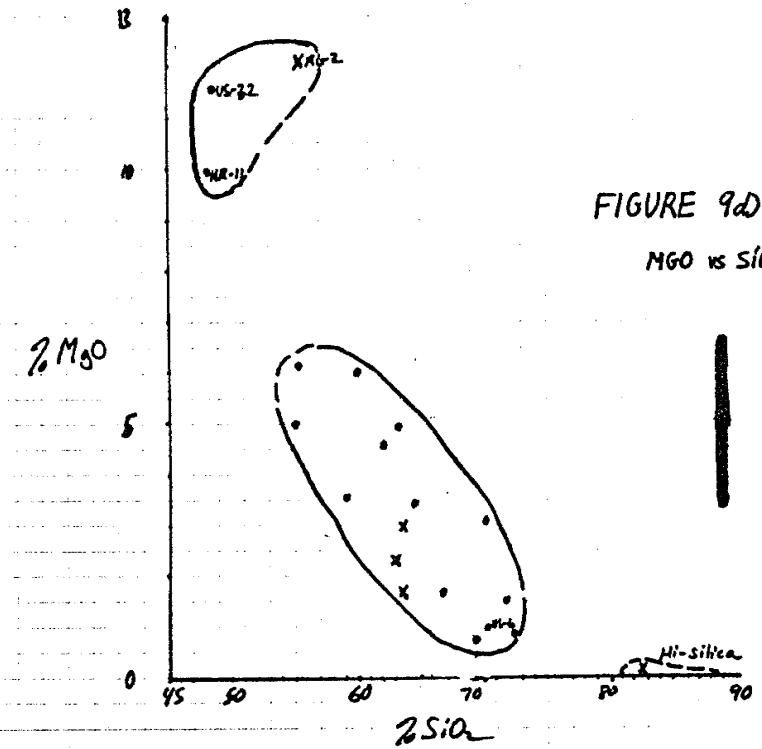


FIGURE 9d

MGO vs $SiO_2$



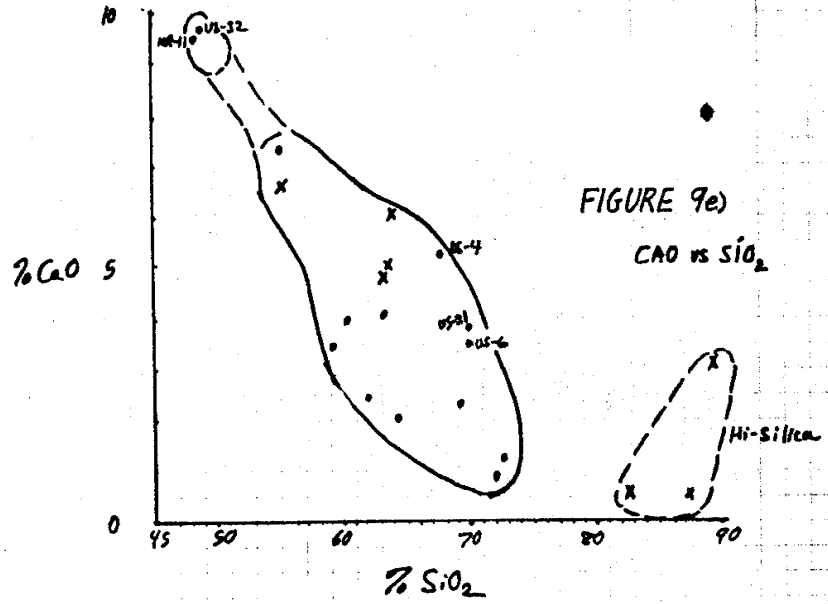


FIGURE 9e)

CAO vs $SiO_2$

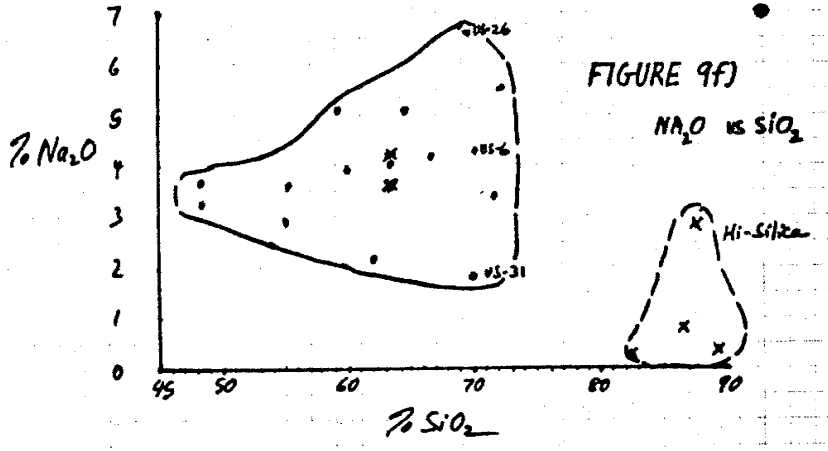


FIGURE 9f)

$NA_2O$ vs $SiO_2$

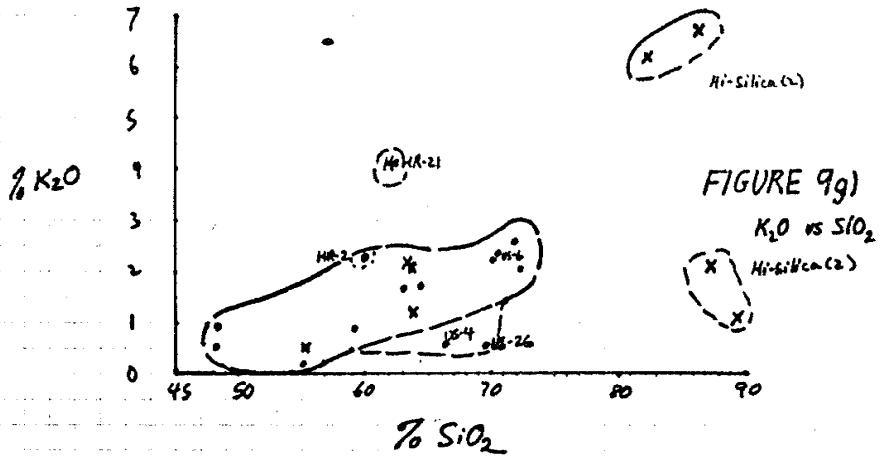


FIGURE 9g)
$K_2O$ vs $SiO_2$

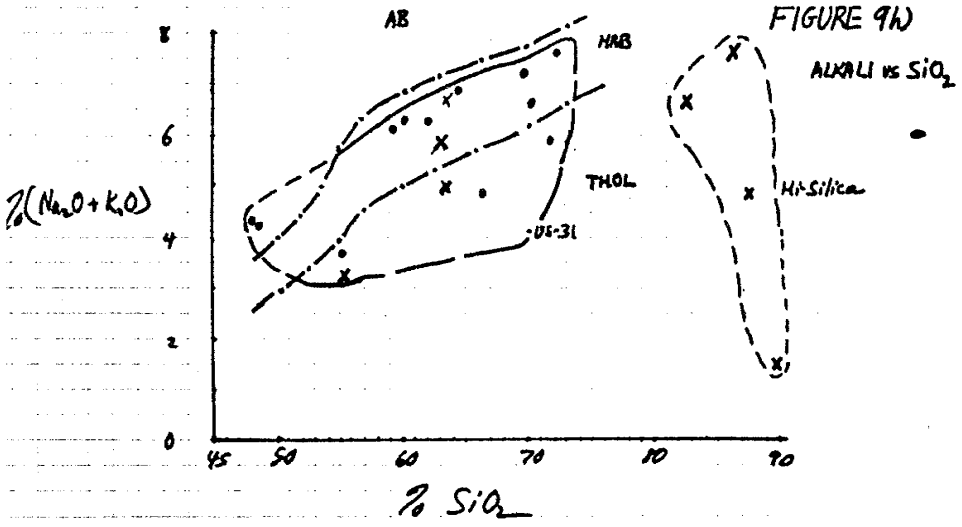


FIGURE 9h)
ALKALI vs $SiO_2$



2) $Al_2O_3$ exhibits a large scatter, with little apparent trend; Alumina is always here than 17%, but in US-32 is less than 12%.

3) Total iron shows a clear trend; three samples (HR-11, US-32 and RL-2) show marked iron enrichment. These same samples display an even more marked Mg enrichment (Figure 9d), setting them apart from the main sequence of samples with less than 7% MgO. This effect is shown best on a plot of MgO vs. FeT.(Figure 12).

4) HR-11 and US-32 also show a clear CaO enrichment, although it falls in line with the main variation. The variation diagram is poorly defined, with several samples (US-6, US-31 and US-4) showing notable CaO enrichment.

5) $Na_2O$ does not define a trend, but shows large scatter. $K_2O$ variation was described in the previous section.

In another silica-based plot (Figure 9h), the value ($Na_2O$ + $K_2O$) may be plotted against $SiO_2$. This may then be compared to the boundaries proposed by Kuno (1966) between tholeiitic, high-alumina and alkali rock series. Hackett River samples fall within the high-alumina basalt field; low Al contents, however, suggest tholeiitic affinities. The mobility of alkali in the system renders further speculation along this line suspect.

The variation characteristics mentioned above indicate a calc-alkaline trend of differentiation. The AFM diagram of the samples (Figure 10) confirms this; it coincides with the diagram of Agricola Lake analyses (Cameron and Durham, 1974).

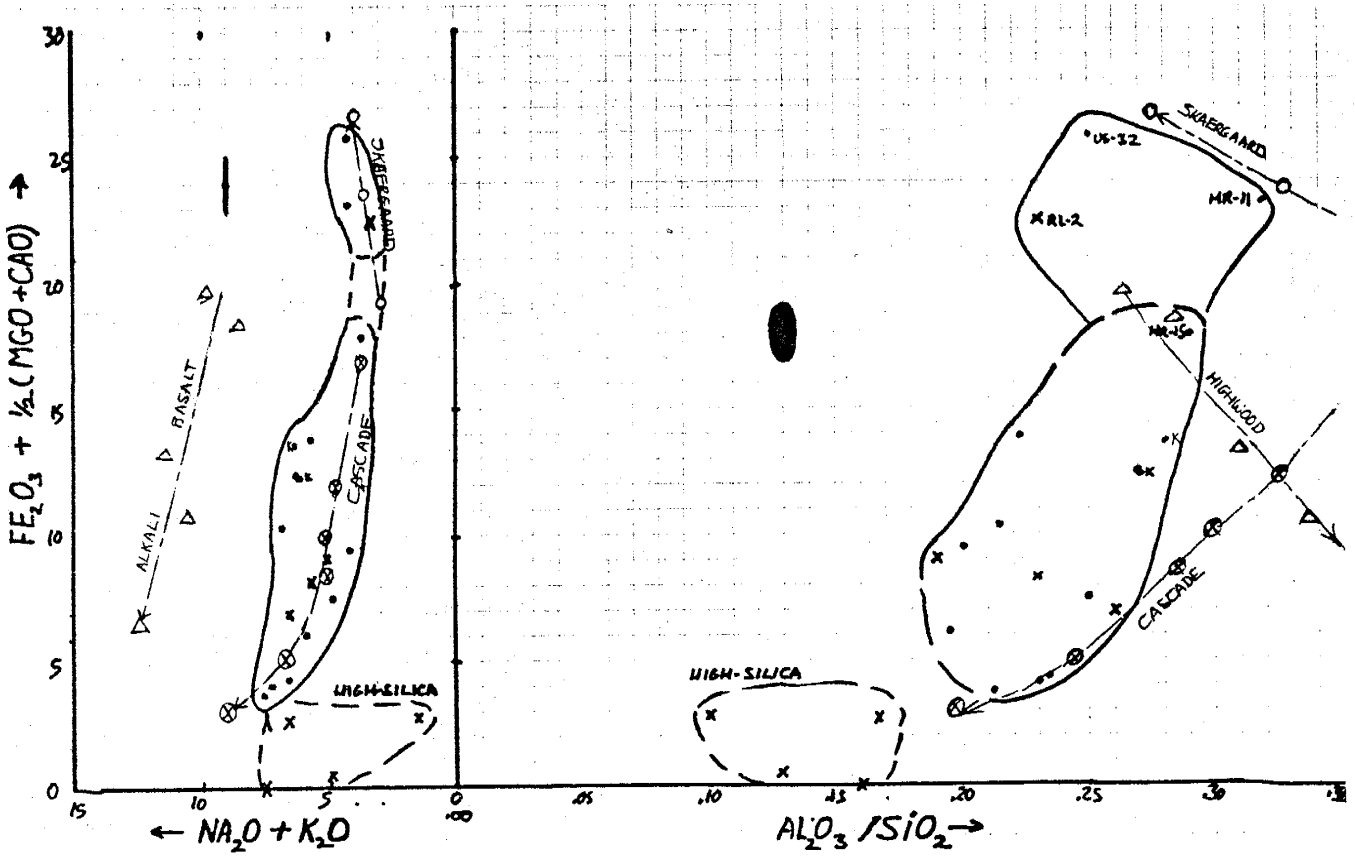


FIGURE 11. CHURCH DIAGRAM (AFTER CHURCH, 1975)

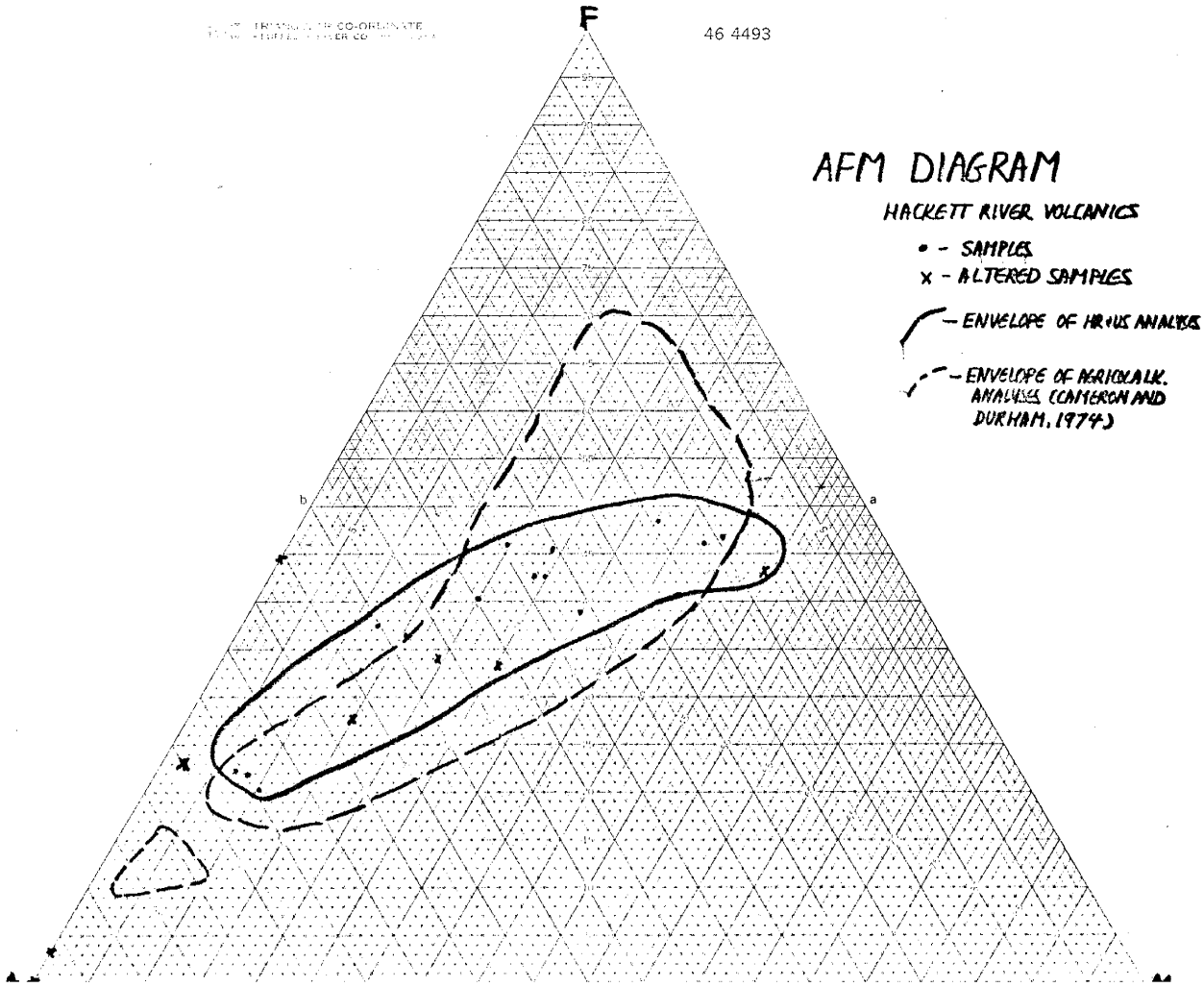

FIGURE 12. MGO vs. $FE_T$

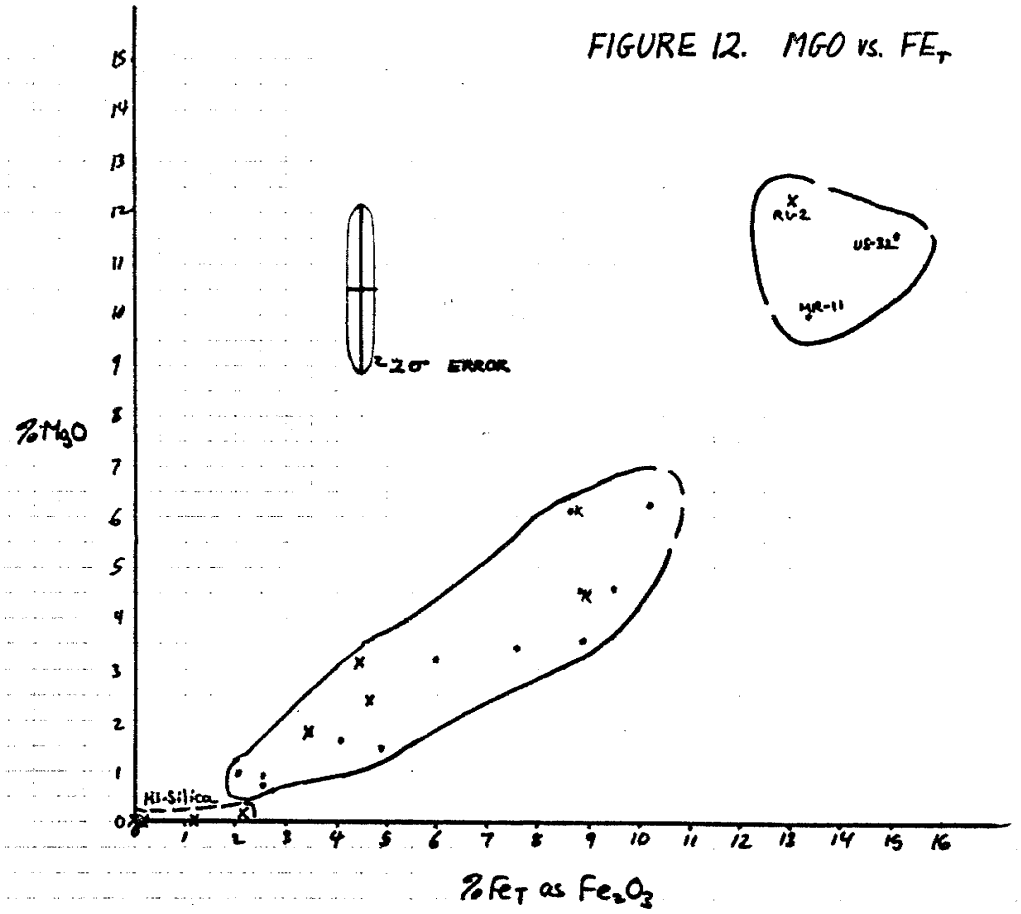




A diagram after Church (1975) of basicity index ($Fe_T + \frac{1}{2}(MgO+CaO)$) versus both total alkali and $Al_2O_3/SiO_2$ (Figure 11) reveals trends similar to the Cascade volcanic suite, but with consistently lower values of $Al_2O_3$ and higher basicity indices in the intermediate and mafic samples. The plot of $Fe_T$ vs. MgO (Figure 12) shows a well-defined variation falling well within the limits of the "primitive (Archean) calcalkaline suite" defined by Jolly (1975) in the Abitibi area. However, this is true only for the intermediate to felsic rocks; the mafic samples display a MgO and $Fe_T$ enrichment more akin to Abitibi komatiites. Further consideration of these matters, and comparisons with other studies, will be made in a later section.

## Correlation Coefficients

The same sort of information as that contained in variation diagrams may be expressed in a briefer manner by using tabulated linear correlation coefficients between the elements. A program STATS was written, using the subroutines BECORI and UERTST from the International Mathematical and Statistical Library. Additional subroutines were added to turn pages after groups of twenty samples during the sample printout, and to break up large charts of correlation coefficients into page-size units.

The major-element results for the analyses reported here, as well as those for the Agricola Lake area (Cameron and Durham, 1974) are shown in Figure 13. The charts are in good agreement, generally higher values for Hackett River samples being due to the lesser number of analyses. Some differences:

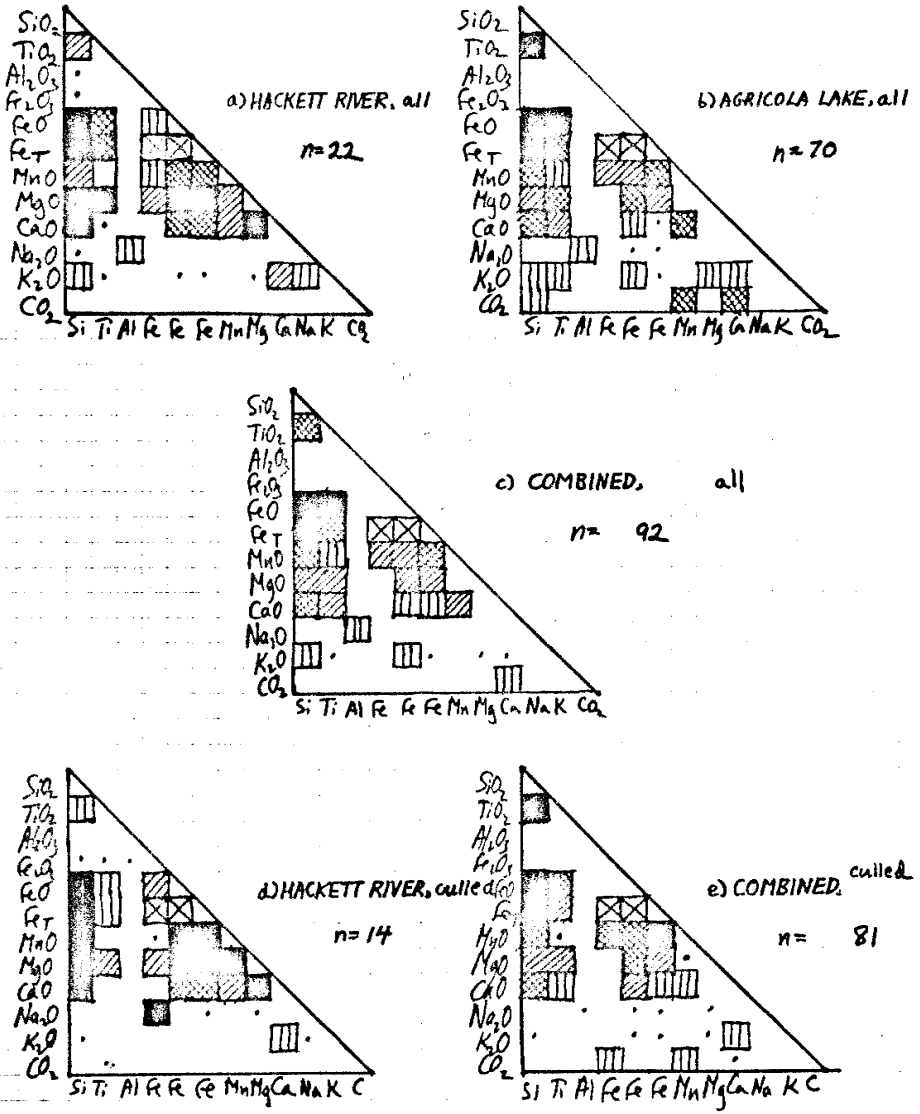


FIGURE 13. MAJOR ELEMENT CORRELATION DIAGRAMS

SEE FIG. 14 FOR LEGEND.



1) Hackett River samples give $Fe_2O_3$ correlations; this is due to the arbitrary splitting of the total iron results into ferric and ferrous oxides, and should be ignored.

2) Correlations with CaO are weak in the Agricola Lake samples. This can be explained by the presence of large numbers of samples with high $CO_2$ contents; the occurrence of calcite "ties up" the Ca, thereby reducing its variation with the other elements.

Combining the results into one diagram (Figure 13c) does not significantly reduce the coefficients. If the combined results are culled of silicified and carbonated samples, the patterns likewise do not change substantially, except for CaO, which loses some correlation with $TiO_2$ and MnO. If these results are compared with the correspondingly culled Hackett River results, two differences are noted:

1) A strong correlation between $Na_2O$ and $Fe_2O_3$ appears in the culled Hackett River diagram. This is almost certainly spurious, as discussed above, due to the splitting of iron.

2) A strong positive correlation between MgO and CaO is noted for the Hackett River samples, but is absent from the Agricola Lake samples. This may be due to the presence of chloritization in the Agricola Lake area, which enriches Mg while leaching Ca, thereby scattering the correlation. This could be tested by rerunning the Agricola Lake samples, removing samples with high chlorite ratios as defined above, then comparing.

In general, however, the agreement is good. In particular,

the identification of groups of covarying elements remains constant. This agreement serves as a check on the consistency of the Hackett River results and those from Agricola Lake, thereby suggesting that the conclusions which can be drawn from the samples discussed here are valid for the entire Hackett River volcanic sequence.

The best-defined group of elements is composed of those elements varying antipathetically to $SiO_2$: FeO, MgO, CaO, $TiO_2$ and MnO. This group is internally coherent, with special affinity between FeO, MgO and MnO. On the other hand, $Al_2O_3$ shows no correlations, as the variation diagram suggested; $K_2O$ and $Na_2O$ show poor correlation, both with each other and with the other oxides--testimony to the mobility of the alkali elements.

This approach, which ties together large amounts of data on numbers of elements, promises to provide a useful survey of trace-element patterns as well. Two correlation diagrams, one representing all analyses, the other representing analyses culled of high-silica and high-carbonate samples, are presented in Figure 14, a and b. Those elements analyzed by neutron actigation only have a smaller sample size (n=11,unculled) than the others (n=22, unculled); to run both at one sample size would induce misleading correlations. Consequently, two runs were made to produce each diagram, one with the larger sample size, the other with the smaller. The two were then combined into one diagram, the elements analyzed by neutron activation only being marked by asterisks in the Figures.



FIGURE 14a.

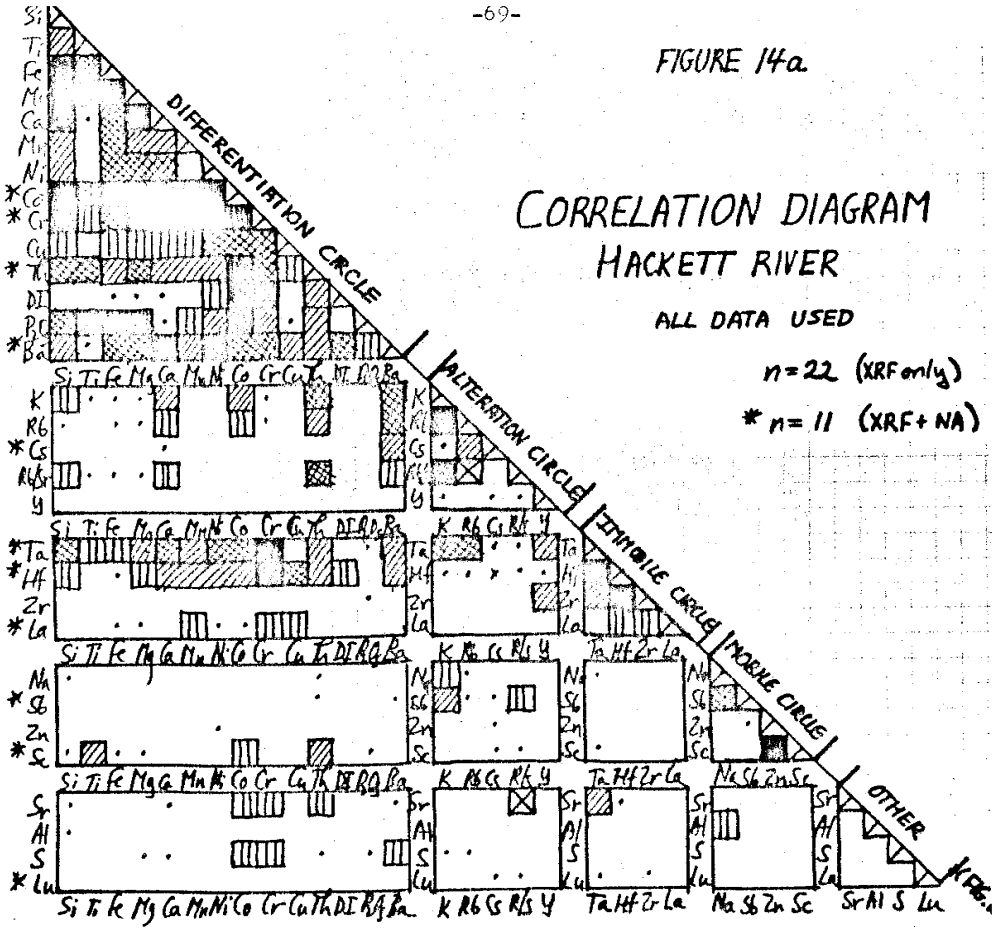


LEGEND FOR FIGS. 13 + 14:

- ■ – Correlation >80%
- ▩ – Correlation 70-80%
- ▨ – Correlation 60-70%
- ▥ – Correlation 50-60%
- ⊡ – Correlation 40-50%
- ⊠ – Not Applicable

*-Analyzed by Neutron Activation; sample size is smaller for these elements

FIGURE 146

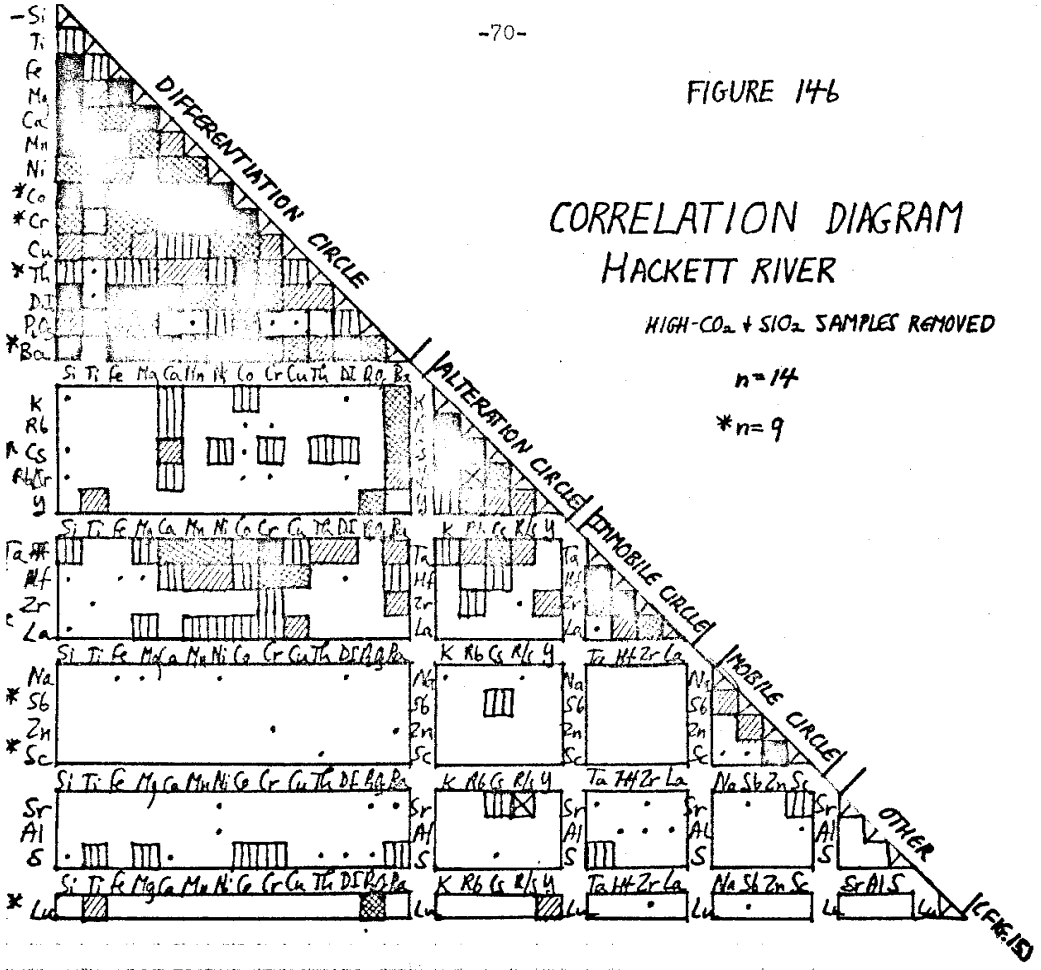




The diagrams are broken up into blocks defined by groups of covarying elements, as labelled along the diagonal in reference to Figure 15.

The strongly correlated group of elements mentioned above are now clustered in the upper-left-hand corner of each diagram. Within this main cluster are: $-SiO_2$, $Fe_T$, MgO, CaO, Mn, Ni, Co, Cr, -(Differentiation Index, normative), and-Ba; Cu, Th and P show strong correlation with some of these elements, while Ta, Hf and La correlate less strongly. (Negative listings indicate antipathetic variation with the remainder of the group.) This cluster comprises those elements and trends classically sought on variation diagrams, here dominated by the ferromagnesian elements which decrease in abundance during calc-alkaline differentiation processes. This group of elements can therefore be called the "Differentiation Circle" (Figure 15).

Two clusters of smaller magnitude can also be discerned. One such is defined by K, Rb and Cs, which show strong affinity; Ba also shows attachment to this group. Additional associates are: Rb/Sr, Ta and Y (but not Lu). Ca, Co and Th show some preference for this group as well. This group seems to be related to alteration processes, as discussed above for K; the cluster may therefore be called the "Alteration Circle". Another cluster is formed by $Na_2O$, Sb, Zn and Sc; it appears in the culled diagram only, suggesting a critical dependence on the absence of carbonate or silica alteration. Because of the demonstrated scatter of $Na_2O$, this can be called the "Mobile Circle".

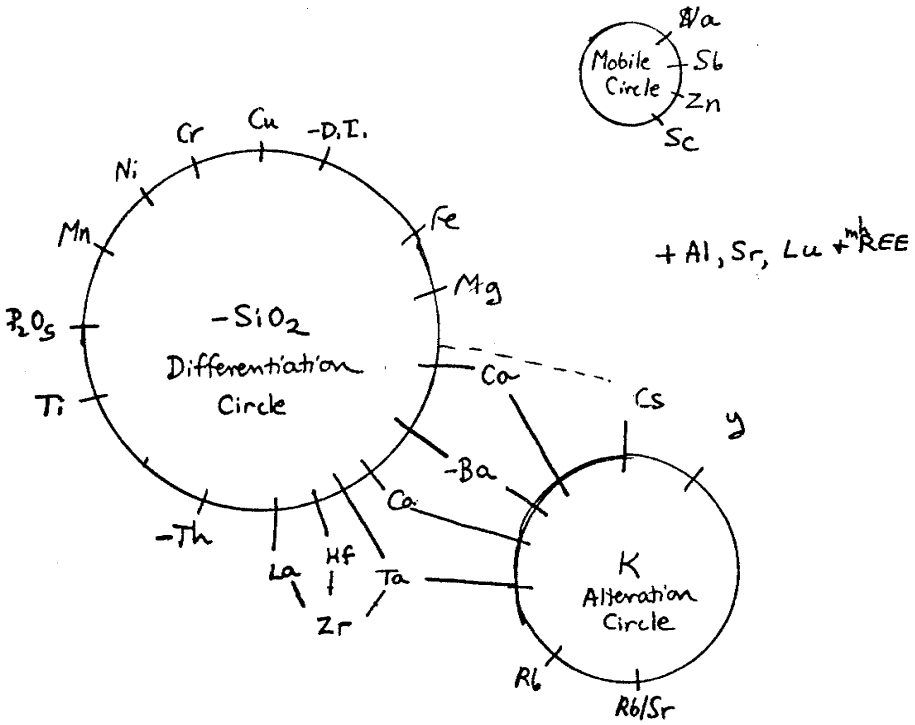


Figure 15. Schematic diagram of correlation clusters, Hackett River analyses.



Some notes on particular elements are in order:

1) Sr shows a lack of significant correlations with any group in the absence of carbonate. Sr associates with the Differentiation Circle when carbonate is present (Figure 14a). Absence of correlation implies either i) erratic mobility, due to leaching or alteration, or ii) variations inherited from processes of magma generation mask the normal correlation with differentiation. Sr has low correlation with the Alteration or Mobile Circles; its variations may therefore represent inherited differences which could "fingerprint" different groups of magmas in the sequence.

2) Ba and Ta show strong correlation to both the Differentiation and Alteration Circles. This indicates that Ba and Ta concentrations are functions of both; that is, reflect both magmatic and alteration processes. Th shows a similar but weaker dual correlation.

3) Trace transition metals generally follow Fe, Mg and Mn, as is expected. Zn, however, shows unpredictable behavior, being associated only with Sc, Sb and indirectly Na in the Mobile Circle. The common factor for these elements' variations is obscure, but may relate to sulfide phases. Cu, however, follows the Differentiation Circle strongly.

4) The behavior of Lu and Y is uncertain. They show only a fair correlation with each other; and, although they behave alike with respect to Ti, P and Zr, they differ in respect to the Alteration Circle, which Y follows while Lu does not. Either Y is subject to alteration, or the high analytical error of Y has created a spurious correlation in this direction.

5) Aluminum is essentially uncorrelated. As with Sr, this may indicate either erratic mobility or masking by inherited characteristics. The latter is preferred, based on the known geochemistry of Al and the observed variation between rock types.

6) Rare earth elements do not show extensive correlations. La correlates fairly well with the Differentiation Circle, especially the transition metals, Hf and Zr. Lu correlates fairly with Y, Ti and P. Within the series (not shown), correlations are good only between adjacent rare-earth elements. The entire series, then, is subject to the same alternatives as mentioned above for Sr and Al; either mobility or inheritance. The latter is again preferred, based on known stability of rare-earth patterns during weathering and alteration, and the established variation with magmatic history.

7) The contrasting behavior of K and Na is striking; whereas K, Rb and Cs form a coherent group, Na correlates only marginally. Na is highly uncorrelated, leading once again to the same alternatives. Na, however, is known to be affected by various alteration processes, such as spilitization and palagonitization, which are not yet well-studied in the Archean. Therefore, Na is considered to vary in response to ill-defined alteration processes unrelated to the Alteration Circle.

8) There are notable differences between the culled and unculled diagrams, which reflect on alteration processes. Ti is poorly correlated in the unculled samples; this may reflect a sharp reduction in Ti contents during silicification and



carbonation. This corresponds to the breakdown of ilmenite and the formation of leucoxene, presumably with extensive Ti loss (Viljoen and Viljoen, 1969). Other correlations appear in the unculled diagram, and are presumably related to alteration: Na with Al and K; Sc with Ti, Fe, Co and Th; Y with Ta, Co and Th; and Ca with K and Rb. On the other hand, some correlations disappear with the addition of carbonated and silicified samples: Y with Lu, K, Rb and Cs, Zn with Sb, and Cs with Ca, Ni, Cr, Th and D.I.

9) Zr is well-correlated with Hf and Ta, but not with any others of the Differentiation Circle. This may be due in part to the large error associated with Zr analyses, but may also indicate a subcircle of Hf, Zr and Ta within the larger cluster.

The relationships of the various major and trace elements in the Hackett River volcanic sequence are illustrated in Figure 15. Most elements correlate with the Differentiation Circle, representing magmatic processes. Alkali and related elements form a separate Alteration Circle, reflecting later redistribution of these elements. A Mobile Circle relates to obscure alteration processes unrelated to the alkali elements. Finally, Al, Sr and the rare earths show the imprint of magmatic processes apart from differentiation, indicating that the volcanic sequence is not a continuous population.

There are three basic limitations in this approach. The first is the restriction of the coefficients to <u>linear</u> correlation. If, foe example, the concentration of a given

element increases with differentiation up to a point, then decreases, the correlation coefficient would be low, although an important relationship does exist. This effect, however, should decrease and not increase the coefficients.

A second limi ation derives from the statistical nature of correlation coefficients. The coefficients measure the scatter of the data points; they can therefore be profoundly influ enced by extreme values, and masked by competing processes. The former may explain, at least in part, the strong correlation between Zn and Sc.

The third limitation is even more fundamental. Variation diagrams and correlation coefficients alike assume that the samples are taken from a single population, or cogenetic sequence of volcanics, that can (in principle) be accurately measured by statistics. Given the large area sampled, absolute homogeneity cannot be obtained. On the other hand, the presence of strong correlations indicate that some degree of homogeneity does exist. The lack of correlation of Al, Sr and rare earths indicate that genetic masking may be taking place--that the population is not homogeneous. The question is: Can the analyzed samples be divided into distinct subgroups?

## Rare Earth Element Distributions

To answer this question, we can turn to the "fingerprint" elements mentioned above, those whose variation may be characteristic of magmatic origins. Preeminent among these are the rare-earth elements (REE). The basic theory of REE analysis is



presented by Haskin and others (1966); application to the problems of tectonic setting and magmatic history have followed (see, for example, Jakes and Gill (1970) on arc th oleiites, Schilling (1969) on Red Sea tholeiites, and Condie (1976) on Archean volcanics). In brief, REE spectra, formed by plotting element abundances (normalized by comparison to abundances in chondritic meteorites to neutralize the odd/even effect of nucleosynthesis) against atomic weight, can be used as a "fingerprint" to identify igneous rocks formed by distinct magmatic processes. Individual features can be related to the presence of absence of specific mineral phases during melting or crystallization of a magma. Such spectra can then be used to distinguish distinct genetic types, and, perhaps, tectonic setting.

The rare-earth spectra for eleven Hackett River samples are shown in Figures 16a-d, using chondrite values from Haskin and others (1968). On the basis of these spectra, with supporting characteristics in trace- and major-element chemistry, five subgroups of samples can be distinghished:

1) Depleted Archean Tholeiite (DATH)--represented by sample US-32. The REE spectrum for this sample is slightly depleted in light REE, but otherwise flat, and correlates with Condie's (1976) DAT category. As mentioned above, this sample is an iron and magnesium-enriched basalt, with relatively low alkali element concentrations.

2) Enriched Archean Tholeiite (EATH)--represented by sample HR-11. This sample is similar in major-element chemistry to

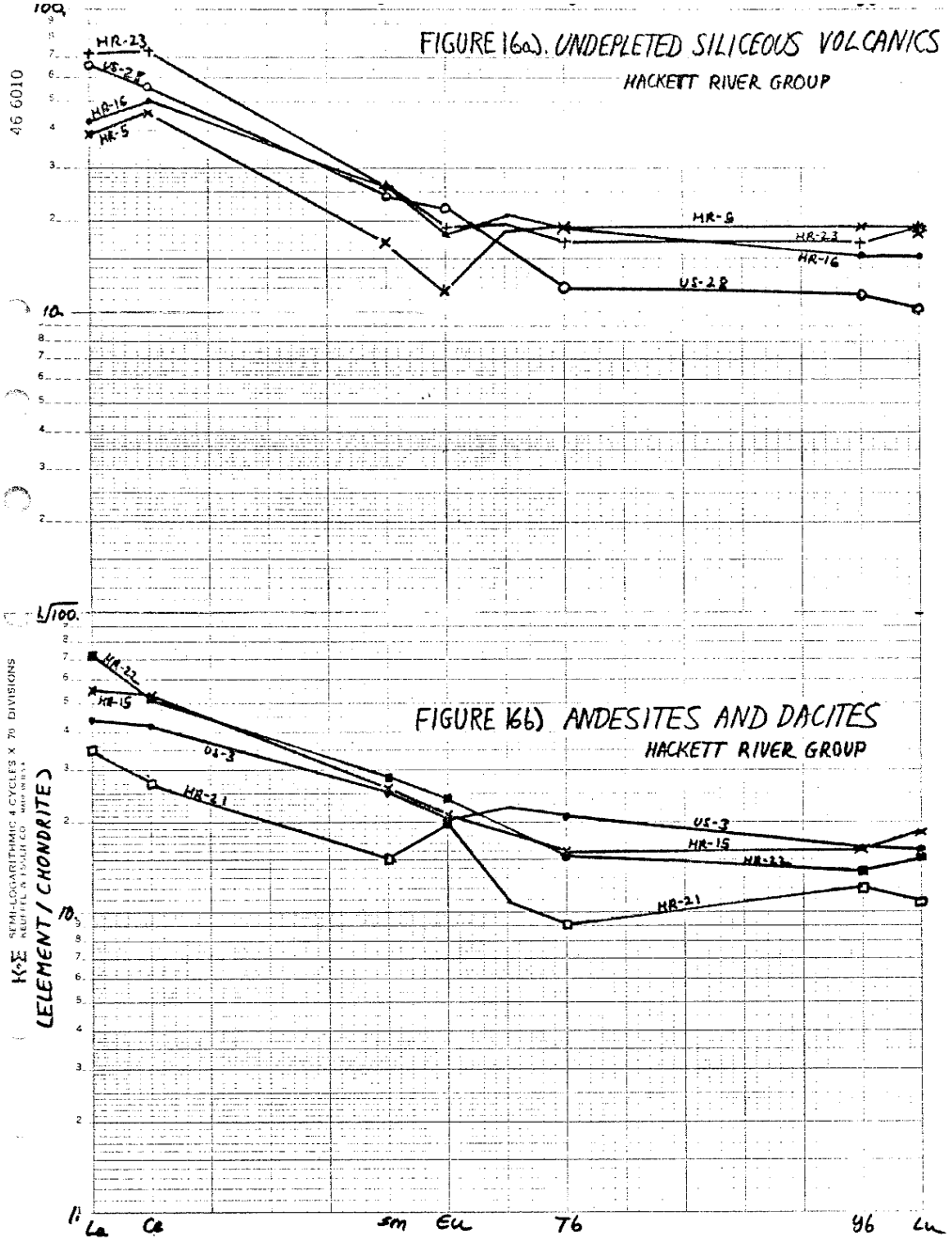
FIGURE 16a). UNDEPLETED SILICEOUS VOLCANICS
HACKETT RIVER GROUP
HR-23
US-28
HR-16
HR-5
HR-5
HR-23
HR-16
US-28
46 6010
La Ce Sm Eu Tb Yb Lu


FIGURE 16b) ANDESITES AND DACITES
HACKETT RIVER GROUP
HR-22
HR-15
US-3
HR-21
US-3
HR-15
HR-22
HR-21
SEMI-LOGARITHMIC 4 CYCLES X 70 DIVISIONS
KEUFFEL & ESSER CO.
(ELEMENT / CHONDRITE)
La Ce Sm Eu Tb Yb Lu

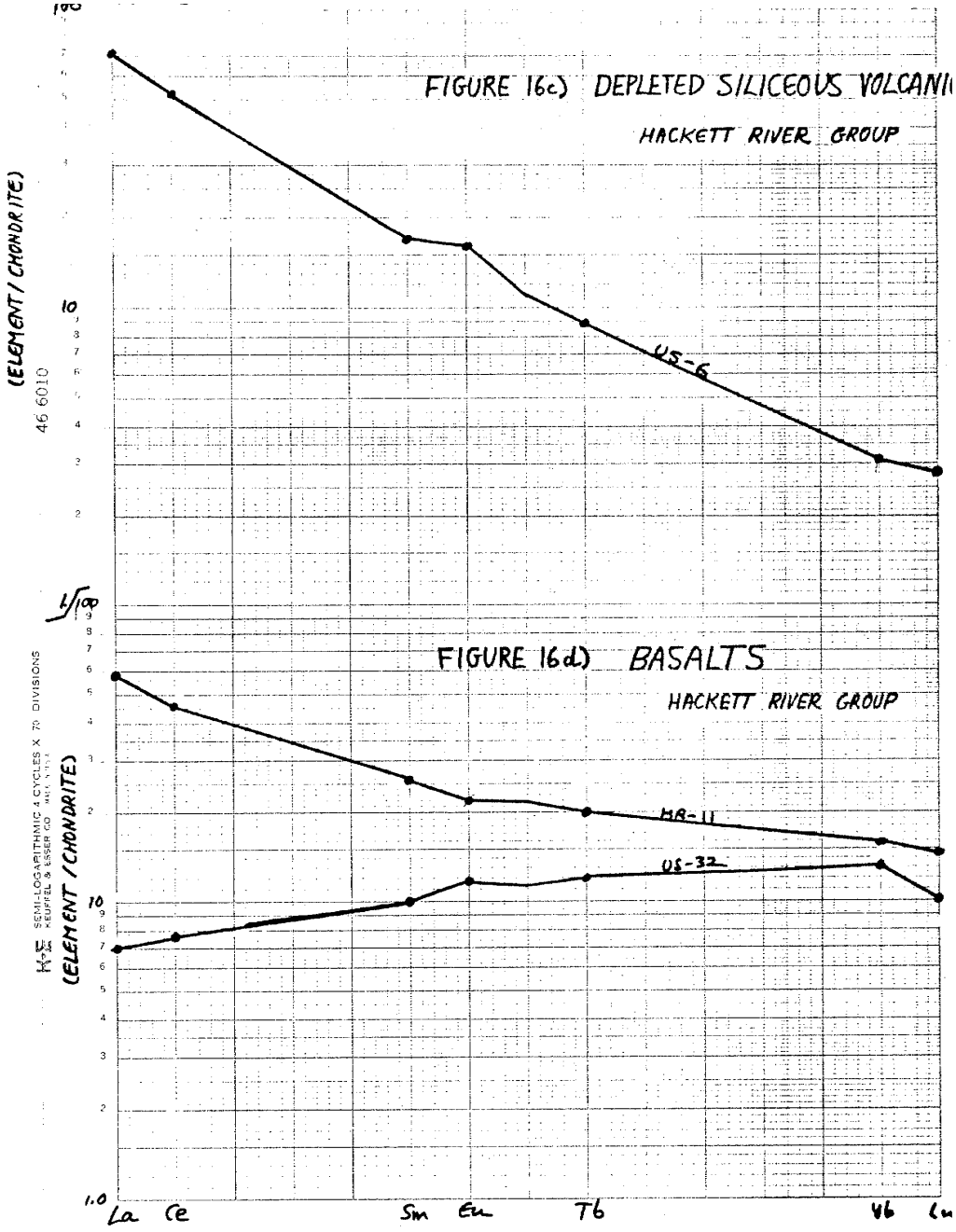
FIGURE 16c) DEPLETED SILICEOUS VOLCANI
HACKETT RIVER GROUP
US-6
46 6010
(ELEMENT / CHONDRITE)


FIGURE 16d) BASALTS
HACKETT RIVER GROUP
HR-11
US-32
SEMI-LOGARITHMIC 4 CYCLES X 70 DIVISIONS
KEUFFEL & ESSER CO.
(ELEMENT / CHONDRITE)
La Ce Sm Eu Tb Yb Lu

US-32; but the rare-earth spectrum is enriched in light REE, corellative with Condie's (1976) EAT category.

3) Archean Andesites and Dacites (AADH)--represented by samples US-3, HR-22 and HR-15. The REE spectra of these rocks correlate with classes LAA (low-alkali Archean andesite) and USV (undepleted siliceous volcanic) of Condie (1976), showing moderate enrichment in light REE, and relatively low alkali contents, within the bulk composition of andesites and dacites ($SiO_2$ content of 55-68%). However, absolute REE contents are significantly lower than Condie's averages.

4) Undepleted Siliceous Volcanics (USVH)--represented by samples HR-16 and US-28. These are rocks of rhyolitic composition ($SiO_2$ greater than 68%) with REE spectra identical to those of AADH. Alkali contents are variable, but higher than DSVH below; at Hackett River, Al and Ca are lower, and Ti higher than DSVH.

5) Depleted Siliceous Volcanics (DSVH)--represented by sample US-6. This sample is a rhyolite with a REE spectrum greatly depleted in heavy REE.

The boundary between AADH and USVH is arbitrary; REE spectra and trace-element contents are not significantly different from 55% to 75% silica. However, DSVH demands a distinct origin which involves garnet, to account for its REE fingerprint. The importance of this distinction cannot be too greatly emphasized; it will appear again when considering the results of trace-element modelling. The basalts EATH and DATH call for separate origins, due to the wide difference in



light REE content between them. This too is borne out by trace-element modelling (see below).

In other words, our previous assumption, that the samples represent one homogeneous population, has been disproved. The analysis of correlation coefficients and variation diagrams, however, indicates a general parallel with magmatic differentiation processes for most of the samples. This indicates that either 1)most major and trace elements are not sensitive to the variations recorded by the REE spectra, or 2) these variations are not strong enough to affect the overall differentiation process. In either case, the REE patterns described above demonstrate that overall trends in element variation, whether described by variation diagrams or correlation coefficients, do not suffice to prove a homogeneous population. Similar conclusions have been reached in work on Recent volcanism (see Carmichael, Turner and Verhoogen (1974) for discussion and references).

## Comparisons

With the sample population divided into subgroups based primarily on REE patterns, comparisons may be made between subgroups and with other analyses of Archean and Recent volcanics. These comparisons look once again for fingerprints of tectonic setting and magma origins, which lead inevitably to a discussion of petrogenesis. In addition, such comparisons aid in assessing the significance of the Hackett River results.

Table 7. Comparison of Hackett River basalts with other Archean and Recent basalts.

| | EATH | DATH | EAT | DAT | 1 | 2 | 3 | 4 | 5 | 6 | 7 | 8 | 9 | 10 | 11 |
|---|---|---|---|---|---|---|---|---|---|---|---|---|---|---|---|
| $SiO_2$ | 48.30 | 48.48 | 49.7 | 51.4 | 49.7 | 51.0 | 51.4 | 47.9 | 47.6 | 47.7 | 51.57 | 50.59 | 49.34 | 50.83 | |
| $TiO_2$ | 1.08 | 0.92 | 1.0 | 1.9 | 1.0 | 1.53 | 0.53 | 0.84 | 2.14 | 1.24 | 0.80 | 1.05 | 1.49 | 2.03 | |
| $Al_2O_3$ | 15.39 | 11.93 | 14.9 | 14.8 | 14.9 | 13.6 | 8.8 | 13.1 | 14.1 | 17.6 | 15.91 | 16.29 | 17.04 | 14.07 | |
| $Fe_2O_3$ | 13.42 | 15.16 | 2.6 | 2.1 | 2.57 | 0.52 | 0.8 | 14.9 | 16.0 | 12.1 | 2.74 | 3.66 | 1.99 | 2.88 | |
| FeO | | | 8.8 | 8.3 | 8.77 | 12.03 | 9.8 | | | | 7.04 | 5.08 | 6.80 | 9.00 | |
| MgO | 9.98 | 11.54 | 6.3 | 6.7 | 6.31 | 6.20 | 10.5 | 10.3 | 5.13 | 5.53 | 6.73 | 8.96 | 7.19 | 6.34 | |
| CaO | 9.52 | 9.78 | 9.4 | 10.7 | 9.39 | 7.88 | 10.7 | 11.2 | 8.40 | 10.5 | 11.74 | 9.50 | 11.72 | 10.42 | |
| $Na_2O$ | 3.76 | 3.32 | 2.0 | 2.7 | 2.11 | 2.45 | 3.0 | 0.93 | 2.65 | 3.75 | 2.41 | 2.89 | 2.73 | 2.23 | |
| $K_2O$ | 0.56 | 0.80 | 0.32 | 0.18 | 0.32 | 0.41 | 0.19 | 0.03 | 0.35 | 0.57 | 0.44 | 1.07 | 0.16 | 0.82 | |
| MnO | 0.22 | 0.28 | NA | NA | 0.19 | 0.25 | 0.19 | 0.19 | 0.25 | 0.15 | 0.17 | 0.17 | 0.17 | 0.18 | |
| $P_2O_5$ | 0.45 | 0.41 | NA | NA | 0.18 | 0.12 | 0.04 | NA | NA | NA | 0.11 | 0.21 | 0.16 | 0.23 | |
| Cr | 123. | 182. | 175. | 350. | 187. | | 735. | 330. | 85. | 108. | 50. | 40. | 300. | | |
| Zn | 130. | 95. | 100. | 115. | 103. | | 80. | | | | (80.) | (80.) | 75. | | |
| Cu | 27. | 83. | 110. | 110. | 109. | | 8. | | | | (80.) | (80.) | 70. | | |
| Co | 38. | 43. | 50. | 60. | 35. | | 37. | | | | (20.) | (40.) | 32. | | |
| Ni | 45. | 85. | 100. | 225. | 103. | | 550. | 158. | 105. | 170. | 30. | 25. | 100. | | |
| Rb | 14. | 16. | 10. | 4. | | | 5.4 | | | | 5. | 10. | 1. | | |
| Sr | 270. | 234. | 165. | 100. | 164. | | 67.6 | | | | 220. | 330. | 135. | | |
| Zr | 250. | 79. | 100. | 55. | 105. | | (38.) | | | | 70. | 100. | 100. | | |
| Ba | 130. | 80. | 90. | 80. | 105. | | 22.7 | | | | 75. | 115. | 11. | | |
| Cs | 1.0 | 0.8 | 0.5 | 0.3 | | | 0.30 | | | | (0.05) | (0.5) | 0.02 | | |
| Y | 11. | 9.8 | 15. | 10. | 15. | | (17.) | | | | -- | 20. | 30. | | |
| Ce | 40. | 7. | 25. | 10. | | | 8.0 | | | | 2.6 | 19. | 12. | | |
| Sm | 4.7 | 1.9 | 3.6 | 2. | | | 1.4 | | | | NA | NA | 3.9 | | |
| Eu | 1.5 | 0.82 | 1.1 | 0.8 | | | 0.48 | | | | NA | NA | 1.5 | | |
| Yb | 3.1 | 2.7 | 2.4 | 1.8 | | | 1.19 | | | | 1.4 | 2.7 | 3. | | |
| Hf | 6.3 | 0.55 | NA | NA | | | 0.7 | | | | 1.0 | 2.6 | NA | | |
| K/Rb | 332. | 464. | 350. | 350. | | | 89. | | | | 1000. | 340. | 1260. | | |
| La/Yb | 6.1 | 0.85 | 5. | 1.5 | | | 2.2 | | | | 1.0 | 3.5 | 1.2 | | |

EABH, DABH; see Table .
EAT, DAT--group averages from Condie(1976).
1 -- Average of Canadian Archean basalts, from Baragar and Goodwin (1968).
2 -- Ely greenstone, Minnesota; from Arth and Hanson (1975);Table 2, col.2.
3 -- Basaltic komatiite,Barberton area,South Africa;from Herrmann(1976),BK-3;values in parentheses from Nesbitt and Sun (1976),high-Mg basalt #364.
4,5,6 -- Abitibi basalts, from Jolly (1975);4 = komatiitic basalt,5=tholeiitic,6-calc-alkaline
7,8,9 -- Recent basalt averages,from Jakes and Gill(1970);7=arc tholeiite,8=high-alumina basalt, 9=abyssal tholeiite. Values in parentheses from Condie(1976)
10 -- Basalt average from Nockolds(1954);represents mostly continental basalts.



Comparative analyses are given for basalts in Table 7, for andesites (55-61% $SiO_2$) in Table 8, for dacites (61-68% $SiO_2$) in Table 9, and for rhyolites in Table 10. The comparative values are plotted with the envelopes of the Hackett River samples on variation diagrams in Figures 17a-g, and on an MgO vs. $Fe_T$ diagram in Figure 18.

Basalts

Two basaltic ($SiO_2$ less than 50%) samples were analyzed; HR-11 (= EATH) and US-32 (= DATH). These were correlated above with the EAT and DAT averages of Condie (1976), and, as shown on Table 7, variations in trace elements roughly match those reported for EAT and DAT. However, these basalts have several unique features, most importantly high iron and magnesium enrichment. As seen on Figure 18, the only results comparable in Fe and Mg contents are basaltic komatiites from Abitibi and Barberton. All Archean averages and modern basalts fall at least 2% short in combined Mg and Fe. Alkali basalts can show comparable enrichment, but $TiO_2$ contents are half that expected from alkali basalts. The norms are nepheline-normative, and the samples plot in the alkali basalt field of Kuno's (1966) diagram (Figure 9h); these, however, may be accounted for by alkali enrichment and mobility. Ti contents of the basalts falls between the curves for Abitibi komatiites and calc-alkaline volcanics (data from Jolly, 1975), but are substantially greater than values reported from komatiites in Barberton (Herrmann and others, 1976) and Munro Twp. (Arndt and

Table 9. Comparison of Hackett River dacites with other Archean and Recent dacites.

| | US-3 | HR-22 | HR-21 | US-4 | AADH | USVd | DSVd | 1 | 2 | 3 | 4 | 5 | 6 | 7 |
|---|---|---|---|---|---|---|---|---|---|---|---|---|---|---|
| $SiO_2$ | 64.42 | 63.23 | 62.12 | 66.83 | 60.94 | 64.0 | 66.2 | 66.8 | 61.74 | 67.16 | 69.6 | 67.0 | 66.80 | 64.90 |
| $TiO_2$ | 0.93 | 0.88 | 1.05 | 0.66 | 0.94 | 0.50 | 0.28 | 0.50 | 1.22 | 0.96 | 0.79 | 0.74 | 0.23 | 0.60 |
| $Al_2O_3$ | 13.77 | 14.04 | 16.69 | 16.75 | 14.67 | 15.8 | 16.5 | 14.8 | 15.17 | 16.73 | 10.3 | 14.1 | 18.24 | 16.0 |
| $Fe_2O_3$ | 7.56 | 9.49 | 8.86 | 4.12 | 0.75 | 2.6 | 0.9 | 1.09 | 1.87 | 0.89 | 6.47 | 6.48 | 1.25 | 3.2 |
| FeO | | | | | 7.51 | 2.9 | 1.0 | 3.01 | 5.74 | 2.77 | | | 1.02 | 1.0 |
| MgO | 3.42 | 4.58 | 4.54 | 1.58 | 4.73 | 3.0 | 1.6 | 1.78 | 2.30 | 1.86 | 1.93 | 2.10 | 1.50 | 1.7 |
| CaO | 2.07 | 4.07 | 2.46 | 5.23 | 4.47 | 3.2 | 3.9 | 2.55 | 4.80 | 3.29 | 3.13 | 3.21 | 3.17 | 4.7 |
| $Na_2O$ | 5.05 | 4.01 | 2.24 | 4.27 | 4.19 | 4.0 | 5.2 | 4.06 | 3.57 | 3.61 | 3.54 | 4.73 | 4.27 | 4.2 |
| $K_2O$ | 1.79 | 1.74 | 4.11 | 0.69 | 1.23 | 2.7 | 2.0 | 1.78 | 0.54 | 1.31 | 0.79 | 1.25 | 1.92 | 1.8 |
| MnO | 0.08 | 0.14 | 0.14 | 0.06 | 0.11 | NA | NA | 0.10 | 0.14 | 0.02 | 0.03 | 0.06 | 0.06 | NA |
| $P_2O_5$ | 0.40 | 0.45 | 0.38 | NA | NA | NA | NA | 0.18 | 0.32 | 0.12 | NA | NA | NA | NA |
| Cr | 9. | 82. | 75. | | 56. | 45. | 30. | 38. | | | 12. | 38. | 5. | 10. |
| Zn | 144. | 142. | 214. | | NA | | | 72. | | | | | | |
| Cu | 15. | 37. | 46. | | 39. | | | 44. | | | | | | |
| Co | 15. | 28. | 23. | | 24. | 15. | 8. | 4. | | | | | 8. | 15. |
| Ni | 15. | 40. | 45. | | 38. | 25. | 25. | 24. | | | 20. | 55. | 1. | 8. |
| Rb | 51. | 38. | 71. | | 33. | 68. | 33. | | | | | | 15. | 40. |
| Sr | 225. | 141. | 167. | | 228. | 390. | 600. | 222. | | | | | 200. | 500. |
| Zr | 225. | 203. | 184. | | 206. | 260. | 50. | 217. | | | | | 80. | 100. |
| Ba | 400. | 170. | 400. | | 240. | 1090. | 590. | 383. | | | | | 250. | 400. |
| Cs | 3.0 | 1.55 | 4.0 | | NA | 3. | 5. | | | | | | 0.2 | 1. |
| Y | 25. | 19. | 18. | | 18, | 8. | 2. | 1.7 | | | | | 25. | 30. |
| Ce | 37. | 46. | 24. | | 43. | 100. | 30. | | | | | | 15. | 26. |
| Sm | 4.5 | 5.1 | 2.7 | | 4.8 | 10. | 2.4 | | | | | | 2. | 2.9 |
| Eu | 2.4 | 1.6 | 1.4 | | 1.5 | 2.3 | 0.7 | | | | | | 0.7 | 1.0 |
| Yb | 2.8 | 3.3 | 2.4 | | 3.1 | 1.4 | 0.5 | | | | | | 2. | 1.4 |
| Hf | 6.9 | 4.8 | 5.5 | | NA | | | | | | | | | |
| K/Rb | 290. | 383. | 483. | | NA | 330. | 503. | | | | | | 800. | 400. |
| La/Yb | 8.2 | 8.6 | 5.0 | | NA | 37. | 26. | | | | | | 3. | 12. |

AADH -- see Table .
USVd,DSVd -- group dacite averages from Condie (1976).
1 -- Canadian Archean salic rocks, average, from Baragar and Goodwin (1968).
2,3 -- Average Archean dacites and rhyodacites, from Wilson and others (1965).
4,5 -- Abitibi tholeiitic and calc-alkaline dacites, respectively, from Jolly (1975).
6 -- Arc dacite, from Jakes and Gill (1970).
7 -- Continental dacite, from Condie (1976).
NA -- Not available.

Table 8. Comparison of Hackett River andesites with other Archean and Recent andesites.

| | HR-15 | HR-2 | RL-2 | US-24 | AADH | LAA | HAA | DAA | 1 | 2 | 3 | 4 | 5 | 6 |
|---|---|---|---|---|---|---|---|---|---|---|---|---|---|---|
| $SiO_2$ | 55.18 | 60.12 | 55.47 | 59.26 | 60.94 | 56.7 | 58.9 | 49.9 | 57.6 | 57.5 | 56.2 | 57.4 | 54.54 | 59.05 |
| $TiO_2$ | 1.02 | 1.40 | 1.88 | 0.73 | 0.94 | 0.92 | 0.65 | 1.1 | 1.0 | 1.23 | 0.93 | 1.25 | 1.13 | 0.69 |
| $Al_2O_3$ | 16.21 | 16.51 | 12.86 | 15.84 | 14.67 | 14.0 | 15.5 | 14.8 | 15.4 | 12.1 | 16.1 | 15.6 | 16.26 | 17.07 |
| $Fe_2O_3$ | 10.24 | 8.65 | 13.04 | 8.80 | 0.75 | 2.3 | 1.5 | 2.4 | 1.82 | 13.3 | 10.07 | 3.48 | 2.31 | 3.90 |
| FeO | | | | | 7.51 | 7.0 | 4.5 | 8.2 | 5.96 | | | 5.01 | 5.40 | 2.57 |
| MgO | 6.18 | 6.08 | 12.26 | 3.52 | 4.73 | 5.4 | 4.5 | 6.4 | 3.75 | 2.85 | 4.18 | 3.38 | 6.97 | 3.25 |
| CaO | 7.27 | 3.95 | 6.53 | 3.48 | 4.47 | 6.6 | 5.1 | 9.8 | 5.64 | 5.77 | 6.84 | 6.14 | 7.50 | 7.09 |
| $Na_2O$ | 3.52 | 3.95 | 2.79 | 5.18 | 4.19 | 3.4 | 4.0 | 2.1 | 3.70 | 3.22 | 4.10 | 4.20 | 3.64 | 3.80 |
| $K_2O$ | 0.16 | 2.36 | 0.57 | 0.93 | 1.23 | 0.67 | 1.9 | 0.25 | 0.84 | 0.67 | 0.82 | 0.43 | 1.49 | 1.27 |
| MnO | 0.10 | 0.11 | 0.11 | 0.22 | 0.11 | NA | NA | NA | 0.15 | 0.12 | 0.11 | NA | 0.12 | 0.15 |
| $P_2O_5$ | 0.42 | 0.54 | 0.54 | 0.26 | NA | NA | NA | NA | 0.22 | NA | NA | 0.44 | 0.23 | 0.20 |
| Cr | 75.5 | | | | 55.5 | 125. | 88. | 175. | 103. | 38. | 70. | 15. | 25. | |
| Zn | 116. | 96. | 152. | 112. | NA | 97. | 81. | 95. | 86. | | | | | |
| Cu | 66. | 21. | 26. | 32. | 39. | 60. | 36. | 76. | 60. | | | | | |
| Co | 28. | | | | 23.6 | 25. | 23. | 32. | 18. | | | | | |
| Ni | 60. | 14. | 34. | 18. | 38. | 70. | 60. | 85. | 63. | 45. | 115. | 20. | 18. | |
| Rb | 9.1 | 79. | 15. | 30. | 33. | 22. | 75. | 7. | | | | 6.0 | 30. | |
| Sr | 319. | 250. | 410. | 247. | 228. | 278. | 580. | 129. | 263. | | | 220. | 385. | |
| Zr | 189. | 250. | 144. | 185. | 206. | 150. | 190. | 103. | 160. | | | 70. | 110. | |
| Ba | 150. | | | | 240. | 230. | 547. | 149. | 248. | | | 100. | 270. | |
| Cs | 0.6 | | | | NA | 0.8 | 1.5 | 0.2 | | | | | | |
| Y | 10. | 20. | 11. | 9.7 | 18. | 25. | 35. | 87. | 14. | | | NA | 21. | |
| Ce | 47. | | | | 43. | 31. | 70. | 30. | | | | 8. | 24. | |
| Sm | 4.7 | | | | 4.8 | 3.6 | 6.7 | 7.3 | | | | | | |
| Eu | 1.45 | | | | 1.5 | 1.1 | 1.7 | 2.0 | | | | | | |
| Yb | 3.2 | | | | 3.1 | 1.8 | 2.4 | 6.1 | | | | 2.4 | 1.9 | |
| Hf | 4.35 | | | | NA | NA | NA | NA | | | | 1.0 | 2.3 | |
| K/Rb | 146. | 247. | 307. | 261. | NA | 253. | 210. | 296. | | | | 890. | 430. | |
| La/Yb | 5.6 | | | | NA | 7.2 | 14. | 2.0 | | | | 1.0 | 6.2 | |

AADH; see Table .
LAA, HAA, DAA -- group averages from Condie (1976).
1 -- Average of Canadian Archean andesites, from Baragar and Goodwin (1968).
2 -- Average tholeiitic andesite, Abitibi (Jolly,1975).
3 -- Average calc-alkaline andesite, Abitibi (Jolly, 1975).
4 -- Average island-arc andesite, from Jakes and Gill (1970).
5 -- Low-silica calc-alkaline andesite, from Jakes and Gill (1970).
6 -- Low-potassium calc-alkaline andesite, from Jakes and Gill (1970).
NOTE: Only one set of trace elements given for calc-alkaline andesite.
NA -- Not available.

Figure 17. Comparison of Hackett River variation diagrams with other Archean and Recent volcanics. Envelopes on each diagram are taken from Figure 9; only anomalous samples are marked on these diagrams, with a dot. Filled triangles are group average values from Condie (1976); filled squares are Archean comparison values; open squares are Recent comparisons. Data is taken from Tables 7-10, with additions from Jolly (1975), from which the Abitibi differentiation trends have been drawn. Solid lines connect the dacite and rhyolite values for USV and DSV reported by Condie (1976).



Table 10. Comparison of Hackett River rhyolites with other Archean and Recent rhyolites.

| | HR-16 | US-28 | DSVH-US-6 | US-26 | US-31 | USVH | USVr | DSVr | 1 | 2 | 3 | 4 | 5 |
|---|---|---|---|---|---|---|---|---|---|---|---|---|---|
| $SiO_2$ | 72.38 | 71.98 | 70.28 | 69.88 | 70.18 | 72.18 | 73.5 | 71.7 | 69.0 | 74.11 | 72.43 | 71.4 | 74.0 |
| $TiO_2$ | 0.84 | 0.93 | 0.50 | 0.55 | 0.67 | 0.88 | 0.14 | 0.19 | 0.54 | 0.14 | 0.16 | 0.58 | 0.25 |
| $Al_2O_3$ | 15.29 | 14.04 | 16.37 | 15.92 | 13.66 | 14.66 | 12.7 | 16.4 | 13.5 | 13.59 | 14.23 | 13.2 | 13.3 |
| $Fe_2O_3$ | 2.60 | 4.88 | 2.04 | 2.51 | 5.97 | 0.72 | 0.9 | 0.7 | 1.24 | 0.64 | 0.84 | 4.31 | 1.3 |
| FeO | | | | | | 2.72 | 1.2 | 0.9 | 3.04 | 1.27 | 1.54 | | 0.5 |
| MgO | 0.91 | 1.48 | 0.98 | 0.72 | 3.18 | 1.20 | 0.8 | 0.5 | 1.42 | 1.04 | 1.47 | 0.82 | 0.3 |
| CaO | 1.34 | 0.93 | 3.50 | 2.39 | 3.80 | 1.14 | 1.1 | 1.7 | 2.22 | 0.60 | 0.88 | 2.03 | 1.5 |
| $Na_2O$ | 5.53 | 3.47 | 4.34 | 6.70 | 1.83 | 4.50 | 3.3 | 5.0 | 4.55 | 2.74 | 4.67 | 4.07 | 4.0 |
| $K_2O$ | 2.05 | 2.51 | 2.31 | 0.52 | 2.36 | 2.88 | 3.0 | 2.0 | 1.44 | 3.82 | 1.32 | 1.60 | 3.5 |
| MnO | 0.04 | 0.08 | 0.11 | 0.02 | 0.07 | 0.06 | NA | NA | 0.08 | 0.02 | 0.02 | 0.03 | NA |
| $P_2O_5$ | 0.28 | 0.24 | 0.18 | 0.19 | 0.26 | NA | NA | NA | NA | 0.12 | 0.20 | NA | NA |
| Cr | 82. | 7.4 | 56. | | | 45. | 12. | 12. | 26. | | | 23. | 2. |
| Zn | 68. | 531. | 42. | 102. | 148. | NA | | | 96. | | | | |
| Cu | 9.5 | 13. | 6.5 | 34. | 33. | 11. | | | 32. | | | | |
| Co | 20. | 15. | 7.1 | | | 18. | 3. | 3. | 5. | | | | 3. |
| Ni | 15. | 15. | 20. | 14. | 36. | 15. | 10. | 10. | 20. | | | 60. | 1. |
| Rb | 35. | 58. | 31. | 21. | 69. | 47. | 43. | 41. | | | | | 100. |
| Sr | 94. | 205. | 278. | 319. | 132. | 150. | 100. | 110. | 218. | | | | 150. |
| Zr | 206. | 200. | 170. | 180. | 190. | 200. | 350. | 30. | 424. | | | | 160. |
| Ba | 460. | 380. | 390. | | | 420. | 750. | 480. | 368. | | | | 900. |
| Cs | 2.2 | 1.6 | 1.3 | | | NA | 0.6 | 2. | | | | | 3. |
| Y | 18. | 11. | 1.7 | 3.2 | 15. | 14. | 30. | 2. | | | | | 10. |
| Ce | 44. | 50. | 46. | | | 47. | 95. | 35. | | | | | 70. |
| Sm | 4.6 | 4.3 | 3.2 | | | 4.4 | 9. | 2.3 | | | | | 5.5 |
| Eu | 1.2 | 1.6 | 1.1 | | | 1.4 | 1.6 | 0.5 | | | | | 1.5 |
| Yb | 3.1 | 2.3 | 0.6 | | | 2.7 | 5.2 | 0.4 | | | | | 3.5 |
| Hf | 4.6 | 6.35 | 4.7 | | | | | | | | | | |
| K/Rb | 485. | 358. | 613. | 209. | 283. | NA | 405. | 580. | | | | | 250. |
| La/Yb | 4.5 | 9.6 | 38. | | | 6.7 | 8.9 | 43. | | | | | 10. |

DSVH, USVH -- See Table .
USVr, DSVr -- group averagesfor Archean rhyolites, from Condie (1976).
1 -- Rhyolite average, Birch-Uchi volcanics, Ontario; from Baragar and Goodwin (1968).
2 -- Archean rhyolite average, from Wilson and others (1965).
3 -- Archean Na-rhyolite average, from Wilson and others (1965).
4 -- Abitibi calc-alkaline rhyolite, from Jolly (1975).
5 -- Recent rhyolite, from Condie (1976).
NA -- Not available.

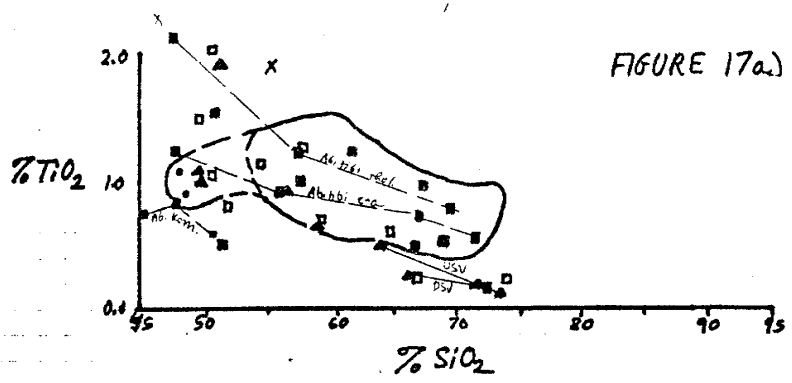


FIGURE 17a)

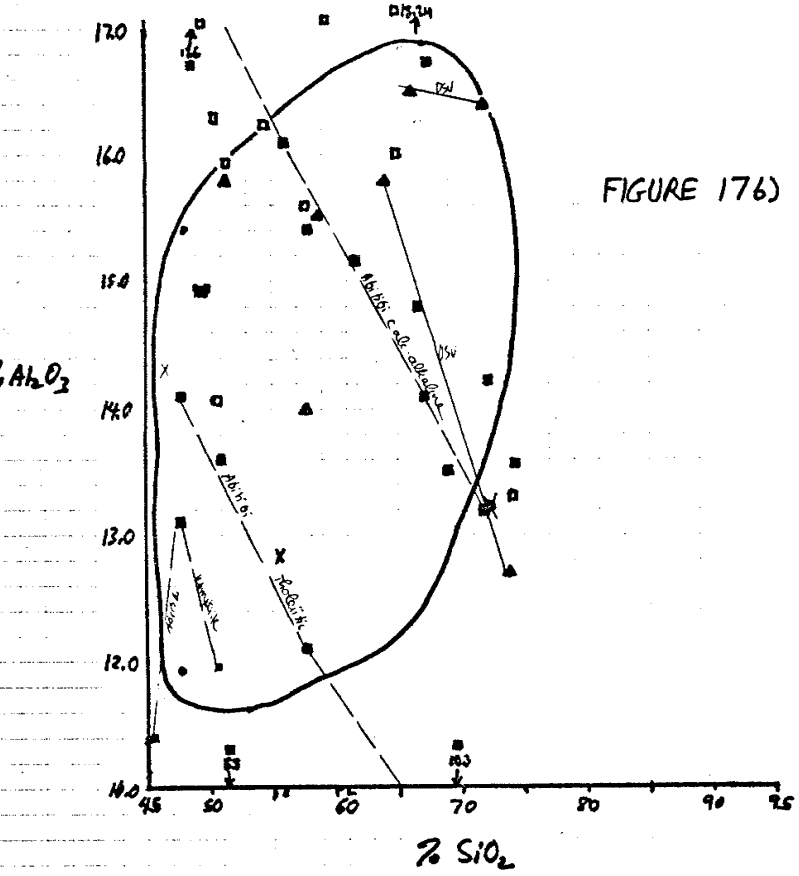


FIGURE 17b)



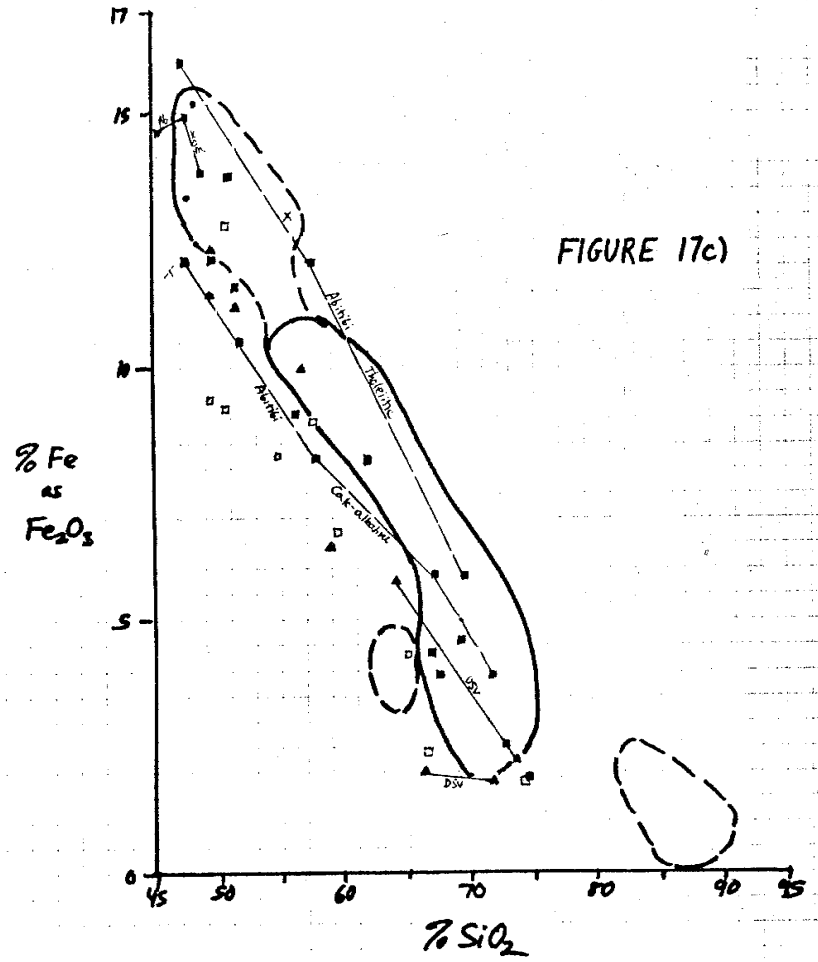


FIGURE 17c)

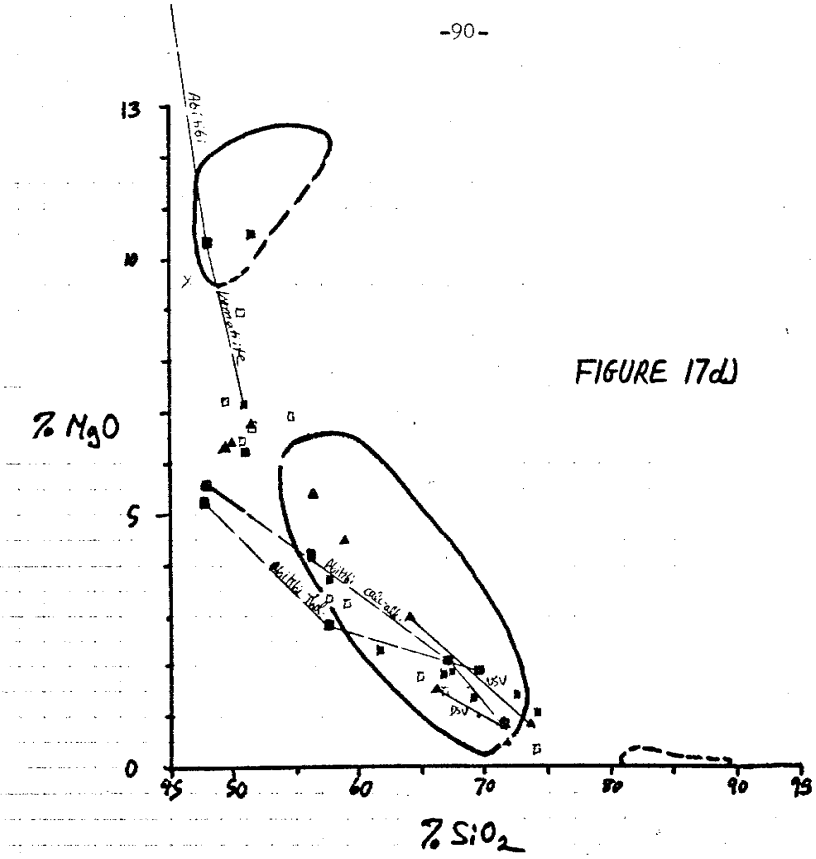


FIGURE 17d)



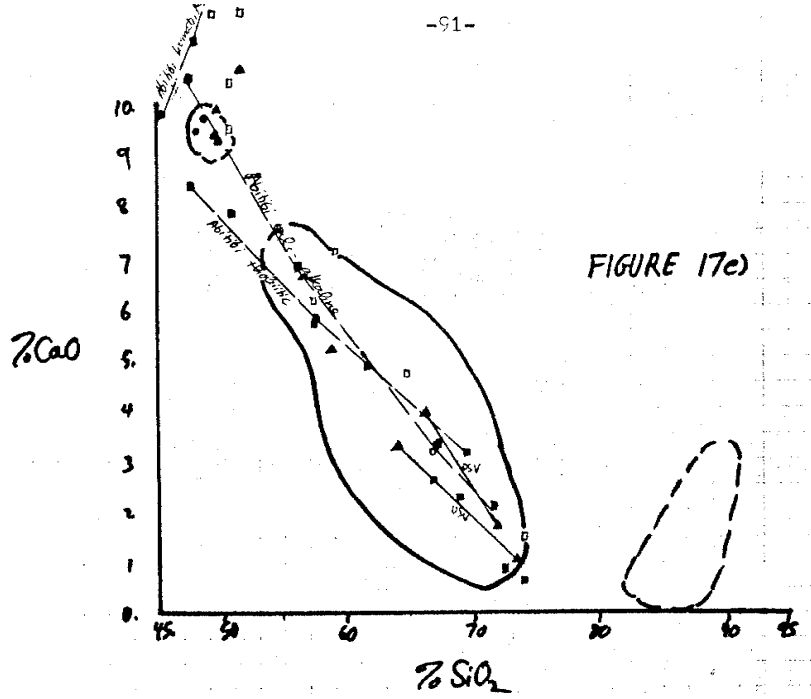


FIGURE 17e)

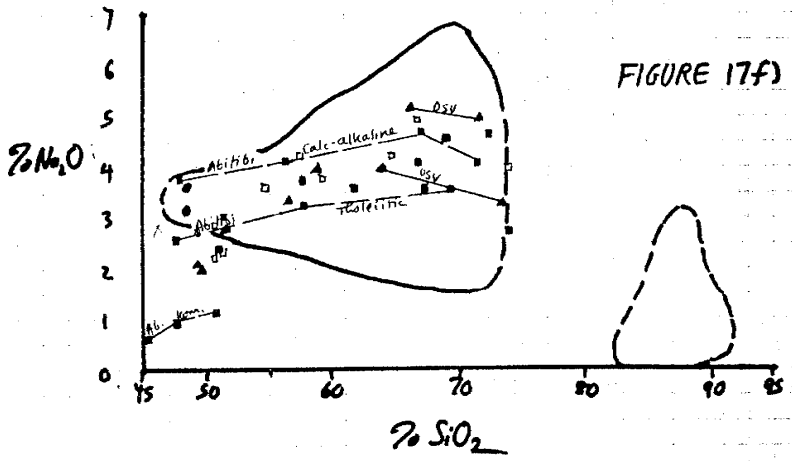


FIGURE 17f)

FIGURE 17g)

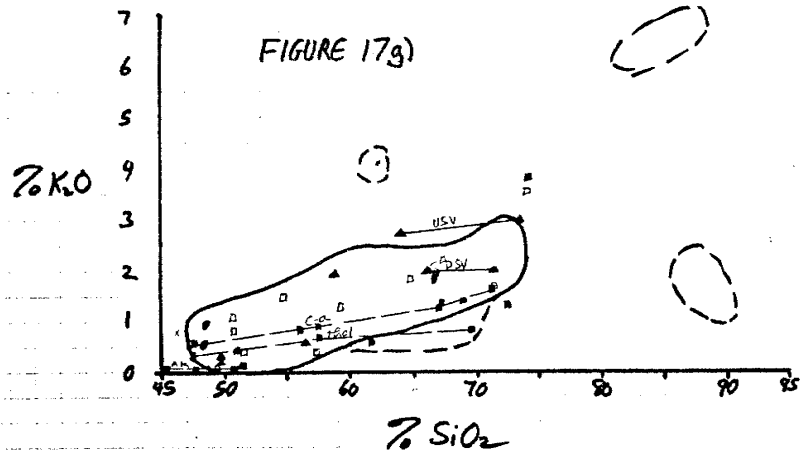




FIGURE 18. MGO vs $FE_T$ COMPARISONS

(SYMBOLS AS IN FIGURE 17)

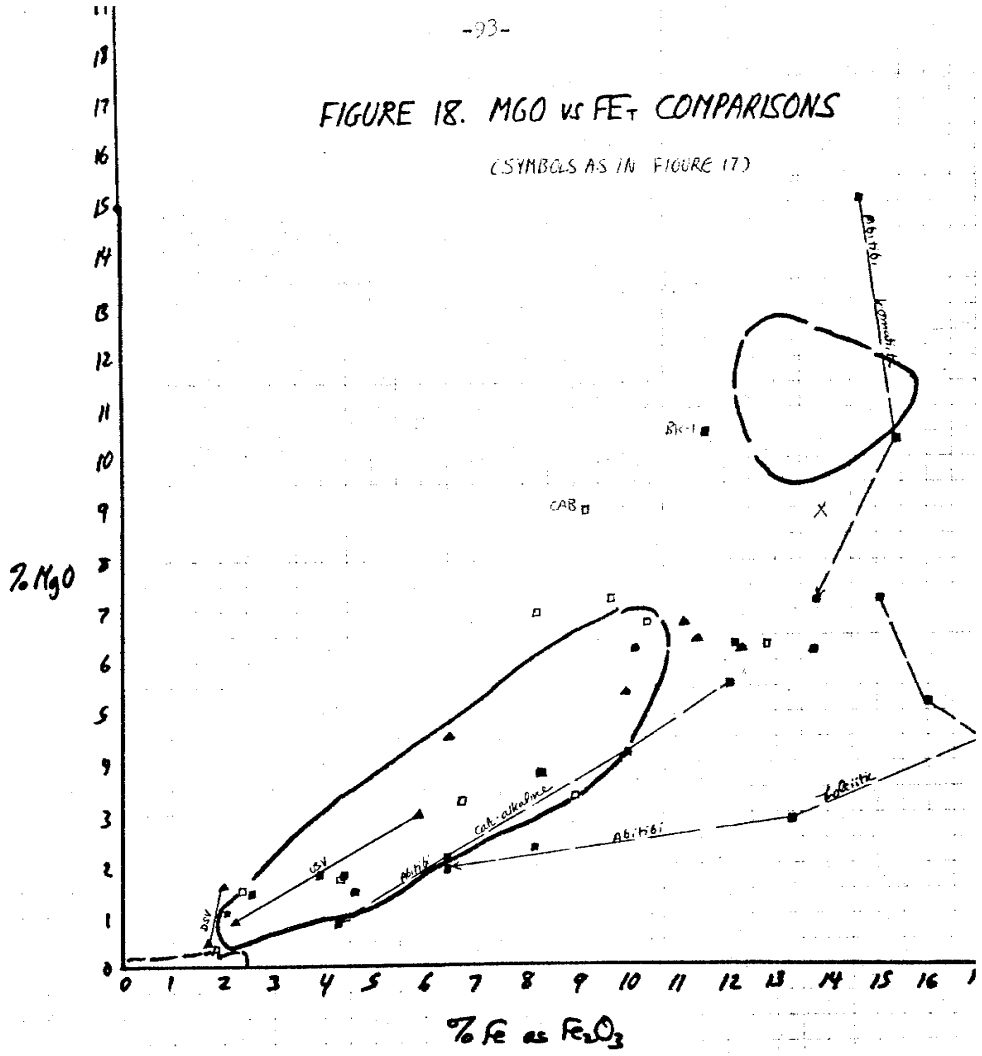

others, 1977).

Much of the evidence, however, militates against a komatiitic affiliation for the basalts. CaO values are lower than komatiitic, and fall on either a calc-alkaline or tholeiitic trend. $TiO_2$ is high, as mentioned above. Particularly strong is the trace-element evidence. Cr and Ni are much too low in the samples, and Ba and Sr too high; values for these elements are more in line with calc-alkaline values (Table 7, cols. 6,7,8). The highly enriched REE pattern of HR-11 has no corollaries among komatiites; the depleted pattern of US-32 still has REE contents more similar to an arc or rise tholeiite than a komatiite.

What remains, then, is the large Mg and Fe enrichment of the samples. Enrichment by chloritization might be considered; however, high Ca and Na cause the alteration index to remain low (see page 49). Considering the few samples available and the poor quality of the MgO analyses, no resolution is possible; the basaltic samples, in particular US-32, show an affinity to the magnesian or komatiitic trend.

Other Archean basalts run no higher than 7.5% MgO, as shown on Figure 18. They also contain about 2% more silica than the Hackett River samples, and may contain more CaO, less Sr, $Na_2O$ and $K_2O$.

Modern basalts do not provide a good analog to the Hackett River samples. As mentioned above, all tholeiitic and high-alumina basalts fall at least 2% short in (Fe+Mg) content. Consideration of other elements favors an analogy to



island-arc tholeiite (Jakes and White, 1970) for DATH, while a calc-alkaline basalt may be closer to DATH (although Al is low); elements used for these analogies are $TiO_2$, CaO, Rb, Sr, Zr and the REE. Values for P, Cr and Ni are higher in the Archean samples (although lower than the group averages of Condie (1976)), while Cu and Co are lower than either Archean or modern values. Abyssal or rise tholeiites are not favored, due to excessive Ti, Al, Cr, Ni, and low Sr and Zr.

Andesites (55-61% $SiO_2$)

Four andesite analyses are compared in Table 8. The one REE analysis available in this silica range (HR-15) reveals an LAA pattern, which major and trace elements generally support. Exceptions are: Al is consistently too high, Cr and Ba are low. The other analyses show a scatter that is hard to interpret. RL-2 shows Fe and Mg enrichment similar to that of the basalts; however, it has been extensively carbonated, and interpretations are suspect.

The Hackett River andesites compare favorably with other analyses of Archean andesites. The andesites lie along the Abitibi calc-alkaline trend (Jolly, 1975), showing no trend to Fe enrichment (except for RL-2). Averages of analyses from Yellowknife, Cameron River, and the Canadian Shield Archean yield similar major and trace-element results. However, Fe, Mg and Sr are higher, and Ba and Cr lower, than these averages (see Baragar and Goodwin, 1968).

Comparison to Recent calc-alkaline volcanics is equivocal.

The REE patterns are similar to calc-alkaline andesites; however, the total REE content is somewhat higher, along with Fe, Mg, Ni and Cr, while Rb is lower. Island arc andesites fit even more poorly, however. Modern calc-alkaline andesites provide the best analog for the Hackett River samples, but several index elements remain unsatisfied.

Dacites (61-68% $SiO_2$)

Four dacite samples are compared in Figure 9. REE patterns correlate with either LAA or USV patterns; however, the slope is not as great as that of USV dacite (Condie, 1976), and many trace elements are in disagreement with the USV average values--in particular, Ba is much lower, as is Sr; Cr, Co and Ni are higher, and Al is lower. US-4 (not analyzed for trace elements) has a high CaO content and low $TiO_2$ which are similar to DSVH values, although dissimilar to DSV dacite values.

The Hackett River dacite values compare well to other Archean dacites, but with more scatter than the andesites. Hackett River samples are rich in Fe and Mg relative to their counterparts elsewhere in the Canadian Shield; they are depleted in Sr and Ba, and enriched in Ti and Cr. The samples correlate with the calc-alkaline dacite of the Abitibi belt; alumina precludes a tholeiitic affiliation. Compared to modern dacites, REE patterns and trace-element contents suggest analogies with the calc-alkaline continental dacites over the arc dacites; but Ti, Fe and Mg contents are higher than in either modern analog.



Rhyolites (over 68% $SiO_2$)

Five rhyolite analyses are contained in Table 10. REE spectra show that both USV and DSV are present. There is striking variation in major and trace-element chemistry between USVH and DSVH; this is most evident in the low Ti, Zr, P, Cs and Y, and high Al, Ca and K/Rb of US-6 relative to HR-16 and US-28. These differences may also be noted between the DSV and USV rhyolite values given by Condie (1976); but the absolute values of some elements is different. In the Hackett River rhyolites, Ti is much higher, Fe, Mg, Ca, Cr, Co, Ni, and Sr are higher, Ba is lower and total rare earths show more difference between depleted and undepleted cases than is the case for Condie's averages. By comparing major and trace elements, US-26 appears to be a DSVH, as does US-4, as mentioned above. US-31, on the other hand, has affinities with the USVH samples.

Hackett River rhyolites show a general resemblance to other Archean and Recent analyses; however, such analyses are not abundant. Fe, Mg and Ti are higher in the Hackett River analyses; but these trends are not as well marked as in the andesites and dacites. The REE patterns for USVH are less enriched in light REE than modern rhyolites; indeed, they are most similar to the AADH results. The DSVH pattern, however, has no modern analogs.

General Considerations

The basalts analyzed from the Hackett River area have

much higher Fe and Mg contents than any reported volcanics of calc-alkaline or tholeiitic trend, but typical of komatiitic basalt; trace-element concentrations, however, seem more related to high-alumina basalts. We may call these "basalts of magnesian affinity"; they do not appear to be cogenetic with the main calc-alkaline trend (but see trace-element modelling results, below).

The andesites, dacites and rhyolites from the Hackett River area fall generally along the trend of both Archean and Recent calc-alkaline volcanism. However, significantly higher values of Fe, Mg, Ti, Ni and Cr, lower Ba and variable Sr persist throughout the differentiation sequence. This suggests that, although the differentiation processes were those of the calc-alkaline suite, the composition of the source rocks or residual phases must have been different, allowing higher contents of Fe, Mg and Ti in the magma. Perhaps this enrichment is related to the high Fe and Mg enrichment of the analyzed basalts; but the enrichment is comparatively small in the intermediate to felsic sequence.

The AADH and USVH values define a continuously varying sequence from 55% to 72% $SiO_2$. The DSVH analysis, however, shows substantial differences from this trend. This may be seen graphically by comparing Figures 9c and 17c, and Figures 9e and 17e. Higher CaO in particular seems to characterize the DSVH samples. The distinction between two varying sequences is shown on an MCA diagram (Figure 19), a ternary plot of $MgO$-$CaO$-$Al_2O_3$ first used by Viljoen and



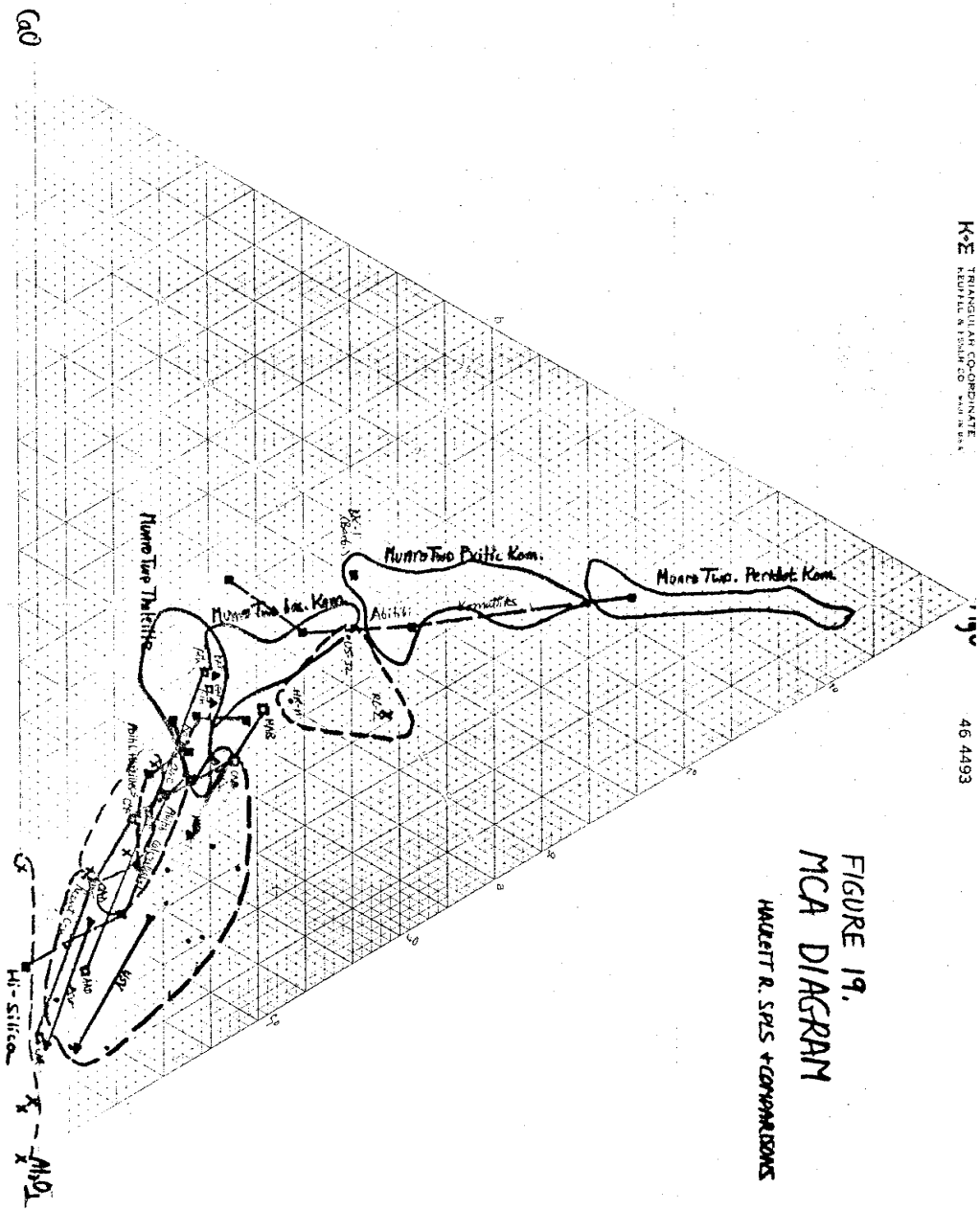


FIGURE 19.
MCA DIAGRAM
HACKETT R. SPLS + COMPARISONS

Viljoen (1969b) to describe komatiitic suites from the Onverwacht Group of South Africa. The Hackett River samples are compared in Figure 19 with: 1)Munro Township komatiites and tholeiites, from Arndt and others (1977); 2) Abitibi differentiation trends, from Jolly (1975); 3) Condie's (1976) Archean group averages, and 4) modern arc and calc-alkaline differentiation trends (data from Jakes and Gill, 1970). The diagram shows the distinction between USV and DSV quite clearly, as well as the komatiitic tendencies of US-32, HR-11 and RL-2. Furthermore, it appears that the dominant USV differentiation trend is distinct from the Abitibi and modern calc-alkaline trends, due to a combination of low CaO and high MgO. DSVH analyses, however, fall along these trends, and also line up with the Back River samples, which, however, are subject to carbonation. Unfortunately, the diagram is more permissive than restrictive, as the MgO uncertainties on Hackett River samples are large. Further use of the MCA diagram for Archean volcanic sequences is indicated.

In summary, the analyzed samples from the Hackett River volcanic sequence contain: 1) two Mg and Fe-rich basalts, one of DAT affinity, the other EAT; 2) a coherent sequence of intermediate to felsic volcanics of LAA and USV affinity; and 3) a few felsic samples of DSV affinity. The members of these three groups may be distinguished both from each other and from other Archean and Recent sequences by a combination of major-element and trace-element criteria.



## Spatial Variation

Before carrying out trace-element modelling of magma formation and speculating on the tectonic consequences of acceptable models, it is important to examine the above-defined sample groups in the light of the field geology.

In the D'Arcy Lake area, three AADH analyses, one USVH and one EATH analysis were collected. The extensive unit of bleached rhyolites yields REE patterns identical to USVH; as REE are generally immobile during alteration (but see Table 6), these samples were likewise USVH. The section at D'Arcy Lake, then, consists of intercalated intermediate and felsic volcanics belonging to the AADH-USVH differentiation sequence, with an EATH pillow basalt near the top of the succession. No mafic base to the sequence has been found; the volcanics are inferred to overly older metasediments. Mafic-to-felsic cycles, characteristic elsewhere in Archean volcanic sequences, are not developed here.

In the Uist Lake region, one DATH, one AADH, one USVH and one DSVH analysis have been collected. The lower volcanic sequence, flanking the Island Lake anticlinorium, contains one DATH sample near its base, with an inferred USVH (US-31) higher up, and a DSVH at its top on the south. The upper volcanic sequence contains, in its basal felsic layers, contains one AADH, one USVH and two inferred DSVH samples. This section has a representative of all three groups of samples, and four of the five sample types (lacking only EATH). No stratigraphic order is evident, except for the DATH sample's

location at the exposed base of the succession (which is probably not the actual base; see p. 23). In particular, DSVH and USVH appear to be intimately intercalated throughout the succession. If these two indeed represent distinct genetic types, as the REE data demand, then at least two sources of magma must have been active contemporaneously. These distinct sources may be defined by either different source compositions or different generative processes. Any petrogenetic model must provide some explanation for two active magma sources within the same volcanic sequence.

Limited sampling of the northern end of the Back River volcanic complex indicates a calc-alkaline trend, with a possible similarity to the DSVH trend (see Figure 19 and discussion). However, because of intense carbonation and sericitization, more cannot be said.

## PETROGENESIS

Having surveyed the variations and correlations of the Hackett River analyses, broken them into genetically distinct groups and compared them both with each other (in time, space and composition) and with other Archean and Recent volcanics, it remains to consider possible source rocks and conditions of magma formation. This may best be done for metamorphosed and altered volcanics such as those under consideration, by use of trace-element modelling techniques.

### Trace-Element Modelling Methods

The theory behind the use of trace elements in petrogenetic studies is summarized in Arth (1976). In brief: A bulk distribution coefficient D may be calculated for each element and each mineralogy which is assumed for a source, by taking a weighted average of the published distribution coefficients for each mineral present. If modal melting is assumed (minerals melt at equal rates), this value is sufficient. If more realistic nonmodal melting is assumed, a bulk melt distribution coefficient P must also be calculated, in which the mineral distribution coefficients are weighted, not by the percentage of each mineral in the rock, but the percentage of the melt that is contributed by the mineral. A realistic percentage of melting is assumed (called F), and a value $c^l/c_o$ is calculated, which is the ratio of the concentration of any element in the melt to its concentration in the parent rock. This is done by using formulas assuming either equilibrium or fractional melting

derived by Shaw (1970). Another value of $c^l/c_o$ can be derived by dividing the concentration of an element in the sample by the concentration in the possible source rock. If the two $c^l/c_o$ values match, the derivation is confirmed. If all nonaltered trace elements match well, the postulated mineralogy and F-value are a likely model for magma generation. A similar procedure may be used for fractional crystallization.

There are many assumptions made in the modelling process; therefore, the matching will not be exact. However, in many cases, close fits are obtained for geologically reasonable compositions and degrees of partial melting.

In this study, the sample averages EATH, DATH, AADH, USVH and DSVH, derived as noted in Tables 7-10, were tested against siliceous, mafic and ultramafic source rocks. The compositions assumed for these sources are given in Table 11; these values are taken from the following sources: LKT from the average Archean tholeiite values of Condie and Hunter (1976); SGNL from the siliceous granulite of Condie and Hunter (1976); and PER from a mixture of one-quarter LKT plus three-quarters the garnet lherzolite values of Condie and Harrison (1976). It should be noted that there appears to be some error in the published LKT values for rare earths; values quoted for Sm, Eu and Tb appear to be too high. The $c^l/c_o$ values calculated using these values were therefore not considered as critically as those for La, Ce, Yb and Lu.

The modal mineralogies and melt fractions assumed for various mafic, siliceous and ultramafic sources are also given

Table 11. Composition of Source Rocks for Modelling Calculations.

a) Chemical Composition of Source Rocks.

| | LKT (Mafic) | SGNL (Silicic) | PER (Ultramafic) |
|---|---|---|---|
| $SiO_2$ | 49.7 | 60.5 | 45.2 |
| $TiO_2$ | 1.0 | 0.9 | 0.7 |
| $Al_2O_3$ | 14.9 | 16.2 | 3.5 |
| $Fe_2O_3$ | 12.4 | 6.2 | 8.3 |
| MgO | 6.3 | 3.1 | 37.5 |
| CaO | 9.4 | 6.0 | 3.1 |
| $Na_2O$ | 2.1 | 3.5 | 0.6 |
| $K_2O$ | 0.25 | 2.1 | 0.13 |
| Sr | 135. | 500. | 55. |
| La | 3.5 | 27. | 1.8 |
| Ce | 12. | 55. | 5.6 |
| Sm | 3.9 | 4.8 | 1.5 |
| Eu | 1.5 | 4.8 | 0.58 |
| Tb | 1.2 | 0.7 | 0.44 |
| Yb | 3.0 | 1.8 | 1.3 |
| Lu | 0.3 | 0.26 | 0.19 |
| Y | 30. | | 14. |
| Co | 32. | 10. | 160. |
| Cr | 300. | 50. | 2600. |
| Ni | 100. | | 1900. |

b) Modal Composition of Source Rocks

| Rock Type | ol | cpx | opx | gar | amp | plag | mgt |
|---|---|---|---|---|---|---|---|
| Mafic:(M) | | | | | | | |
| 1.amphibolite | | 30% | | | 50% | 15% | 5% |
| 2.garnet granulite | | 25% | | 20% | | 55% | |
| 3.gabbro | 10% | 40% | 10% | | | 50% | |
| 4.hbl-gar granulite | | 30% | | 15% | 50% | 15% | |
| 5.eclogite I | | 50% | | 50% | | | |
| 6.eclogite II | | 60% | | 40% | | | |
| Silicic:(S) | | | | | | | |
| 1.siliceous granulite | | 15% | | | | 85% | |
| Ultramafic:(U) | | | | | | | |
| 1.peridotite | 70% | 15% | 15% | | | | |
| 2.plagioclase per. | 70% | 10% | 10% | | | 10% | |
| 3.amphib. perid. | 70% | 10% | 10% | | 10% | | |
| 4.garnet perid. | 70% | 10% | 10% | 10% | | | |
| 5.gar-amphib. per. | 70% | 5% | 5% | 10% | 10% | | |
| 6.plag-amphib. per. | 70% | 5% | 5% | | 10% | 10% | |

Table 11. Composition of Source Rocks (continued).

c) Melt Fractions of Source Rocks.

| Rock Type | ol | cpx | opx | gar | amp | plag | mgt |
|---|---|---|---|---|---|---|---|
| Mafic:(M) | | | | | | | |
| 1.amphibolite | | 10% | | | 37% | 52% | 1% |
| 2.garnet granulite | | 25% | | 20% | | 55% | |
| 3.gabbro | 10% | 40% | 10% | | | 50% | |
| 4.hbl-gar granulite | | 10% | | 10% | 30% | 50% | |
| 5.eclogite I | | 50% | | 50% | | | |
| 6.eclogite II | | 60% | | 40% | | | |
| Silicic:(S) | | | | | | | |
| 1.siliceous granulite | | 15% | | | | 85% | |
| Ultramafic:(U) | | | | | | | |
| 1.peridotite | 10% | 50% | 40% | | | | |
| 2.plagioclase per. | 10% | 20% | 20% | | | 50% | |
| 3.amphibole per. | 10% | 30% | 20% | | 40% | | |
| 4.garnet per. | 20% | 30% | 20% | 30% | | | |
| 5.gar.-amphib. per. | 10% | 10% | 10% | 30% | 40% | | |
| 6.plag.-amph. per. | 6% | 7% | 7% | | 30% | 50% | |



in Table 11. These values were assumed in part from known mineralogies of source rocks, and in part from testing linear combinations of minerals in a major-element mixing program modified from Wright and Doherty (1970). Perturbations of up to 5% in the quoted values will not generally affect the results. Garnet granulite, gabbro and eclogite are assumed to melt modally, as is siliceous granulite; all other models were calculated on a nonmodal melting basis, in which olivine is assumed to melt much less, and plagioclase, amphibole and pyroxenes more, than their modal percentage.

Reasonable values for F, the degree of partial melting, were taken from a compilation by Condie (unpublished data) of results from extensive experimentation with the major-element mixing program mentioned above. Small variations in this value do not substantively affect the results.

Mineral distribution coefficients for this study have been taken from compilations in Condie and Harrison (1976) and Condie and Hunter (1976), and are listed in Table 12. There are two sets of coefficients; one applies to mafic to andesitic rocks, the other to dacitic to rhyolitic rocks. EATH and DATH were considered with the former, USVH and DSVH with the latter. For AADH modelling, bulk distribution coefficients were calculated using both tables, then compared.

Modelling was conducted using the elements, Sr, La, Ce, Sm, Eu, Tb, Yb, Lu, Y, Co, Cr and Ni. Use of Rb and Ba was attempted, but the results proved unuseable due to mobilization of these elements by alteration processes.

Table 12. Distribution Coefficients for Model Calculations.

a) Mafic to andesitic

| | ol | cpx | opx | gar | amp | plag | mag |
|---|---|---|---|---|---|---|---|
| Rb | 0.01 | 0.03 | 0.03 | 0.01 | 0.2 | 0.1 | 0.0 |
| Sr | 0.01 | 0.1 | 0.02 | 0.02 | 0.5 | 2.0 | 0.0 |
| Ba | 0.01 | 0.05 | 0.02 | 0.02 | 0.1 | 0.5 | 0.0 |
| La | 0.01 | 0.05 | 0.03 | 0.01 | 0.2 | 0.1 | 0.0 |
| Ce | 0.01 | 0.1 | 0.05 | 0.01 | 0.2 | 0.1 | 0.0 |
| Sm | 0.01 | 0.2 | 0.05 | 1.0 | 0.25 | 0.1 | 0.0 |
| Eu | 0.01 | 0.3 | 0.05 | 1.0 | 0.3 | 0.6v | 0.0 |
| Tb | 0.015 | 0.3 | 0.08 | 5.0 | 0.3 | 0.1 | 0.0 |
| Yb | 0.02 | 0.3 | 0.1 | 7.0 | 0.3 | 0.1 | 0.0 |
| Lu | 0.02 | 0.3 | 0.1 | 7.0 | 0.3 | 0.1 | 0.0 |
| Co | 6. | 1.0 | 2.5 | 1.5 | 1.0 | 0.0 | 10. |
| Cr | 0.1 | 7.0 | 2. | 5.0 | 9.0 | 0.0 | 50. |
| Ni | 30. | 4.0 | 6. | 2.0 | 2.5 | 0.0 | 0.0 |
| Zr | 0.0 | 1.0 | 1.0 | 5.0 | 5.0 | 0.01 | 0.0 |
| Y | 0.01 | 0.8 | 0.5 | 10.0 | 2.0 | 0.01 | 0.0 |

b) Dacitic to rhyolitic

| | ol | cpx | opx | gar | amp | plag | mag |
|---|---|---|---|---|---|---|---|
| Rb | 0.01 | 0.04 | 0.04 | 0.01 | 0.2 | 0.1 | 0.0 |
| Sr | 0.01 | 1.0 | 0.1 | 0.02 | 0.2 | 10. | 0.0 |
| Ba | 0.01 | 0.05 | 0.02 | 0.02 | 0.05 | 0.5 | 0.0 |
| La | 0.01 | 0.3 | 0.1 | 0.1 | 1.0 | 0.3 | 0.0 |
| Ce | 0.01 | 0.5 | 0.2 | 0.3 | 2.0 | 0.3 | 0.0 |
| Sm | 0.01 | 0.5 | 0.2 | 3.0 | 7.0 | 0.15 | 0.0 |
| Eu | 0.01 | 1.0 | 0.15 | 3.0 | 5.0 | 1.v | 0.0 |
| Tb | 0.015 | 1.5 | 0.3 | 15.0 | 6.0 | 0.15 | 0.0 |
| Yb | 0.02 | 2.0 | 0.8 | 25.0 | 5.0 | 0.05 | 0.0 |
| Lu | 0.02 | 2.0 | 0.8 | 25.0 | 5.0 | 0.05 | 0.0 |
| Co | 6.0 | 7.0 | 10. | 15.0 | 30.0 | 0.0 | 10. |
| Cr | 0.1 | 25.0 | 5. | 15.0 | 100. | 0.0 | 50. |
| Ni | 30. | 20.0 | 10. | 5.0 | 30. | 0.0 | 0.0 |
| Zr | 0.0 | 4.0 | 4.0 | 15.0 | 30. | 0.01 | 0.0 |
| Y | 0.01 | 3.0 | 1.0 | 30.0 | 10. | 0.01 | 0.0 |

Values are taken from Condie and Harrison (1976), Condie and Hunter (1976).
v -- values for Eu distribution in plagioclase are highly variable.



## Results of Modelling

### Siliceous Volcanics

The calculated $c^l/c_o$ for the derivation of USVH amd DSVH from various source rocks are compared to model results in Table 13a. From comparison of values, several observations result:

1) Siliceous granulite is not an acceptable source for either USVH or DSVH (the REE pattern is entirely wrong);

2) No mafic source is entirely acceptable for either USVH or DSVH. Total REE concentrations are not high enough in any model for production of USVH from LKT or DATH; nor is there an acceptable fit to the EATH/USVH values. Garnet granulite (model M2) is the best fit for the LKT/DSVH values, but total REE content is still too low.

3) Ultramafic sources provide the best approximations to both USVH and DSVH. The best solution for USVH is 1% melting of a plagioclase-amphibole peridotite, although this yields a somewhat low Sr value. The quantities of both plagioclase and amphibole in this model (U6) have probably been overestimated; much less of both is called for. Indeed, a peridotite with neither mineral (U1) also yields a good solution; but a small amount of plagioclase would help reduce the Sr value. In all models, Cr values are too high; this may be remedied by assuming that chromite is present as a residual phase. The best solution for DSVH is a garnet peridotite (U4), again with chromite residuum necessary. Other peridotite models do not give melts with trace-element

Table 13. Trace element Modelling Results, continued.

b) Intermediate Volcanics

| M | LKT/ AADH | DATH/ AADH | EATH/ AADH | M1 F | M1 M | M2 F | M2 M |
|---|---|---|---|---|---|---|---|
| Sr | 1.7 | 0.97 | 0.84 | 1.0 | 1.9 | 0.18 | 0.89 |
| La | 5.4 | 8.3 | 1.0 | 1.4 | 3.3 | 3.2 | 7.4 |
| Ce | 3.5 | 6.1 | 1.08 | 0.83 | 3.2 | 2.5 | 6.8 |
| Sm | 1.3 | 2.5 | 1.02 | | 2.7 | 1.2 | 2.8 |
| Eu | 1.0 | 1.8 | 1.0 | 0.38 | 2.3 | 0.73 | 1.6 |
| Tb | 0.70 | 1.64 | 0.91 | | 2.4 | 0.30 | 0.89 |
| Yb | 1.0 | 1.15 | 1.0 | 0.35 | 2.4 | 0.19 | 0.67 |
| Lu | 1.0 | 1.68 | 1.16 | 0.35 | 2.4 | 0.19 | 0.67 |
| Y | 0.60 | 1.84 | 1.64 | 0.35 | 0.78 | 0.16 | 0.47 |
| Co | 0.74 | 0.55 | 0.62 | 0.066 | 0.72 | 0.22 | 0.72 |
| Cr | 0.19 | 0.30 | 0.45 | 0.018 | 0.12 | 0.12 | 0.38 |
| Ni | 0.38 | 0.45 | 0.84 | 0.054 | 0.42 | 0.18 | 0.68 |
| F | | | | 20% | 20% | 7% | 7% |

| Sil | SGNL/ AADH | S1(F) | PER/ AADH | U1 F | U1 M | U2 F | U2 M | U3 F | U3 M | U4 F | U4 M | U5 F | U5 M | U6 F | U6 M |
|---|---|---|---|---|---|---|---|---|---|---|---|---|---|---|---|
| Sr | 0.46 | 0.23 | 4.15 | 4.9 | 11.0 | 1.2 | | 5.6 | 8.2 | 6.5 | 14.6 | 8.0 | 9.6 | 1.3 | |
| La | 0.70 | 1.5 | 10.6 | 8.1 | 11.6 | 7.6 | 11.1 | 5.5 | 10.2 | 10. | 15.7 | 6.1 | 12.9 | 6.0 | 9.7 |
| Ce | 0.78 | | 7.7 | 6.3 | 10.5 | 6.4 | 10.4 | 3.6 | 9.7 | 7.0 | 14.5 | 3.6 | | 3.5 | |
| Sm | 1.0 | | 3.2 | 6.3 | 9.5 | 6.8 | 9.5 | 1.6 | 8.7 | 2.7 | 6.2 | 1.1 | | 1.5 | |
| Eu | 0.88 | 0.93 | 2.6 | 4.8 | 8.5 | 4.15 | 6.8 | 1.9 | 7.9 | 2.4 | 4.8 | 1.3 | | 1.7 | |
| Tb | 1.2 | | 1.9 | 3.5 | 8.0 | | | 1.5 | 7.6 | 0.67 | 1.9 | 0.53 | | 1.55 | |
| Yb | 1.7 | 1.4 | 2.4 | 2.4 | 7.7 | 3.0 | 8.0 | 1.5 | 7.3 | 0.41 | 1.45 | 0.37 | 1.4 | 1.6 | 7.6 |
| Lu | 2.2 | 1.4 | 3.0 | 2.4 | 7.7 | 3.0 | 8.0 | 1.5 | 7.3 | 0.41 | 1.45 | 0.37 | 1.4 | 1.6 | 7.6 |
| W | 1.1 | 0.45 | 1.3 | 1.8 | 4.4 | 2.4 | 5.3 | 0.89 | 3.1 | 0.34 | 1.01 | 0.28 | 0.89 | 0.95 | |
| Co | 2.4 | 0.98 | 0.15 | 0.16 | 0.22 | 0.18 | 0.22 | 0.13 | 0.22 | 0.14 | 0.21 | 0.12 | 0.22 | 0.14 | |
| Cr | 1.1 | 0.45 | 0.021 | 0.28 | 0.84 | 0.37 | 1.09 | 0.10 | 0.66 | 0.25 | 0.81 | 0.09 | 0.60 | 0.11 | |
| Ni | | | 0.020 | 0.041 | 0.045 | 0.04 | 0.05 | 0.04 | 0.05 | 0.04 | 0.04 | 0.04 | 0.05 | 0.041 | |
| F | | 55% | | 7% | 7% | 7% | 7% | 7% | 7% | 5% | 5% | 5% | 5% | 7% | 7% |

See notes on previous page
F, M in headings; felsic or mafic values of D, from Table 12.



Table 13. Trace-element Modelling Results. $C^1/C_o$ compared between sample/source and model.

a) Siliceous Volcanics

| Mod | LKT/ USVH | DATH/ USVH | EATH/ USVH | M1 | M2 | M3 | M4 | M5 | M6 | LKT/ DSVH | DATH/ DSVH | EATH/ DSVH |
|---|---|---|---|---|---|---|---|---|---|---|---|---|
| Sr | 1.1 | 0.64 | 0.56 | 0.63 | 0.18 | 0.19 | | 1.79 | 1.54 | 2.1 | 1.2 | 1.0 |
| La | 5.1 | 7.8 | 0.95 | 1.5 | 3.5 | 3.6 | | 3.6 | 3.4 | 6.6 | 10. | 1.2 |
| Ce | 3.9 | 6.7 | 1.2 | 0.83 | 2.7 | 2.8 | | 2.2 | | 3.8 | 6.6 | 1.15 |
| Sm | 1.1 | 2.3 | 0.94 | | 1.2 | 3.6 | | 0.60 | | 0.82 | 1.7 | 0.68 |
| Eu | 0.93 | 1.7 | 0.93 | 0.35 | 0.72 | 1.2 | | 0.53 | | 0.73 | 1.3 | 0.73 |
| Tb | 0.62 | 1.5 | 0.82 | | 0.30 | 1.7 | | 0.13 | | 0.33 | 0.80 | 0.44 |
| Yb | 0.90 | 1.0 | 0.87 | 0.33 | 0.19 | 1.4 | | 0.082 | 0.10 | 0.20 | 0.22 | 0.19 |
| Lu | 1.43 | 1.3 | 0.88 | 0.33 | 0.19 | 1.4 | | 0.082 | 0.10 | 0.30 | 0.26 | 0.18 |
| Y | 0.47 | 1.4 | 1.3 | 0.17 | 0.15 | 0.95 | | 0.067 | 0.080 | 0.06 | 0.17 | 0.15 |
| Co | 0.55 | 0.41 | 0.46 | 0.06 | 0.22 | 0.28 | | 0.10 | 0.11 | 0.22 | 0.17 | 0.19 |
| Cr | 0.15 | 0.25 | 0.37 | 0.017 | 0.11 | 0.13 | | 0.055 | 0.053 | 0.19 | 0.31 | 0.46 |
| Ni | 0.15 | 0.18 | 0.33 | 0.050 | 0.17 | 0.10 | | 0.088 | 0.080 | 0.20 | 0.24 | 0.44 |
| F | | | | 7% | 3% | 4% | | 10% | 10% | | | |

| Sil | SGNL/ USVH | S1 | SGNL/ DSVH | PER/ USVH | U1 | U2 | U3 | U4 | U5 | U6 | PER/ DSVH |
|---|---|---|---|---|---|---|---|---|---|---|---|
| Sr | 0.30 | 0.16 | 0.56 | 2.7 | 5.7 | 0.93 | 7.0 | 8.0 | 10.9 | 0.98 | 5.05 |
| La | 0.67 | 1.96 | 0.85 | 10. | 13. | 11.8 | 6.1 | 15. | 7.0 | 7.4 | 13. |
| Ce | 0.85 | | 0.84 | 8.4 | 8.4 | 8.8 | 3.6 | 8.8 | 3.7 | 3.6 | 8.2 |
| Sm | 0.92 | | 0.67 | 2.9 | 8.4 | 10.0 | 1.3 | 2.7 | 0.99 | 1.3 | 2.1 |
| Eu | 0.82 | 0.89 | 0.69 | 2.4 | 5.4 | 4.4 | 1.6 | 2.4 | 1.2 | 1.5 | 1.9 |
| Tb | 1.06 | | 0.57 | 1.7 | 3.6 | 4.7 | 1.3 | 0.61 | 0.47 | 1.4 | 0.91 |
| Yb | 1.5 | 1.86 | 0.33 | 2.1 | 2.3 | 3.3 | 1.3 | 0.37 | 0.33 | 1.5 | 0.46 |
| Lu | 1.6 | 1.86 | 0.35 | 2.3 | 2.3 | 3.3 | 1.3 | 0.37 | 0.33 | 1.5 | 0.47 |
| Y | | | | 1.0 | 1.7 | 2.4 | 0.73 | 0.30 | 0.24 | 0.84 | 0.12 |
| Co | 1.76 | 0.97 | 0.71 | 0.11 | 0.15 | 0.17 | 0.11 | 0.14 | 0.11 | 0.13 | 0.044 |
| Cr | 0.90 | 2.93 | 1.12 | 0.017 | 0.22 | 0.33 | 0.079 | 0.22 | 0.079 | 0.089 | 0.022 |
| Ni | | | | 0.008 | 0.039 | 0.042 | 0.037 | 0.041 | 0.039 | 0.039 | 0.011 |
| F | | 30% | | | 1% | 1% | 1% | 1% | 1% | 1% | |

M1, etc--model numbers from Table 11.
LKT/USVH, etc.--calculated $c^1/c_o$, as (USVH)/(LKT); acronyms from Tables 7-10 and 11.

contents such as those found for USVH and DSVH.

Intermediate Volcanics

Calculated $c^l/c_o$ values for the derivation of AADH from various source rocks by partial melting are compared to model results in Table 13b. From comparison of values:

1) As with siliceous volcanics, a siliceous granulite source is not acceptable for the formation of AADH.

2) No mafic source is acceptable for the formation of AADH. The slope of the REE pattern cannot be reproduced by the mafic models considered; furthermore, due to the similarities between USVH and AADH patterns, sources ruled out for USVH need not be considered for AADH.

3) Ultramafic sources provide the best approximations to AADH. The best solution is a 7% melt of a peridotite with neither plagioclase, amphibole nor garnet (U1). For this model, all PER/AADH values fall between the felsic and mafic calculated values, except for Sr which is low, and the middle REE. Cr is again too low, and demands chromite in the source. Some plagioclase and perhaps some amphibole in the source rock would help the fit.

Mafic Volcanics

Calculated $c^l/c_o$ values for the derivation of EATH and DATH from various source rocks are compared to model results in Table 13c. From comparison of values:

1) Mafic sources cannot reproduce either the light REE enrichment of EATH, nor the depletion of DATH; transition metal



Table 13. Trace-element Modelling Results, continued.

c) Mafic Volcanics

| M | LKT/ EATH | DATH/ EATH | M1 | M2 | M3 | M4 | M5 | M6 | LKT/ DATH |
|---|---|---|---|---|---|---|---|---|---|
| Sr | 2.0 | 1.15 | 2.1 | 0.92 | | 2.0 | | 1.9 | 1.7 |
| La | 5.4 | 8.3 | 1.9 | 2.5 | | 2.1 | | 1.9 | 0.66 |
| Ce | 3.3 | 5.7 | 1.9 | 2.5 | | 2.0 | | 1.9 | 0.58 |
| Sm | 1.8 | 2.5 | 1.7 | 1.8 | | 1.5 | | 1.3 | 1.49 |
| Eu | 1.0 | 1.83 | 1.7 | 1.3 | | 1.5 | | 1.3 | 0.55 |
| Tb | 0.75 | 1.33 | 1.6 | 0.92 | | 0.88 | | 0.63 | 0.42 |
| Yb | 1.03 | 1.15 | 1.6 | 0.74 | | 0.74 | | 0.50 | 0.90 |
| Lu | 1.6 | 1.44 | 1.6 | 0.74 | | 0.74 | | 0.50 | 1.13 |
| Y | 0.37 | 1.12 | 0.76 | 0.56 | | 0.41 | | 0.36 | 0.33 |
| Co | 1.2 | 0.88 | 1.0 | 1.4 | | 0.83 | | 0.91 | 1.34 |
| Cr | 0.41 | 0.68 | 0.2 | 0.47 | | 0.16 | | 0.28 | 0.61 |
| Ni | 0.45 | 0.53 | 0.43 | 0.75 | | 0.38 | | 0.48 | 0.85 |
| F | | | 45% | 35% | | 40% | | 50% | |

| U | PER/ EATH | U1,U2 | U3 | U4 | U5 | U6 | PER/ DATH |
|---|---|---|---|---|---|---|---|
| Sr | 4.9 | 4.7 | 4.5 | 3.8 | 3.8 | | 4.2 |
| La | 10.6 | 4.7 | 4.7 | 3.9 | 3.9 | 4.6 | 1.3 |
| Ce | 7.1 | 4.6 | 4.6 | 3.8 | | | 1.2 |
| Sm | 3.1 | 4.5 | 4.5 | 3.5 | | | 1.3 |
| Eu | 2.6 | 4.4 | 4.4 | 3.4 | | | 1.4 |
| Tb | 2.0 | 4.3 | 4.3 | 2.5 | | | 1.1 |
| Yb | 2.4 | 4.2 | 4.2 | 2.2 | 2.2 | 4.2 | 2.1 |
| Lu | 2.6 | 4.2 | 4.2 | 2.2 | 2.2 | 4.2 | 1.8 |
| Y | 0.79 | 3.5 | 3.2 | 1.9 | 1.9 | | 0.70 |
| Co | 0.24 | 0.22 | 0.22 | 0.22 | 0.23 | | 0.27 |
| Cr | 0.047 | 1.24 | 1.18 | 1.6 | 1.5 | | 0.07 |
| Ni | 0.024 | 0.047 | 0.047 | 0.047 | 0.048 | | 0.045 |
| F | | 20% | 20% | 25% | 25% | 20% | |

See Notes on previous pages.

values are also inexplicable by mafic models.

2) Once again, peridotite sources provide the closest approximations to the observed values. No model, however, adequately accounts for all trace-element features of either EATH or DATH. The best solution for EATH is a garnet peridotite (model U4), again with residual chromite; however, the enrichment in light REE is insufficient in this (or any other tested) model. It is therefore necessary to call on either 1)pre-enrichment of ultramafic material with light REE; 2) concentration of light REE in low-melting minor phases; or 3) enrichment of HR-11 in light REE during alteration after emplacement. The best approximation to DATH values is a non-garnet-bearing peridotite (models U1, U2, U3, U6). However, all these models yield REE contents two to four times too high. One therefore needs a depleted peridotite to produce DATH. It was attempted to derive this depleted rock from the residuum after partial melting to produce AADH as described above; however, the degree of depletion was only half that needed.

Summary of Preferred Models

The preferred models gleaned from the comparisons of Table 13 are shown schematically in Figure 20. Both USVH and AADH are derived from a common source; this is in keeping with the arbitrary nature of the division between them. DSVH and EATH are both derived from a source with garnet present. DATH, on the other hand, requires a source highly depleted in rare earths. Because of the necessity of assuming



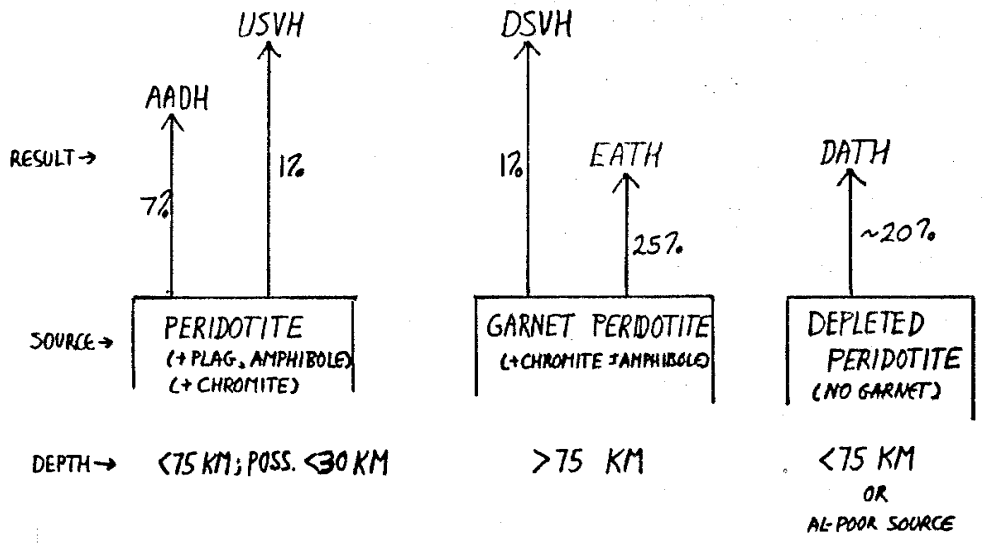


FIGURE 20. SCHEMATIC DIAGRAM OF MAGMA ORIGINS

a different composition for the DATH source from PER, the degree of melting is uncertain..

A depth of origin for each magma can be inferred from consideration of a whole-rock phase diagram for peridotite mineral assemblages (Ringwood, 1969, quoted in Condie, 1976). The presence of garnet in peridotite at melting temperatures requires a source greater than about 75 km, whereas the presence of plagioclase requires a source less than about 30 km. These depths are quoted on Figure 20. The source of AADH and USVH does not contain garnet, hence is less than 75 km deep; if plagioclase is present, as is possible, it is less than 30 km. The source for DSVH and EATH contains garnet, hence is over 75 km deep. The source for DSVH contains no garnet; this would indicate a depth of less than 75 km. However, as the PER composition is not valid for this source, this depth determination is not strictly valid.

## Tectonic Significance

Several facets of the assemblage of models outlined above bear upon the problems of tectonic evaluation of the Hackett River volcanic belt. It is not possible, with the limited sampling and restricted range of models considered, to attempt a tectonic reconstruction solely on geochemical grounds. However, some constraints on any such reconstruction can be placed from the model results.

A striking feature of the diagram of preferred models is the absence of mafic models. This is in contrast to the



summary of models presented in Condie (1976), where DSV, LAA and EAT are derived from an eclogite source. This absence implies that the source of magma can be neither a subducted mafic oceanic crust, nor the base of a subsiding pile of mafic volcanics--both models which have been proposed for formation of intermediate and felsic volcanic rocks in the Archean volcanic sequences. The Hackett River volcanics demand either a ultramafic mantle source or an ultramafic oceanic crust undergoing subduction.

The models presented above demand two sources of magmas; one deep, one shallow. These two sources must have been active concurrently, as USVH/AADH and DSVH samples appear to be intricately interbedded in the Uist Lake area, and EATH occurs within a sequence of AADH and USVH volcanics. Therefore, any model for the formation of the Hackett River volcanic sequence must satisfy these conditions:

1) It must provide for two simultaneous sources of magma, one at a depth greater than 75 km, the other shallower, preferably less than 30 km.

2) It should not depend on melting of mafic source rocks;

3) It must provide for a depleted ultramafic source for DSVH.

This last constraint is not perhaps as severe as it seems. The REE pattern for DSVH falls at the bottom of the range of rise and arc tholeiites. Presumably, therefore, one can call upon the same depleted source as today produces these rocks, perhaps ascribing the Mg and Fe enrichment to a higher temperature

due to a higher geothermal gradient during the Archean. However, the inclusion of garnet peridotite as a source of magma suggests a geothermal gradient during the Archean not much greater than the present-day oceanic geotherm (see Condie, 1976b, p. 47).

## Further Work

Confirmation of the intercalating nature of the two types of siliceous volcanics (USVH and DSVH) is needed; rare-earth analyses should be run on US-31, US-4 and US-26. Adjacent sample localities should be reexamined for possible analysis.

Further chemical study of the Back River volcanic complex should be undertaken, beginning with the RL-series samples, to determine if the same intercalating pattern occurs in this later sequence. Evaluation of the effects of carbonation should be made in this regard.

More sophisticated modelling needs to be done, taking into account details of the petrology of mantle systems and observed mineralogies of source rocks. The Mg and Fe enrichment of the basaltic samples was not considered in the selection of F-values for trace-element modelling; the major-element mixing program needs to be used to define any differences in this regard.

The methods of correlation coefficients and cluster analysis applied to discerning differentiating, mobile and inheritance-masked elements needs to be applied to better-known volcanic



sequences with larger numbers of samples to establish its usefulness in geochemical studies.

Better analytical precision should be obtained for MgO and the transition elements than was achieved in this study.

More detailed mapping and sampling should be undertaken in the Hackett River sequence. Such study would include the tracing of individual beds or flow units, the evaluation of within-unit geochemical variation and alteration, and trace-element analysis.

Finally, better methods for computerized data processing, statistical analysis and optimization techniques, and chemical modelling should be developed to speed and complete the manipulations performed manually in this project.

REFERENCES CITED

Anhaeusser, C.R., 1973, The evolution of the early Precambrian crust of southern Africa; Roy. Soc. London Philos. Trans., Series A, v.273, p.359-388.

Anhaeusser, C.R., Mason, R., Viljoen, M.J., Viljoen, R.P., 1969, A reappraisal of some aspects of Precambrian shield geology; Geol. Soc. Am. Bull., v.80, p.2175-2200.

Arth, J.G., 1976, Behavior of trace elements during magmatic processes--a summary of theoretical models and their applications; Jour. Research U.S. Geol. Survey, v.4,p.41-47.

Arth, J.G., Hanson, G.N., 1975, Geochemistry and origin of the early Precambrian crust of northeastern Minnesota; Geochim. Cosmochim. Acta, v.39, p.325-362.

Arndt, N.T., Naldrett, A.J., Pyke, D.R., 1977, Komatiitic and iron-rich tholeiitic lavas of Munro Township, northeast Ontario; Jour. Petrology, v.18, Part 2, in press.

Baragar, W.R.A., 1966, Geochemistry of the Yellowknife volcanic rocks; Can. Jour. Earth Sci., v.3, p.9-30.

Baragar, W.R.A., Goodwin, A.M., 1969, Andesites and Archean volcanism of the Canadian Shield; in Proceedings of the Andesite Conference; Bull. 65, Oregon Dept. Geology and Mineral Industries, p. 121-142.

Bowen, R.W., 1971, Graphic Normative Analysis Program; U.S. Geol. Survey Computer Contribution #13, 43pp.

Boyle, R.W., 1961, The geology, geochemistry and origin of the gold deposits of the Yellowknife district; Geol. Survey Canada, Memoir 310 193pp.

Bryan, W.P.D., Padgham,W.A., Jefferson, C.W., Shegelski,R.J., Remayne, E.A., and Vandor, H.E., 1975, Geology of 76-F-9, E.G.S. Map 1976-5-preliminary edition; DIAND,Ottawa.

Cameron, E.M., 1974, Geochemical methods of exploration for massive sulphide mineralization in the Canadian Shield; Proceedings 5th Intl. Geochemical Exploration Symposium, Vancouver.

Cameron, E.M., 1975, Integrated studies on mineral resource appraisal in the Beechey Lake belt of the northern Shield; in Report of Activities, Part A; Geol. Surv. Canada Paper 75-1, p.189-192.

Cameron, E.M., Durham,C.C., 1974, Geochemical studies in the eastern part of the Slave Structural Province, 1973; Geol. Surv. Canada Paper 74-22, 22pp.

Carmichael, I.S.E., Turner, F.J., Verhoogen, J., 1974, Igneous Petrology. New York, McGraw Hill, 739pp.

Chayes, F., 1975, A priori and experimental approximation of simple ratio correlations; Chapter 5 of R.B. McCammon, ed., Concepts in Geostatistics; Springer-Verlag, pp.106-137.

Church, B.N., 1975, Quantitative classification and chemical comparison of common volcanic rocks; Geol. Soc. Am. Bull., v.86, p.257-263.

Condie, K.C., 1976a, Trace-element geochemistry of Archean greenstone belts; Earth Science Reviews, v.12, pp.

Condie, K.C., 1976b, Plate tectonics and crustal evolution. New York, Pergamon, 288pp.

Condie, K.C., Baragar, W.R.A., 1974, Rare-earth element distributions in volcanic rocks from Archean greenstone belts; Contrib. Mineral. Petrol., v.45, p.237-246.

Condie, K.C., Harrison, N.M., 1976, Geochemistry of the Archean Bulawayan Group, Midlands greenstone belt, Rhodesia; Precambrian Research, v.3, pp.

Condie, K.C., Hunter, D.R., 1976, Trace element geochemistry of the Archean granitic rocks from the Barberton region, South Africa; Earth Plan. Sci. Letters, v.29, p.389-400.

Condie, K.C., Lo, H.H., 1971, Trace element geochemistry of the Louis Lake batholith of early Precambrian age, Wyoming; Geochim. Cosmochim. Acta, v.35, p.1099-1120.

Engel, A.E.J., Engel, C.E., 1962, Progressive metamorphism of amphibolite, northwest Adirondack mountains, New York; Geol. Soc. Am. Bull., Buddington vol., pp.37-82.

Field, D., Elliott, R.B., 1974, The chemistry of gabbro/amphibolite transitions in South Norway. II. Trace elements; Contrib. Min. Petrol., v.47, p.63-76.

Fraser, J.A., 1964, Geological notes on the northeastern District of Mackenzie, Northwest Territories; Geol. Surv. Canada, Paper 63-40,

Frith, R., Frith, R.A., Doig, R., 1977, The geochronology of the granitic rocks along the Bear-Slave Structural Province boundary, northwest Canadian Shield; Can. Jour. Earth Sci., v.14, p.1356-1373.

Frith, R.A., Fyson, W.K., Hill, J.D., 1977, The geology of the Hackett-Back River greenstone belt--second preliminary report; in Report of Activities, Part A; Geol. Surv. Can. Paper 77-1A, p.415-423.



Frith, R.A., Hill, J.D., 1975, The geology of the Hackett-Back River greenstone belt--preliminary account; Geol. Surv. Can., Paper 75-1C, p.367-370.

Frith, R.A., Roscoe, S.M., 1977, Tectonic setting and sulphide deposits of the Hackett River greenstone belt, Slave Province (abs); CIM Bulletin, v.70, p.69-70.

Glikson, A.Y., 1971, Primitive Archaean elemental distribution patterns: Chemical evidence and geotectonic significance; Earth Plan. Sci. Letters, v.12, p.309-320.

Gordon, G.E., Randle, K., Goles, G.G., Corliss, J.B., Beeson, M.H., Oxley, S.S., 1968, Instrumental activation analysis of standard rocks with high-resolution -ray detectors; Geochim. Cosmochim. Acta, v.32, p.369-396.

Green, D.C., Baadsgaard, H., 1971, Temporal evolution and petrogenesis of an Archean crustal segment at Yellowknife, N.W.T.; Jour. Petrology, v.12, p.177-217.

Hart, S.R., Brooks, C., Krogh, T.E., Davis, G.L., Nava, D., 1970, Ancient and modern volcanic rocks: a trace element model; Earth Plan. Sci. Letters, v.10, p.17-28.

Haskin, L.A., Haskin, M.A., Frey, F.A., Wildeman, T.R., 1968, Relative and absolute terrestrial abundances of the rare earths; in L.H. Ahrens, ed., Origin and distribution of the elements. Pergamon Press, Oxford, p.889-912.

Hayslip, D.L., 1973, Geochemistry of the bimodal Quaternary volcanism in the Medicine Lake Highland, northern California;

M.S. thesis, New Mexico Institute of Mining and Technology, 129pp.

Henderson, J.B., 1975, Sedimentology of the Archean Yellowknife Supergroup at Yellowknife, District of Mackenzie; Geol. Surv. Canada, Bulletin 246, 62pp.

Henderson, J.F., Brown, I.C., 1966, Geology and structure of the Yellowknife greenstone belt, District of Mackenzie; Geol. Surv. Canada, Bulletin 141.

Herrmann, A.G., and others, 1976, Major, minor and trace element compositions of komatiites from the Precambrian crust of southern Africa; Contrib. Min. Petrol., v.59, p.1-12.

Hodgman, C.D., Weast, R.C., Shankland, R.S., Selby, S.M., eds., 1962, Handbook of chemistry and physics. Cleveland, Chemical Rubber, 3604pp.

Jahn, B.-M., Shih, Chi-Yu, Murthy, V.R., 1974, Trace element geochemistry of Archean volcanic rocks; Geochim. Cosmochim. Acta, v.38, p.611-627.

Jakes, P., Gill, J., 1970, Rare earth elements and the island arc tholeiitic series; Earth Plan. Sci. Letters, v.9, p.17-28.

Jefferson,C.W.,Padgham,W.A.,Bryan,M.P.D.,Shegelski,R.J., Ronayne,E.A.,Vandor,H.,Thorstad,L.E.,1976,Geology 76-K-2, E.G.S.Map 1976-4-preliminary edition, DIAND, Ottawa.

Jefferson,C.W.,Padgham,W.A.,Bryan,M.P.D.,Ronayne,E.A.,Shegelski, R.J.,Vandor,H.,Thorstad,L.E.,1976, Geology 76-F-15, E.G.S. Map 1976-4-preliminary edition, DIAND, Ottawa.

Jefferson,C.W.,Padgham,W.A.,Bryan,M.P.D.,Ronayne,E.A.,Shegelski, R.J.,Sterenberg,V.Z.,Vandor,H.,Thorstad,L.E.,1976, Geology



Hackett River, 76-F-16,E.G.S. Map 1976-4-preliminary edition, DIAND, Ottawa.

Jolly, W.T., 1975, Subdivision of the Archean lavas of the Abitibi area, Canada from Fe-Mg-Ni-Cr relations; Earth Plan. Sci. Letters, v.27, p.200-210.

Krumbein, W.C., Graybill,F.A., 1965, An introduction to statistical models in geology. New York, McGraw Hill, 475pp.

Kuno, H., 1966, Lateral variations of basalt magma type across continental margins and island arcs; Bull. volcanol., v.29, p.195-222.

Lambert, M.B., 1976, The Back River volcanic complex, District of Mackenzie; in Report of Activities, Part A; Geol.Surv. Canada Paper 76-1A, pp.363-367.

Langford, F.F., Morin, J.A., 1976, The development of the Superior Province of northwestern Ontario by merging island arcs; Am. Jour. Sci., v.276, p.1023-1034.

McGlynn, J.C., Henderson, J.B., 1972, The Slave Province; in Variations of tectonic styles in Canada; Geol. Assoc. Canada Spec. Paper 11, p.505-526.

Nesbitt, R.W., Sun, S.S., 1976, Geochemistry of Archean spinifex-textured peridotites and magnesian and low-magnesian tholeiites; Earth Plan. Sci. Letters, v.31,p.433-453

Nockolds, S.R., 1954, Average chemical compositions of some igneous rocks; Geol. Soc. Am. Bull., v.65, p.1007-1032.

Padgham,W.A.,Jefferson,C.W.,Ronayne,E.A.,Sterenberg,V.Z.,1974a, Geology of Index Lake, 76-G-13,perliminary edition;DIAND,Ottaw

Padgham,W.A.,Bryan,M.P.D.,Ronayne,E.A.,Sterenberg,V.Z.,1974b, Geology of Hackett River, 76-F-16, preliminary edition; DIAND, Ottawa.

Padgham,W.A.,Bryan,M.P.D.,Ronayne,E.A.,Sterenberg,V.Z.,1974c, Geology of 76-F-9, preliminary edition; DIAND, Ottawa.

Padgham,W.A.,Sterenberg,V.Z.,Bryan,E.A.,Ronayne,E.A.,Jefferson,C.W., 1974d, Geology of 76-G-5, preliminary edition;DIAND, Ottawa.

Padgham,W.A.,Bryan,M.D.P.,Jefferson,C.W.,Ronayne,E.A., Sterenberg,V.Z.,1974e, Geology of Agricola Lake, 76-G-12, preliminary edition; DIAND, Ottawa.

Padgham,W:A.,Jefferson,C.W.,Shegelski,R.J.,Bryan,M.P.D.,Ronayne,E.A., Vandor,H.,Thorstad,L.E.,1976, Geology 76-K-1,E.G.S. Map 1976-6-preliminary edition; DIAND, Ottawa.

Ridler, R.H., 1973, Exhalite concept--a new tool for exploration; Northern Miner, v.59, no.37, p.59-62.

Ringwood, A.E., 1969, Composition and evolution of the upper mantle; Am. Geophys. Union Mon., No.13, p.1-17.

Schilling, J., 1969, Red Sea floor origin: rare-earth evidence; Science, v.165, p.1357.

Shaw, D.M., 1970, Trace element fractionation during anatexis; Geochim. Cosmochim. Acta, v.34, p.237-243.

Stockwell, C.H., 1972, Revised Precambrian time scale for the Canadian Shield; Geol. Surv. Canada, Paper 72-52, 4pp.

Thomas, M.D., Gibb, R.A., Quince, J.R., 1976, New evidence from offset aeromagnetic anomalies for transcurrent faulting associated with the Barthurst and McDonald Faults, Northewst Territories; Can. Jour. Earth Sci., v.13, p.1244-1250.



Viljoen, R.P., Viljoen, M.J., 1969a, The effects of metamorphism and serpentinization on the volatile contents of associated rocks of the Barberton region; in Upper Mantle Project, Geol. Soc. South Africa Spec. Pub. 2, pp.29-53.

Viljoen, R.P., Viljoen, M.J.,1969b, Geology and geochemistry of the lower formations, Onverwacht Group and a proposed new class of igneous rocks; in Upper Mantle Project, Geol. Soc. South Africa Spec. Pub. 2, p.55-85.

Viljoen, M.J., Viljoen, R.P., 1969c, The geological and geochemical significance of the upper formations of the Onverwacht Group; in Upper Mantle Project, Geol. Soc. South Africa Spec. Pub. 2, p.113-152.

Wilson, H.D.B., Andrews, P., Maxham, R.L., Ramlal, K., 1965, Archean volcanism in the Canadian Shield; Can. Jour. Earth Sci., v.2, p.161-175.

Wright, G.M., 1957, Geological notes on the eastern District of Mackenzie, Northwest Territories; Geol. Surv. Canada Paper 56-10.

Wright, T.L., Doherty, P.C., 1970, A linear programming and least squares computer method for solving petrologic mixing problems; Geol. Soc. Am. Bull., v.81, p.1995-2008.

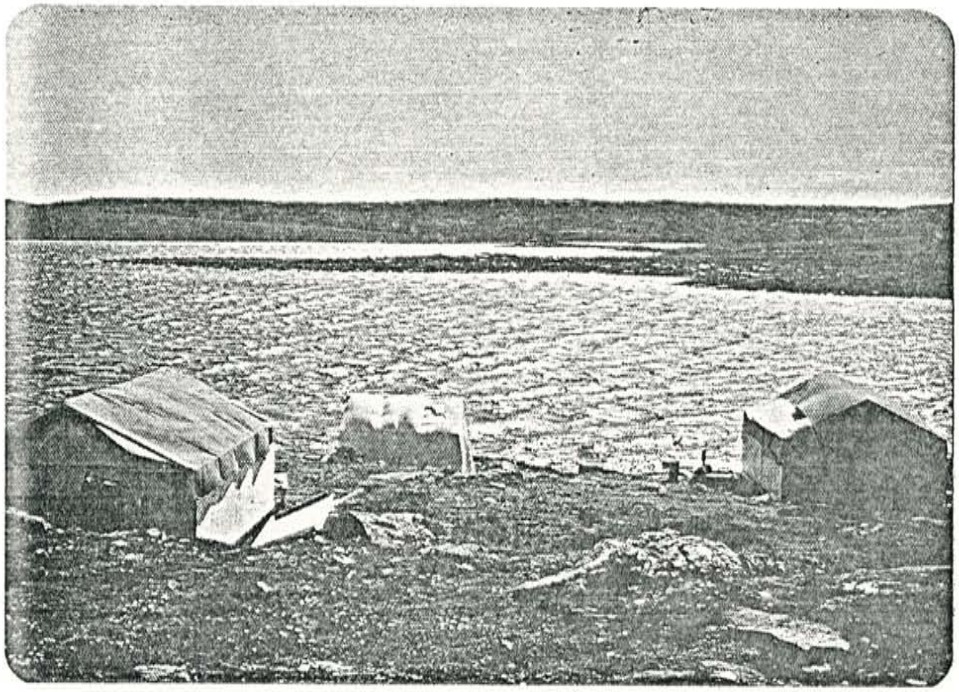

Photo 1. D'Arcy Lake camp, showing general nature of the terrain and the excellence of outcrop. View to SE; outcrops in foreground are bleached rhyolite.

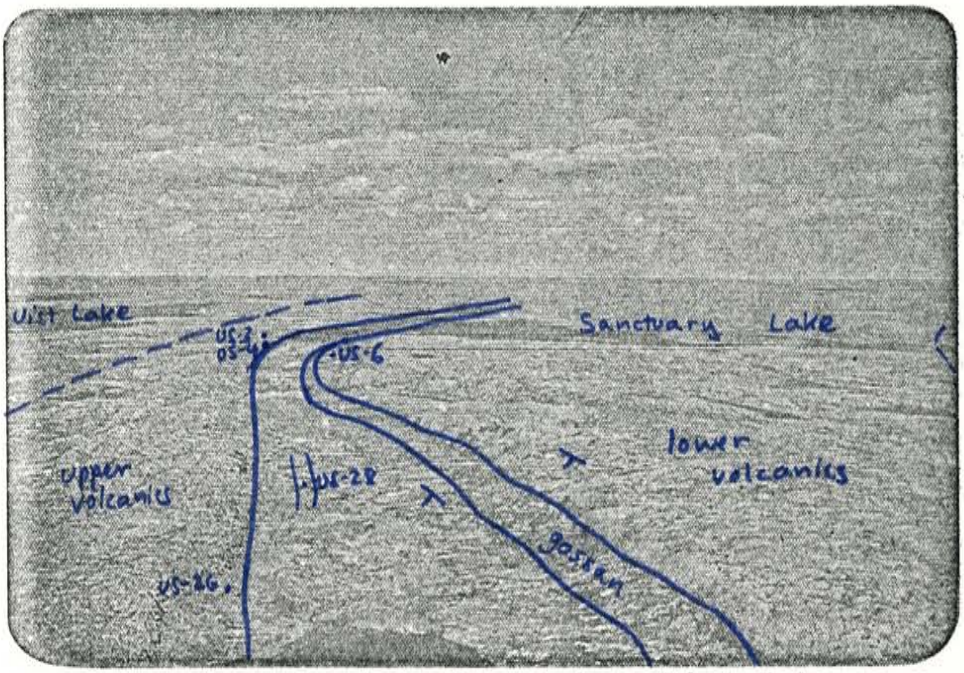


Photo 2. Aerial view W from Uist Lake camp. A trench is developed on shaley sediments (unit 3, Fig. 4), with gossan on the N wall. To N are S-dipping older volcanics.

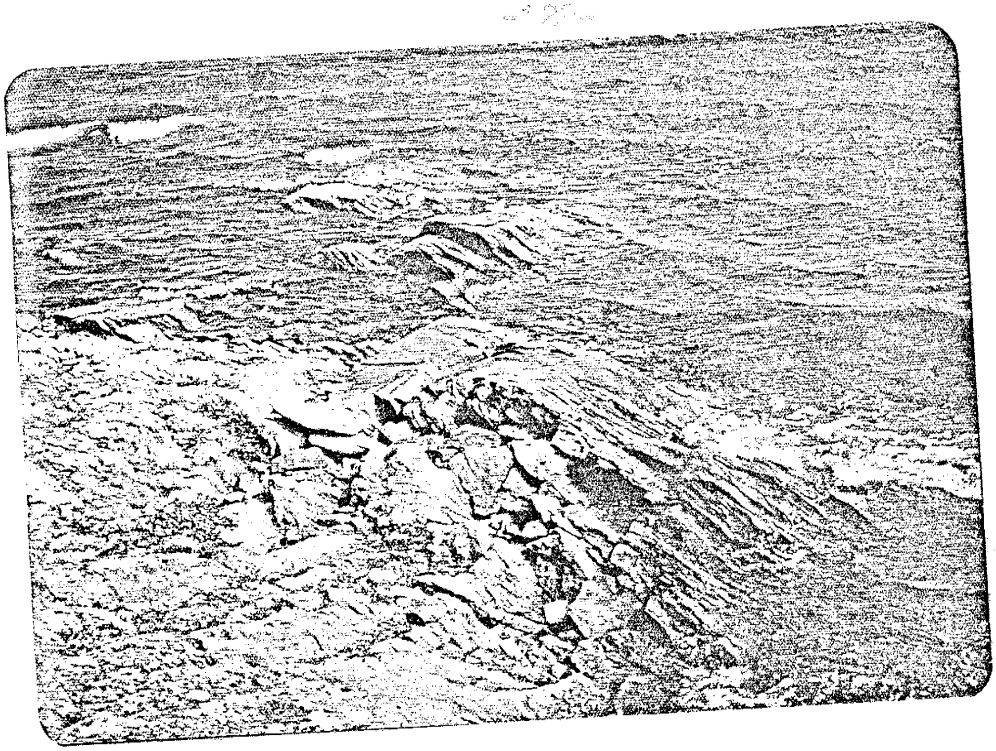

Photo 3. $F_2$ isocline fold, on shore of D'Arcy Isle northeast of Camp. Axis plunges to the NE.

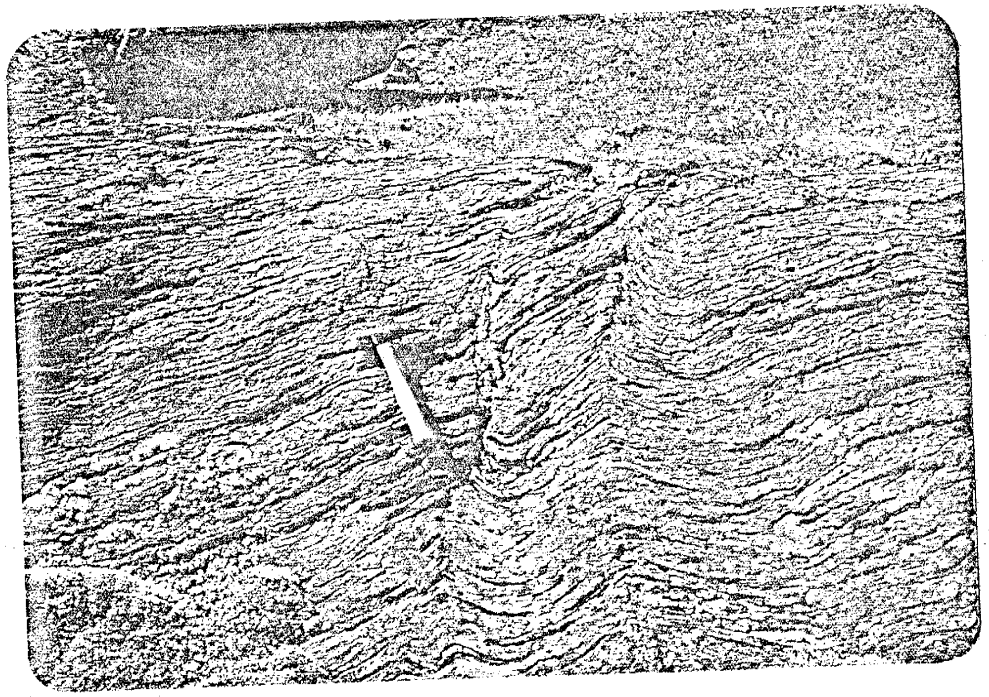

Photo 4. $F_2$ crenulation folds in basaltic tuff unit of upper volcanic sequence, West Lake.

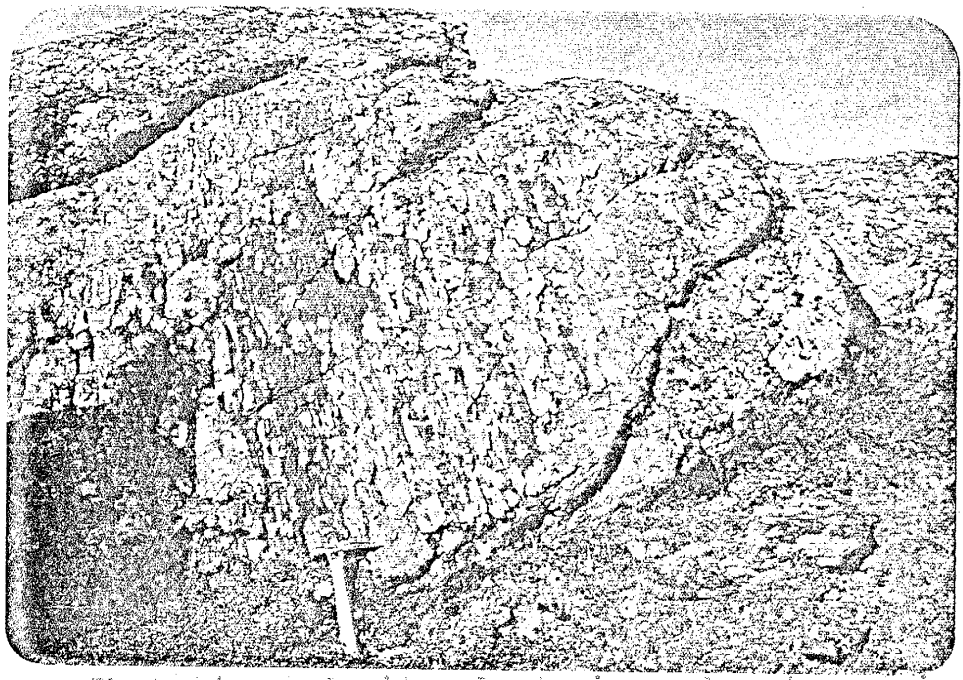

Photo 5. Andesite clasts in carbonate matrix, with strong SE-plunging lineation. West of D'Arcy Lake.

Photo 6. Graded bedding in Yellowknife sediments, west of Dist Lake Camp. No cremulation is developed in mudstone tops of graded beds, but dies out in sandy bottoms. Penny gives scale.

I. HACKETT RIVER ANALYSES--MAJOR ELEMENTS

| | HR-23 | HR-5 | HR-16 | US-28 | US-6 | US-3 | HR-22 | HR-21 | HR-15 | HR-11 | US-32 | errors |
|---|---|---|---|---|---|---|---|---|---|---|---|---|
| $SiO_2$ | 87.58 | 82.74 | 72.38 | 71.98 | 70.28 | 64.42 | 63.23 | 62.12 | 55.18 | 48.30 | 48.48 | 0.51 |
| $TiO_2$ | 0.41 | 0.25 | 0.84 | 0.93 | 0.50 | 0.93 | 0.88 | 1.05 | 1.02 | 1.08 | 0.92 | 0.022 |
| $Al_2O_3$ | 11.24 | 13.84 | 15.29 | 14.04 | 16.37 | 13.77 | 14.04 | 16.69 | 16.21 | 15.39 | 11.93 | 0.30 |
| $Fe_2O_3$ | 0.18 | 2.22 | 2.60 | 4.88 | 2.04 | 7.56 | 9.49 | 8.86 | 10.24 | 13.42 | 15.16 | 0.26 |
| MgO | 0.0 | 0.18 | 0.91 | 1.48 | 0.98 | 3.42 | 4.58 | 4.54 | 6.18 | 9.98 | 11.54 | 1.65 |
| CaO | 0.57 | 0.65 | 1.34 | 0.93 | 3.50 | 2.07 | 4.07 | 2.46 | 7.27 | 9.52 | 9.78 | 0.084 |
| $Na_2O$ | 2.84 | 0.35 | 5.53 | 3.47 | 4.34 | 5.05 | 4.01 | 2.24 | 3.52 | 3.76 | 3.32 | 0.054 |
| $K_2O$ | 2.15 | 6.34 | 2.05 | 2.51 | 2.31 | 1.79 | 1.74 | 4.11 | 0.16 | 0.56 | 0.90 | 0.021 |
| $P_2O_5$ | 0.07 | 0.10 | 0.28 | 0.24 | 0.18 | 0.40 | 0.45 | 0.38 | 0.42 | 0.45 | 0.41 | 0.05 |
| MnO | 0.01 | 0.07 | 0.04 | 0.08 | 0.11 | 0.08 | 0.14 | 0.14 | 0.10 | 0.22 | 0.28 | 0.01 |
| $CO_2$ | 0.0 | 0.0 | 0.0 | 0.0 | 0.58 | 0.0 | 0.0 | 0.0 | 0.0 | 0.12 | 0.0 | 15% |
| S | 0.0 | 0.0 | 0.0 | 0.0 | 0.10 | 0.0 | 0.0 | 0.0 | 0.0 | 0.40 | 0.17 | 60% |
| $Fe^3/Fe_T$ | 0.55 | 0.55 | 0.22 | 0.18 | 0.21 | 0.09 | 0.09 | 0.15 | 0.07 | 0.08 | 0.08 | |
| FeO | 0.08 | 0.90 | 1.83 | 3.60 | 1.45 | 6.19 | 7.77 | 6.78 | 8.57 | 8.64 | 9.75 | |
| $Fe_2O_3$ | 0.10 | 1.22 | 0.57 | 0.87 | 0.43 | 0.69 | 0.86 | 1.33 | 0.71 | 0.75 | 0.85 | |
| minor | 0.05 | 0.08 | 0.09 | 0.07 | 0.07 | 0.07 | 0.06 | 0.07 | 0.06 | 0.06 | 0.06 | |
| total | 105.14 | 106.72 | 101.20 | 100.46 | 100.52 | 98.93 | 102.88 | 101.96 | 99.44 | 101.56 | 101.44 | |
| rem: | hi-silica | hi-silica | | | | | | K-enr. | | | | |
| K/Na | 0.76 | 18.1 | 0.37 | 0.72 | 0.53 | 0.35 | 0.43 | 1.83 | 0.05 | 0.15 | 0.27 | 1.8% |
| Al/Si | 0.13 | 0.17 | 0.21 | 0.20 | 0.23 | 0.21 | 0.22 | 0.27 | 0.29 | 0.32 | 0.25 | 2.5% |
| $\frac{Mg+Fe}{Ca+Na}$ | 0.05 | 2.40 | 0.46 | 1.45 | 0.39 | 1.54 | 1.74 | 2.85 | 1.52 | 1.76 | 2.04 | 17% |



APPENDIX

I. Hackett River Analyses--Major Elements

II. Hackett River Analyses--Trace Elements

III. Hackett River Analyses--Modes

IV. Hackett River Analyses--CIPW Norms

II. HACKETT RIVER ANALYSES--TRACE ELEMENTS

| | HR-23 | HR-5 | HR-16 | US-28 | US-6 | US-3 | HR-22 | HR-21 | HR-15 | HR-11 | US-32 | errors |
|---|---|---|---|---|---|---|---|---|---|---|---|---|
| Sb | 0.45 | 0.3 | 0.5 | 0.35 | 0.4 | 0.4 | 0.4 | 0.35 | 0.45 | 0.4 | 0.4 | 33% |
| Zn | 2.1 | 105. | 68. | 531. | 42. | 144. | 142. | 219. | 116. | 130. | 95. | 25% |
| Cu | 9.8 | 15. | 9.5 | 13. | 6.5 | 15. | 37. | 46. | 66. | 27. | 83. | 37% |
| Ni | 10.0 | 15. | 15. | 15. | 20. | 15. | 40. | 45. | 60. | 45. | 85. | 43% |
| Co | 3.2 | 2.5 | 20.1 | 15.1 | 7.1 | 14.8 | 28.3 | 23.3 | 27.6 | 37.9 | 43. | 4.5% |
| Mn | 84. | 570. | 328. | 658. | 872. | 589. | 1117. | 1080. | 777. | 1725. | 2165. | 3.2% |
| Cr | 0.0 | 2.9 | 82. | 7.35 | 56. | 9. | 82. | 75. | 75.5 | 123. | 182. | 14.6% |
| Rb | 26.7 | 85.0 | 35.1 | 58.2 | 31.3 | 51.3 | 37.7 | 70.6 | 9.10 | 14.0 | 16.1 | 3.4% |
| Sr | 46.0 | 29.9 | 94.0 | 205. | 278. | 225. | 141. | 167. | 319. | 270. | 234. | 4.0% |
| Cs | 0.55 | 1.55 | 2.2 | 1.65 | 1.3 | 3.0 | 1.55 | 4.0 | 0.6 | 1.0 | 0.8 | 25% |
| Ba | 250. | 400. | 460. | 380. | 390. | 400. | 170. | 400. | 150. | 130. | 80. | 7.5% |
| Th | 4.85 | 8.1 | 1.9 | 2.75 | 4.4 | 5.5 | 2.2 | 2.85 | 2.25 | 1.2 | 0.8 | 5.6% |
| Sc | 5.5 | 6.15 | 16.2 | 49. | 8.7 | 12.4 | 21.3 | 18.8 | 21.2 | 22.6 | 33.3 | 3.1% |
| Y | 14. | 23. | 18. | 11. | 1.7 | 25. | 19. | 18. | 10. | 11. | 9.8 | 43% |
| Zr | 179. | 230. | 206. | 200. | 170. | 225. | 203. | 184. | 189. | 250. | 79. | 31% |
| Hf | 5.9 | 7.15 | 4.6 | 6.35 | 4.7 | 6.9 | 4.8 | 5.5 | 4.35 | 6.3 | 0.55 | 11.4% |
| Ta | 1.04 | 1.54 | 0.79 | 0.91 | 0.67 | 1.11 | 0.93 | 1.04 | 0.70 | 0.65 | 0.20 | 16.6% |
| La | 24. | 13. | 14. | 22. | 23. | 14. | 24. | 12. | 18. | 19. | 2.3 | 10.1% |
| Ce | 65. | 40. | 44. | 50. | 46. | 37. | 46. | 24. | 47. | 40. | 7. | 3.7% |
| Sm | 4.7 | 3.1 | 4.6 | 4.3 | 3.2 | 4.5 | 5.1 | 2.7 | 4.7 | 4.7 | 1.9 | 1.2% |
| Eu | 1.3 | 0.8 | 1.2 | 1.6 | 1.1 | 1.4 | 1.6 | 1.4 | 1.45 | 1.5 | 0.82 | 15% |
| Tb | 0.8 | 0.9 | 0.9 | 0.58 | 0.4 | 1.0 | 0.74 | 0.4 | 0.73 | 0.9 | 0.5 | 24% |
| Yb | 3.6 | 3.8 | 3.1 | 2.3 | 0.6 | 3.3 | 2.8 | 2.4 | 3.2 | 3.1 | 2.7 | 8.0% |
| Lu | 0.64 | 0.65 | 0.52 | 0.34 | 0.09 | 0.55 | 0.53 | 0.37 | 0.63 | 0.49 | 0.34 | 8.7% |
| K/Rb | 668. | 619. | 485. | 358. | 613. | 290. | 383. | 483. | 146. | 332. | 464. | 3.5% |
| Rb/Sr | 0.58 | 2.84 | 0.37 | 0.28 | 0.11 | 0.23 | 0.27 | 0.42 | 0.03 | 0.05 | 0.07 | 5.2% |
| Zr/Y | 12.8 | 10. | 11. | 18. | 100. | 9.0 | 11. | 10. | 19. | 23. | 8.1 | 53% |
| La/Yb | 6.7 | 3.4 | 4.5 | 9.6 | 38. | 4.2 | 8.6 | 5.0 | 5.6 | 6.1 | 0.85 | 13% |
| Eu/Eu* | 0.83 | 0.67 | 0.78 | 1.15 | 1.19 | 0.86 | 1.01 | 1.54 | 0.93 | 0.92 | 1.13 | 20% |

-134-

I. HACKETT RIVER ANALYSES--MAJORS (continued)

| | HR-2 | HR-13 | HR-28 | US-26 | US-31 | RL-10 | RL-3 | RL-7 | US-24 | RL-2 | US-4 | ERRORS |
|---|---|---|---|---|---|---|---|---|---|---|---|---|
| $SiO_2$ | 60.12 | 89.47 | 86.65 | 69.88 | 70.18 | 63.64 | 63.73 | 63.16 | 59.26 | 55.47 | 66.83 | 0.51 |
| $TiO_2$ | 1.40 | 0.17 | 0.11 | 0.55 | 0.67 | 0.32 | 0.40 | 0.48 | 0.73 | 1.88 | 0.66 | 0.022 |
| $Al_2O_3$ | 16.51 | 9.27 | 13.56 | 15.92 | 13.66 | 16.57 | 12.33 | 14.50 | 15.84 | 12.86 | 16.75 | 0.30 |
| $Fe_2O_3$ | 8.65 | 1.20 | 0.0 | 2.51 | 5.97 | 3.46 | 4.45 | 4.67 | 8.80 | 13.04 | 4.12 | 0.26 |
| MgO | 6.08 | 0.0 | 0.0 | 0.72 | 3.18 | 1.72 | 3.11 | 2.45 | 3.52 | 12.26 | 1.58 | 1.65 |
| CaO | 3.95 | 3.27 | 0.0 | 2.39 | 3.80 | 5.29 | 6.14 | 4.77 | 3.48 | 6.53 | 5.23 | 0.084 |
| $Na_2O$ | 3.95 | 0.47 | 0.83 | 6.70 | 1.83 | 4.37 | 3.68 | 3.59 | 5.18 | 2.79 | 4.27 | 0.054 |
| $K_2O$ | 2.36 | 1.03 | 6.82 | 0.52 | 2.36 | 2.20 | 1.35 | 2.23 | 0.93 | 0.57 | 0.69 | 0.021 |
| $P_2O_5$ | 0.54 | 0.05 | 0.05 | 0.19 | 0.26 | 0.14 | 0.15 | 0.18 | 0.26 | 0.54 | ND | 0.05 |
| MnO | 0.11 | 0.13 | 0.01 | 0.02 | 0.07 | 0.09 | 0.06 | 0.08 | 0.22 | 0.11 | 0.06 | 0.01 |
| $CO_2$ | 0.0 | 0.71 | 0.0 | 0.18 | 1.30 | 13.29 | 14.62 | 5.51 | 0.0 | 14.34 | 0.0 | 15% |
| S | 0.48 | 0.05 | 0.0 | 0.10 | 0.14 | 0.0 | 0.10 | 0.0 | tr | 0.0 | 0.0 | 60% |
| $Fe^3/Fe_T$ | 0.10 | 0.55 | 0.55 | 0.20 | 0.21 | 0.12 | 0.15 | 0.10 | 0.08 | 0.07 | 0.16 | |
| $Fe_2O_3$ | 0.86 | 0.66 | 0.0 | 0.50 | 1.26 | 0.41 | 0.67 | 0.47 | 0.70 | 0.91 | 0.66 | |
| FeO | 7.01 | 0.49 | 0.0 | 1.81 | 4.25 | 2.74 | 3.40 | 3.78 | 7.29 | 10.91 | 3.11 | |
| minor | 0.03 | 0.02 | 0.02 | 0.02 | 0.03 | 0.02 | 0.02 | 0.02 | 0.02 | 0.02 | 0.0 | |
| total | 103.40 | 105.79 | 108.05 | 99,50 | 102.96 | 110.80 | 109.76 | 101.22 | 97.43 | 119.17 | 99.84 | |
| rem: | K-enr. | hi-silica K-enr. | hi-silica K-enr. | K-depl. | | hi-$CO_2$ | hi-$CO_2$ | hi-$CO_2$ | | hi-$CO_2$ | K-depl. | |
| K/Na | 0.60 | 2.19 | 8.2 | 0.08 | 1.29 | 0.50 | 0.37 | 0.62 | 0.18 | 0.20 | 0.16 | 1.8% |
| Al/Si | 0.28 | 0.10 | 0.16 | 0.23 | 0.20 | 0.26 | 0.19 | 0.23 | 0.27 | 0.23 | 0.25 | 2.5% |
| $\frac{Mg+Fe}{Ca+Na}$ | 1.86 | 0.32 | 0.0 | 0.35 | 1.63 | 0.54 | 0.77 | 0.85 | 1.42 | 2.71 | 0.60 | 17% |

-133-

III. HACKETT RIVER ANALYSES--MODES

| | HR-23 | HR-5 | HR-16 | US-28 | US-6 | US-3 | HR-22 | HR-21 | HR-15 | HR-11 | US-32 |
|---|---|---|---|---|---|---|---|---|---|---|---|
| ground-mass | 88. | 81. | 83. | 75. | 88. | 76. | 70. | 65. | 59. | 38. | 22. |
| biotite | 1.0 | 5. | 9. | 12.5 | 1.1 | 20. | 28. | 29. | 3. | 2. | 0. |
| muscov. | 11. | 10. | 6. | 10.9 | 7.2 | 0. | 0.4 | 5. | 0. | 2. | 6. |
| chlorite | 0.6 | 4. | 0. | 0.1 | 2. | 0. | 0. | 0. | 0. | 8. | 4. |
| hbl | 0. | 0. | 0. | 0. | 0. | 0. | 0. | 0. | 36. | 47. | 67. |
| mag | tr | 0. | 2. | 1.3 | 0.2 | 1. | 1.2 | 0.4 | 3. | 2. | 0.6 |
| calcite | 0. | 0. | 0. | 0. | 0. | 1.3 | 0. | 0. | 0. | 0.3 | 0. |
| cordier | 0. | 0. | 0. | 0. | 0. | 0. | 3. | 0. | 0. | 0. | 0. |
| pyrite | 0. | 0. | 0. | 0. | 0. | 0.2 | 0. | 0. | 0. | 0. | 0.4 |
| garnet | | | | | | | | | | | |
| leucox. | | | | | | | | | | | |
| epidote | | | | | | | | | | | |
| hem,etc. | | | | | | | | | | | |
| density | 2.64 | 2.64 | 2.73 | 2.73 | 2.69 | 2.71 | 2.77 | 2.74 | 2.92 | 3.00 | 3.06 |

| | HR-2 | HR-13 | HR-28 | US-26 | US-31 | RL-10 | RL-3 | RL-7 | US-24 | RL-2 | US-4 |
|---|---|---|---|---|---|---|---|---|---|---|---|
| ground-mass | 70. | 80. | 87. | 92. | 60. | 63. | 60. | 42. | 66. | 32. | 77. |
| bio | 29. | tr | 0. | 3.8 | 18. | 0. | 0. | 39. | 14. | 0. | 4.4 |
| musc | 0. | 14. | 12. | 1.2 | 8. | 6. | 5. | 6.8 | 3. | 4. | 16. |
| hbl | 0. | 0. | 0. | 0. | 4. | 0. | 0. | 0. | 0. | 0. | 0.6 |
| chlor | 0. | 3.5 | 0. | 3. | 2. | 0.4 | 1.5 | 0. | 15. | 20. | 0.8 |
| mag | 0. | 0.2 | 0. | tr | 0. | 0.6 | 0.2 | 0. | tr | 0. | 1.2 |
| calc | 0. | 1.6 | 0. | 0.4 | 3. | 30. | 33. | 13. | 0. | 35. | 0. |
| cord | | | | | | | | | | | |
| pyrite | 1.0 | 0. | 0. | 0.2 | 0.3 | 0. | 0.2 | 0. | tr | 0. | 0. |
| gar | | 0.6 | | | | | | | 3. | | |
| leuc. | | | 0.2 | | | | | | | | |
| epidote | | | | | 5. | | | | | | 0.4 |
| hem,etc. | | | | | | | | | | 5.0 | |
| density | 2.76 | 2.68 | 2.66 | 2.63 | 2.75 | 2.69 | 2.69 | 2.77 | 2.78 | 2.91 | 2.71 |

II. HACKETT RIVER ANALYSES--TRACE ELEMENTS (continued)

| | HR-2 | HR-13 | HR-28 | US-26 | US-31 | RL-10 | RL-3 | RL-7 | US-24 | RL-2 | US-4 | errors |
|---|---|---|---|---|---|---|---|---|---|---|---|---|
| Sb | | | | | | | | | | | | |
| Zn | 96. | 29. | 0. | 102. | 148. | 175. | 69. | 354. | 112. | 152. | | 25% |
| Cu | 21. | 23. | 34. | 34. | 33. | 29. | 34. | 28. | 32. | 26. | | 37% |
| Ni | 14. | 9.2 | 20. | 14. | 36. | 29. | 24. | 23. | 18. | 34. | | 43% |
| Co | | | | | | | | | | | | |
| Mn | 837. | 1000. | 53. | 181. | 560. | 688. | 453. | 643. | 1683. | 817. | 459. | 3.2% |
| Cr | | | | | | | | | | | | |
| Rb | 79.2 | 42.4 | 130. | 20.7 | 69.2 | 70.4 | 35.3 | 70.2 | 29.6 | 15.4 | | 3.4% |
| Sr | 250. | 127. | 58.0 | 319. | 132. | 445. | 814. | 671. | 247. | 410. | | 4.0% |
| Cs | | | | | | | | | | | | |
| Ba | | | | | | | | | | | | |
| Th | | | | | | | | | | | | |
| Sc | | | | | | | | | | | | |
| Y | 20. | 9.3 | 14. | 3.2 | 15. | 6.3 | 8.3 | 13. | 9.7 | 11. | | 43% |
| Zr | 250. | 130. | 140. | 180. | 190. | 140. | 180. | 180. | 185. | 144. | | 31% |
| Hf | | | | | | | | | | | | |
| Ta | | | | | | | | | | | | |
| La | | | | | | | | | | | | |
| Ce | | | | | | | | | | | | |
| Sm | | | | | | | | | | | | |
| Eu | | | | | | | | | | | | |
| Tb | | | | | | | | | | | | |
| Yb | | | | | | | | | | | | |
| Lu | | | | | | | | | | | | |
| K/Rb | 247. | 202. | 426. | 209. | 283. | 259. | 317. | 264. | 261. | 307. | | 3.5% |
| Rb/Sr | 0.32 | 0.33 | 2.24 | 0.07 | 0.52 | 0.16 | 0.04 | 0.10 | 0.12 | 0.04 | | 5.2% |
| Zr/Y | 12.5 | 14. | 10. | 56. | 13. | 22. | 22. | 14. | 19. | 13. | | 53% |
| La/Yb | | | | | | | | | | | | |

IV. HACKETT RIVER ANALYSES--CIPW NORMS (continued)

| | HR-2 | HR-13 | HR-28 | US-26 | US-31 | RL-10* | RL-3* | RL-7 | US-24 | RL-2 | US-4 |
|---|---|---|---|---|---|---|---|---|---|---|---|
| Q | 7.70 | 73.50 | | 23.02 | 38.24 | 16.06 | 22.06 | 29.70 | 8.34 | 20.69 | 24.24 |
| C | 1.52 | 3.03 | | 0.87 | 4.68 | | | 6.11 | 0.62 | 6.42 | |
| or | 13.49 | 5.75 | | 3.09 | 13.54 | 13.33 | 8.39 | 13.02 | 5.64 | 2.83 | 4.08 |
| ab | 32.32 | 3.76 | | 56.98 | 15.04 | 37.92 | 32.76 | 30.01 | 44.99 | 19.81 | 36.19 |
| an | 15.54 | 10.78 | | 9.52 | 8.68 | 19.59 | 13.82 | | 15.98 | | 24.54 |
| ne | | | | | | | | | | | |
| di | | | | | | 5.28 | 14.04 | | | | 1.20 |
| hy | 23.41 | 0.20 | | 3.64 | 13.03 | 6.22 | 6.70 | 7.46 | 21.33 | 20.66 | 7.54 |
| ol | | | | | | | | | | | |
| Z | 0.04 | 0.03 | | 0.03 | 0.04 | 0.03 | 0.03 | 0.03 | 0.03 | 0.02 | |
| mt | 1.21 | 0.90 | | 0.73 | 1.77 | 0.61 | 1.02 | 0.67 | 1.04 | 1.11 | 0.96 |
| hm | | | | | | | | | | | |
| il | 2.57 | 0.30 | | 1.05 | 1.24 | 0.62 | 0.80 | 0.90 | 1.42 | 3.00 | 1.26 |
| cm | | | | | | | | | | | |
| ru | | | | | | | | | | | |
| ap | 1.24 | 0.11 | | 0.45 | 0.60 | 0.34 | 0.37 | 0.42 | 0.63 | 1.07 | |
| pr | 0.87 | 0.09 | | | | * | * | | | | |
| cc | | 1.53 | | 0.41 | 2.87 | * | * | 7.99 | | 8.71 | |
| mg | | | | | | * | * | 3.70 | | 15.71 | |
| D.I. | 53.52 | 83.02 | | 83.09 | 66.82 | 67.32 | 63.22 | 72.72 | 58.96 | 43.32 | 64.51 |

HR-28 norm not computable; insufficient CaO to form ap.

*--Norms for RL-10 and RL-3 computed on a $CO_2$ and S-free basis.



IV. HACKETT RIVER ANALYSES--CIPW NORMS

| | HR-23 | HR-5 | HR-16 | US-28 | US-6 | US-3 | HR-22 | HR-21 | HR-15 | HR-11 | US-32 |
|---|---|---|---|---|---|---|---|---|---|---|---|
| Q | 58.78 | 51.42 | 27.84 | 36.50 | 28.28 | 15.64 | 13.52 | 17.53 | 5.44 | | |
| C | 3.19 | 5.10 | 2.15 | 4.46 | 2.09 | 0.70 | | 4.87 | | | |
| or | 12.09 | 35.11 | 11.98 | 14.80 | 13.49 | 10.70 | 10.10 | 23.83 | 0.95 | 3.24 | 5.24 |
| ab | 22.86 | 2.78 | 46.26 | 29.30 | 36.29 | 43.22 | 33.32 | 18.60 | 29.96 | 23.16 | 18.94 |
| an | 2.31 | 2.46 | 4.85 | 3.11 | 12.44 | 7.82 | 14.90 | 9.61 | 28.13 | 22.99 | 14.76 |
| ne | | | | | | | | | | 4.35 | 4.73 |
| di | | | | | | | 1.72 | | 4.48 | 16.10 | 24.88 |
| hy | | 0.76 | 3.79 | 8.18 | 3.87 | 18.13 | 22.48 | 20.78 | 27.00 | | |
| ol | | | | | | | | | | 24.43 | 26.64 |
| Z | 0.03 | 0.04 | 0.04 | 0.04 | 0.03 | 0.04 | 0.04 | 0.03 | 0.04 | 0.04 | 0.02 |
| mt | | 1.66 | 0.82 | 1.26 | 0.62 | 1.01 | 1.22 | 1.89 | 1.04 | 1.52 | 1.74 |
| hm | 0.10 | | | | | | | | | | |
| il | 0.18 | 0.44 | 1.58 | 1.76 | 0.94 | 1.79 | 1.64 | 1.96 | 1.95 | 2.01 | 1.72 |
| cm | | | 0.02 | | 0.02 | | 0.01 | 0.01 | 0.02 | 0.03 | 0.04 |
| ru | 0.30 | | | | | | | | | | |
| ap | 0.16 | 0.22 | 0.66 | 0.57 | 0.42 | 0.96 | 1.05 | 0.88 | 1.00 | 1.04 | 0.96 |
| pr | | | | | 0.18 | | | | | 0.73 | 0.31 |
| cc | | | | | 1.30 | | | | | 0.27 | |
| mg | | | | | | | | | | | |
| D.I. | 93.73 | 89.30 | 86.08 | 80.60 | 78.05 | 69.55 | 56.94 | 59.96 | 36.36 | 30.75 | 28.90 |